N1-methylpseudouridine and pseudouridine mRNA Modifications Modulate Translation Rate and Fidelity

by

Jeremy Monroe

A dissertation submitted in partial fulfillment
of the requirements for the degree of
Doctor of Philosophy
(Chemistry)
in the University of Michigan
2022

Doctoral Committee:

Assistant Professor Kristin Koutmou, Chair
Assistant Professor Aaron Frank
Research Professor Anna Mapp
Assistant Professor Kaushik Ragunathan

Jeremy G. Monroe

monroejg@umich.edu

ORCID iD: 0000-0002-1901-8345

Dedication

This dissertation is dedicated to all the scientists who understand that good science is about the search for and reporting of the truth. Many these scientists have had their careers stymied or curtailed because they refused to fabricate and fudge the data. While the majority of academic scientists are more concerned about making the correct allies and obtaining funding than conducting repeatable, reproducible, and falsifiable science, these few true investigators are pushing the frontiers of humanity's knowledge. In the future when the junk science has been pushed aside and only the truth remains the forgotten scientists of today will be remembered and it is to them that I dedicate my humble PhD work.

Acknowledgements

I would like to acknowledge my parents who raised me to respect the truth and to understand the value of hard work. I am the scientist and person I am today because of them.

They brought me up to be uncompromising with the truth and to speak my mind. While these principles have not always made my life easy, they have allowed me to live a moral and productive life. Everything I have accomplished both personally and professionally is the result of the values they instilled in me.

Table of Contents

List of Tables

List of Figures

List of Equations

List of Appendices

Abstract

The discovery of modifications within the coding region of mRNA have highlighted the importance of uncovering how modifications alter the transformation of the information encoded in RNA transcripts into functional protein. Prominent among mRNA modifications are the N1-methylpseudouridine ($m^1\Psi$) and pseudouridine (Ψ) modifications, which are both incorporated into RNA therapeutic platforms, with $m^1\Psi$ being a prominent component in the Pfizer and Moderna COVID-19 vaccines. Using a fully reconstituted prokaryotic *in vitro* system detailed molecular level insights can be gained about how mRNA modifications can modify the rate and fidelity of translation. Alterations to either the rate or fidelity of translation can result in varying levels of protein production or miscoded protein products. My studies have demonstrated that both Ψ and $m^1\Psi$ are able to modulate ribosome fidelity in a codon and anticodon dependent manner. This alteration of ribosome fidelity was confirmed by *in cellular* studies in HEK293 cells which displayed the same pattern of altered ribosomal accuracy. Using molecular modeling we deduced that isomerization and increased base stacking interactions are partially responsible for the changes in translational accuracy. Understanding if and how these modifications impact translation is important for understanding the epigenetic landscape and potential avenues of mRNA therapeutics development.

Chapter 1 Introduction

An organism's survival depends upon its ability to express its genetic information.[1] This expression is accomplished through the transformation of genetic information reposited in DNA into messenger RNA (mRNA) through transcription and then the mRNA being translated into functional protein. This orchestration of informational transfer was described by Francis Crick as the *Central Dogma of Biology*.[2] Messenger RNA occupancies a unique position within this information flow serving as the transitory carrier of the genetic information to be expressed. [3,4]. The ability to produce proteins with both rapidity and accuracy is vital for maintenance of a cell's homeostasis[5]. Given the importance of protein synthesis to the cell fitness and viability, alterations to the biochemical properties of mRNA through modifications could potentially impact translation and thus the cell's genetic expression.

1.1 Ribosome

Translation occupies a strategic position in the Central Dogma being the final step in gene expression and the actual transition point between information and functionality. Translation occurs at the ribosome, a macromolecule consisting of proteins and ribosomal RNA (rRNA)[6]. The ribosome enzymatically converts single amino acids attached to transfer RNAs (tRNAs) into a polypeptide chain. Ribosomes consists of a large and a small subunit that form a tight coupled unit during translation. The exact size and composition of these subunits varies between kingdoms but the enzymatic chemistry of protein synthesis remains highly conserved (**Figure 1)**[6,7]. The small ribosomal subunit (30S in prokaryotes and 40S in eukaryotes) monitors the interaction between the mRNA codons and the tRNA's anticodon at the decoding center. The large subunit (50S in prokaryotes and 60S in eukaryotes) contains the site of peptide bond formation during elongation and the site of peptide hydrolysis during termination at the peptidyl transfer center (PTC). Spanning both the large and small subunit are three tRNA binding sites. The aminoacyl site (A-site), the peptidyl site (P-site), and the exit site (E-site). While prokaryotic and eukaryotic ribosomes differ in several aspects including size and composition, the molecular structures and mechanisms of translation are highly conserved between kingdoms.

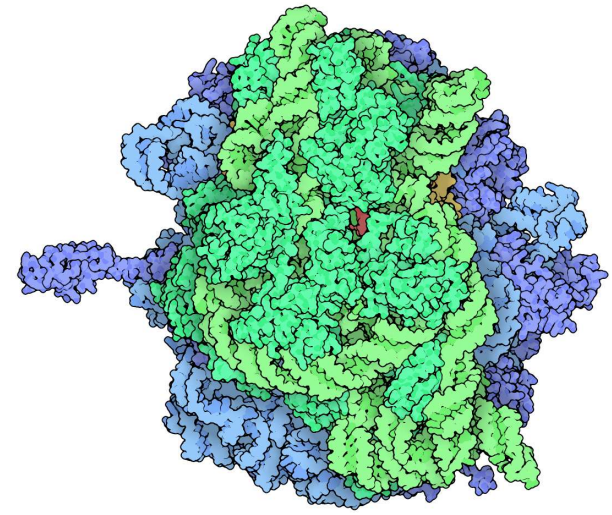

Figure 1 *Bacterial Ribosome with the small subunit in green and the large subunit in blue (PDB entry 4v5d)*

1.2 Protein Synthesis

Prokaryotic translation occurs in four main steps: initiation, elongation, termination, and recycling. Each of these steps is a highly dynamic multi-step process involving various factors. Translation starts during initiation when the subunits of the ribosome, assisted by protein initiation factors, assemble on the start codon (AUG) of the mRNA and an aminoacylated formyl-methionine tRNA (^{f}met tRNA) is bound to the P-site of the ribosome. During elongation the ribosome decodes the codons of the mRNA messages and incorporates the corresponding amino acid into a polypeptide chain[8]. Termination occurs when the ribosome encounters a stop codon (UAA, UGA, UAG) and a release factor (RF) binds to the A-site of the ribosome resulting in a peptide hydrolysis reaction[9]. During recycling the ribosome dissociates into its respective subunits to start the next round of translation. Given the complex and multistep nature of translation, I focused my investigation on the elongation, particularly amino acid addition, and termination steps of translation[10].

1.2.1 Elongation

Elongation consists of repeating cycles of tRNA decoding, amino acid addition, peptide bond formation, and translocation. The cycle proceeds from the open reading frame (ORF) codon immediately following the AUG start codon as the ribosome decodes the mRNA sequence. Amino acid addition can be broken down into seven kinetically definable proofreading and/or conformational steps[10,11]. (**Figure 2) .** Understanding these steps permits the elucidation of how modification can alter them.

A ternary complex (TC) consisting of acylated tRNA, EF-Tu protein, and GTP is recruited to the A-site with transient binding to the L7/L12 stalks of the ribosome, step 1 of Figure 2[13,14]. The tRNA anticodon is able to rapidly and reversibly sample the codon in the A-site. The tRNA anticodon is recognized by the mRNA through codon : anticodon base pairing interactions in a step 2 of Figure 2[15]. The decoding of aminoacyated tRNA does not rely entirely upon the base pairing interaction especially given the low free energy difference between cognate and near cognate interactions, -3 kcal/mol or less[15,16]. Correct decoding occurs when the cognate tRNA in the TC binds to the codon creating a stabilizing codon-anticodon complex due to the correct Watson Crick geometry of the base pairs. This complex interacts with the 16S rRNA located in the small subunit of the ribosome, causing the A1492 and A1493 residues to reconfigure from a flipped-in conformation to a flipped-out conformation[7,10]. These residues are then able to interact with the first and second positions of the stabilized codon-anticodon complex bound in the A-site.

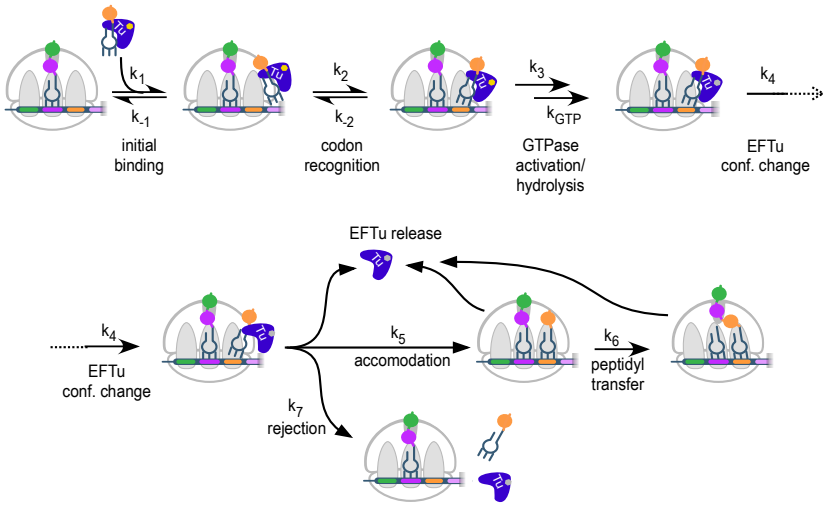

Figure 2 *The Seven Kinetically Definable Steps of Amino Acid Selection*

Once decoding occurs GTP activation and GTP hydrolysis rapidly proceed, (Steps 3 and 4, **Figure 2**). GTP activation occurs as a result of conformational changes in the EF-Tu GTP binding domain bound to the sarcin-ricin loop (SRL) of the 23S rRNA in the ribosome's large subunit[10]. The SRL is the primary element responsible for the activation of GTP. GTP

hydrolysis utilizes a universally conserved histone residue to position a nucleophilic water molecule to hydrolyze the GTP's γ-phosphate. The L12 stalk of the ribosome has been speculated to also contribute to this reaction [10]. GTP activation and hydrolysis serves as an additional proofreading step of amino acid addition with noncognate codon-anticodon complexes resulting in decreased rates of GTP hydrolysis[11,15]. After GTP hydrolysis the EF-Tu undergoes a conformation change and the GDP-EF-Tu complex dissociates from the ribosome (Step 4, **Figure 2**). Accommodation fully seats the tRNA in the A-site of the ribosome, moving the 3' CCA end of the tRNA into the PTC on the large subunit (Step 5, **Figure 2**). The rate of accommodation for noncognate tRNA has been observed to be slower which allows the ribosome another chance to reject incorrectly selected tRNA. Once the incoming tRNA is fully seated in the A-site the ribosome uses ordered water molecules and nucleophilic attacks in the PTC to form a peptide bond and transfer the polypeptide chain from the P-site tRNA to the A-site tRNA. [16,21]. When the peptide bond is formed the ribosomal subunits rotate to translocate the tRNA in the P site into the E site and the A site tRNA into the P site and exposing the next codon on the mRNA[21]. The steps preceding GTP hydrolysis (Steps 1 and 2, **Figure 2**) can be defined as the selectivity of the ribosome since the ribosome is selecting the cognate tRNA, while the subsequent steps deal with the proofreading ability of the ribosome. The process of amino acid addition then continues as the ribosome translates the mRNA sequence into a polypeptide chain. mRNA modifications have the ability to change multiple steps of this process by altering the hydrogen bonding, sterics, base stacking, and stability both within the mRNA and intermolecularly between the codon:anticodon which could result in different rates of amino acids addition and changes to the decoding ability of the ribosome.

1.2.2 Termination

Elongation continues until the ribosome encounters a stop codon (UAA, UAG, UGA) in the mRNA sequence **(Figure 2)**. These codons are recognized by two Class 1 protein release factors in prokaryotes., release factor 1 (RF1) which recognized the UAG codon and release factor 2 (RF2) which recognizes the UGA codon. The UAA is recognized by both RF1 and RF2 and as a result is referred to as the universal stop codon[22]. While eukaryotes have the same stop codons, they are all recognized by a single release factor (eRF1)[9]. Release factors function by binding to the stop codon in the A-site with a tripeptide motif that mimics the anticodon of tRNA. This anticodon motif varies slightly with RF1 having a PA(V)T and RF2 having a SPF motif[23,24]. The universally conserve GGQ motif in RFs binds to the PTC site and hydrolyzes the polypeptide chain from the P-site tRNA, thus releasing the polypeptide chain from the ribosome[25]. This reaction is catalyzed by class 2 release factor RF3. RF3 is a small GTPase which enhances the rate RF dissociation from the ribosome by binding to the ribosome and hydrolyzing a GTP to cause a ribosomal conformational change that induces the dissociation of class 1 RFs[26]. Modified residues within a stop codon could result in changes to termination rates which may cause reduced/accelerated rates of translation or recoding of the stop codon resulting in readthrough and an aberrant protein product.

1.3 References

[1] Darwin C, Wallace A. On the Tendency of Species to form Varieties; and on the Perpetuation of Varieties and Species by Natural Means of Selection. Journal of the Proceedings of the Linnean Society of London Zoology 1858;3:45–62. https://doi.org/10.1111/j.1096-3642.1858.tb02500.x.

[2] Crick F. Central Dogma of Molecular Biology. Nature 1970;227:561–3. https://doi.org/10.1038/227561a0.

[3] Nirenberg MW, Matthaei JH. The dependence of cell-free protein synthesis in E. coli upon naturally occurring or synthetic polyribonucleotides. PNAS 1961;47:1588–602. https://doi.org/10.1073/pnas.47.10.1588.

[4] Crick FH, Barnett L, Brenner S, Watts-Tobin RJ. General nature of the genetic code for proteins. Nature 1961;192:1227–32. https://doi.org/10.1038/1921227a0.

[5] Lin J, Amir A. Homeostasis of protein and mRNA concentrations in growing cells. Nat Commun 2018;9:4496. https://doi.org/10.1038/s41467-018-06714-z.

[6] Wilson DN, Doudna Cate JH. The Structure and Function of the Eukaryotic Ribosome. Cold Spring Harb Perspect Biol 2012;4:a011536. https://doi.org/10.1101/cshperspect.a011536.

[7] Javed A, Orlova EV. Unravelling Ribosome Function Through Structural Studies. Subcell Biochem 2019;93:53–81. https://doi.org/10.1007/978-3-030-28151-9_3.

[8] Initiation of mRNA translation in bacteria: structural and dynamic aspects n.d. https://www.ncbi.nlm.nih.gov/pmc/articles/PMC4611024/ (accessed November 14, 2019).

[9] Adio S, Sharma H, Senyushkina T, Karki P, Maracci C, Wohlgemuth I, et al. Dynamics of ribosomes and release factors during translation termination in n.d.:24.

[10] Rodnina MV. Translation in Prokaryotes. Cold Spring Harb Perspect Biol 2018;10. https://doi.org/10.1101/cshperspect.a032664.

[11] Pape T, Wintermeyer W, Rodnina MV. Complete kinetic mechanism of elongation factor Tu-dependent binding of aminoacyl-tRNA to the A site of the E. coli ribosome. EMBO J 1998;17:7490–7. https://doi.org/10.1093/emboj/17.24.7490.

[12] Dever TE, Dinman JD, Green R. Translation Elongation and Recoding in Eukaryotes. Cold Spring Harb Perspect Biol 2018;10. https://doi.org/10.1101/cshperspect.a032649.

[13] Ogle JM, Carter AP, Ramakrishnan V. Insights into the decoding mechanism from recent ribosome structures. Trends Biochem Sci 2003;28:259–66. https://doi.org/10.1016/S0968-0004(03)00066-5.

[14] Youngman EM, Brunelle JL, Kochaniak AB, Green R. The Active Site of the Ribosome Is Composed of Two Layers of Conserved Nucleotides with Distinct Roles in Peptide Bond Formation and Peptide Release. Cell 2004;117:589–99. https://doi.org/10.1016/S0092-8674(04)00411-8.

[15] Gromadski KB, Rodnina MV. Kinetic Determinants of High-Fidelity tRNA Discrimination on the Ribosome. Molecular Cell 2004;13:191–200. https://doi.org/10.1016/S1097-2765(04)00005-X.

[16] Rodnina MV, Wintermeyer W. Ribosome fidelity: tRNA discrimination, proofreading and induced fit. Trends Biochem Sci 2001;26:124–30. https://doi.org/10.1016/s0968-0004(00)01737-0.

[17] Durant PC, Bajji AC, Sundaram M, Kumar RK, Davis DR. Structural effects of hypermodified nucleosides in the Escherichia coli and human tRNALys anticodon loop: the effect of nucleosides s2U, mcm5U, mcm5s2U, mnm5s2U, t6A, and ms2t6A. Biochemistry 2005;44:8078–89. https://doi.org/10.1021/bi050343f.

[18] Konevega AL, Soboleva NG, Makhno VI, Peshekhonov AV, Katunin VI. Effect of modification of tRNA nucleotide 37 on the tRNA interaction with the A and P sites of the Escherichia coli 70S ribosome. Mol Biol 2006;40:597–610. https://doi.org/10.1134/S0026893306040121.

[19] Murphy FV, Ramakrishnan V, Malkiewicz A, Agris PF. The role of modifications in codon discrimination by tRNA(Lys)UUU. Nat Struct Mol Biol 2004;11:1186–91. https://doi.org/10.1038/nsmb861.

[20] Phizicky EM, Hopper AK. tRNA processing, modification, and subcellular dynamics: past, present, and future. RNA 2015;21:483–5. https://doi.org/10.1261/rna.049932.115.

[21] Dunkle JA, Dunham CM. Mechanisms of mRNA frame maintenance and its subversion during translation of the genetic code. Biochimie 2015;114:90–6. https://doi.org/10.1016/j.biochi.2015.02.007.

[22] Baggett NE, Zhang Y, Gross CA. Global analysis of translation termination in E. coli. PLOS Genetics 2017;13:e1006676. https://doi.org/10.1371/journal.pgen.1006676.

[23] Svidritskiy E, Korostelev AA. Conformational control of translation termination on the 70S ribosome. Structure 2018;26:821-828.e3. https://doi.org/10.1016/j.str.2018.04.001.

[24] Korostelev AA. Structural aspects of translation termination on the ribosome. RNA 2011;17:1409. https://doi.org/10.1261/rna.2733411.

[25] Dinçbas-Renqvist V, Engström Å, Mora L, Heurgué-Hamard V, Buckingham R, Ehrenberg M. A post-translational modification in the GGQ motif of RF2 from Escherichia coli stimulates termination of translation. EMBO J 2000;19:6900–7. https://doi.org/10.1093/emboj/19.24.6900.

[26] Freistroffer DV, Pavlov MYu, MacDougall J, Buckingham RH, Ehrenberg M. Release factor RF3 in E.coli accelerates the dissociation of release factors RF1 and RF2 from the ribosome in a GTP-dependent manner. EMBO J 1997;16:4126–33. https://doi.org/10.1093/emboj/16.13.4126.

Chapter 2 A Molecular Level Perspective on the Frequency, Distribution, and Consequences of mRNA Modifications

Chapter 2 is reprinted with permission from Wiley Interdiscip Rev RNA. 2020 Jul;11(4). Manuscript was written by Jeremy Monroe, Josh Jones, and Dr. Kristin Koutou. Josh Jones created the figures for the paper 3-6 for the paper and wrote the Quantitative sections. Jeremy Monroe helped to edit figure 7 and wrote the consequences of mRNA modification abundance and frequency and consequence of mRNA modifications on translation sections. Kristin Koutmou wrote the remaining sections and edited the manuscript.

2.1 Introduction

Chemical modifications have been studied as key modulators of RNA biogenesis, function, and stability for over half a century [1–5]. Until recently, post-transcriptional modifications were thought to be largely limited to non-coding RNAs (ncRNA), as only three modifications, N7-methylguanosine (m^7G), N6-methyladenosine (m^6A) and inosine (I), were known in protein coding messenger RNAs (mRNAs) [4,6–9]. The discovery of over a dozen enzymatically incorporated modifications in mRNAs has shifted this paradigm and generated tremendous interest because mRNA modifications have the potential to control protein expression (**Figure 3**) [10,11].

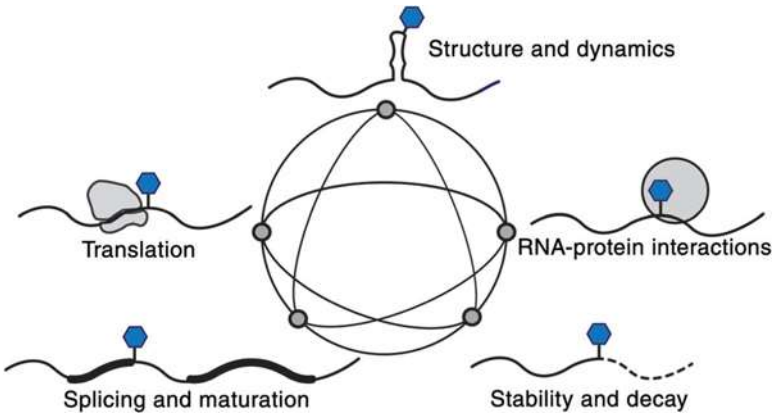

Figure 3 *Chemical modifications have the potential to individually influence mRNA structure and dynamics, splicing and maturation, RNA-protein interactions, translation, and stability.The interconnected nature of the mRNA lifecycle can intensify the effect of a modification through the modulation of downstream processes. For example, several mRNA modifications, m^6A, m^1A, m^1G, Ψ and f^5C, have been shown to change the stability of RNA structures and would be predicted to redistribute the ensemble of mRNA secondary structures present in a cell [82,152,159–163] . This alteration can modulate the ability to form RNA-protein interactions, which can in turn impact mRNA maturation, translation, and decay through pathways dependent on these interactions. Additionally, mRNA translation rates and mRNA decay rates are coupled, with poorly translated mRNAs being targeted more robustly for decay [97,98] . Thus, if an mRNA modification strongly impacts one step in an mRNA's life, this perturbation is likely to be observed in the outcome of related processes (e.g. modification induced perturbations in mRNA structure could slow translation, which in turn reduces the mRNA's half-life).*

It is still unclear if most modifications result from background off-target activities of ncRNA modifying enzymes, or if they represent a new layer of post-transcriptional control. Regardless, there are likely to be biological consequences for mRNA modifications, as these chemical tags can influence the interactions between mRNAs and the cellular machinery. The study of mRNA modifications (the epitranscriptome, Figure 2) is a rapidly emerging field as researchers seek to establish the influence of mRNA modifications on biology and human health [8,12–16]. Initial correlative studies have revealed links between a sub-set of modifications and essential biological functions including development, sex determination and *circadian rhythm maintenance*, multiple cancers and diseases [15,17–27]. However, key fundamental questions regarding the incorporation and molecular level consequences of mRNA modification need to be

investigated to understand how mRNA modification status contributes to discrete biological processes and disease states (Figure 3).

The mRNA epitranscriptome is chemically diverse, containing nucleoside isomers, methyl-, acetyl-, hydroxymethyl- and formyl-modifications (Figure 2) [22,28–37]. Modifications are present in mRNAs in eukaryotic, bacterial and viral mRNAs [38,39]. Advances in sequencing technologies enabled the development of techniques to identify the location of modifications transcriptome wide [30,40,41]. These approaches have given us an expansive bird's-eye view of mRNA modifications by providing detailed maps of where twelve modifications can be incorporated into the transcriptome [N6-methyladenosine (m^6A) pseudouridine (Ψ), N4-acetylcytidine (ac^4C), N1-methyladenosine (m^1A), N7-methylguanosine (m^7G), 2'O-methyl modifications (Cm, Am, Gm, Um), 5-methylcytidine (m^5C), and 5-hydroxymethylcytidine (hm^5C), and inosine (I)] [28–30,33–35,40,42–55].

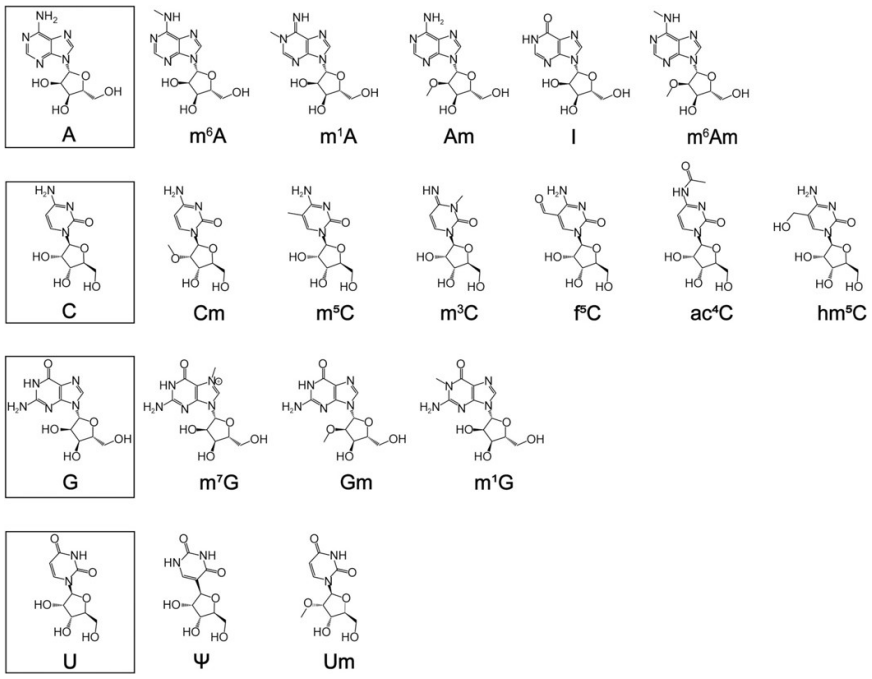

Figure 4 *Reported mRNA modifications.Unmodified nucleosides are shown in boxes, while the modified nucleosides are unboxed. The full names of the nucleosides are: A, adenosine; m6A, N6-methyladenosine; m1A, 1-methyladenosine; Am, 2'-O-methyladenosine; I, inosine; m6Am, N6, 2'-O-dimethyladenosine; C, cytidine; Cm, 2'-O-methylcytidine; m5C, 5-methylcytidine; m3C, 3-methylcytidine; f5C, 5-formylcytidine; ac4C, N4-acetylytidine; hm5C, 5-hydroxymethylcytidine; G, guanosine; m7G, 7-methylguanosine; Gm, 2'-O-methylguanosine; m1G, 1-methylguanosine; U, uridine; Ψ, pseudouridine; Um, 2'-O-methyluridine.*

Our best understanding of how mRNA modifications can influence gene expression comes from a long-standing body of work of inosine, and overlying the findings of transcriptome wide studies with genetic and biochemical investigations of m^6A [56,57]. Inosine can contribute to mRNA stability, splicing and translational recoding [58–64] . Similarly, the primary consequence of m^6A is mRNA degradation, though effects on transcript maturation and translation have also been reported [65–69] . Eukaryotes possess a series of "reader" and "eraser" proteins that bind m^6A-containing transcripts to mediate these effects [57,70–72] . Inosine prevalence and the conservation of m^6A reader proteins across a variety of eukaryotic species suggests that at least some modifications could contribute to biological function. Despite our in-depth knowledge of where mRNA modifications can exist and growing molecular level insight into inosine and m^6A function, we have a limited (or no) picture of the biological role for the other 14 reported mRNA modifications.

Establishing a quantitative, biochemical framework for understanding individual mRNA modifications to complement existing transcriptome wide datasets is one of the next milestones for the epitranscriptome field. In particular, measurements of the frequency (stoichiometry) of individual modification sites under a variety of cellular conditions and disease states will be required to determine which sites are the most biologically meaningful. Additionally, *in vitro* structural, thermodynamic and kinetic studies characterizing how interactions between proteins, ncRNAs, decay machinery, and the ribosome are changed by modified mRNAs will provide a deep understanding of how post-transcriptional modifications can influence protein production. Such work can also potentially reveal additional functions of modifications that might not be immediately obvious from correlative studies. Together, these data will enable us to critically

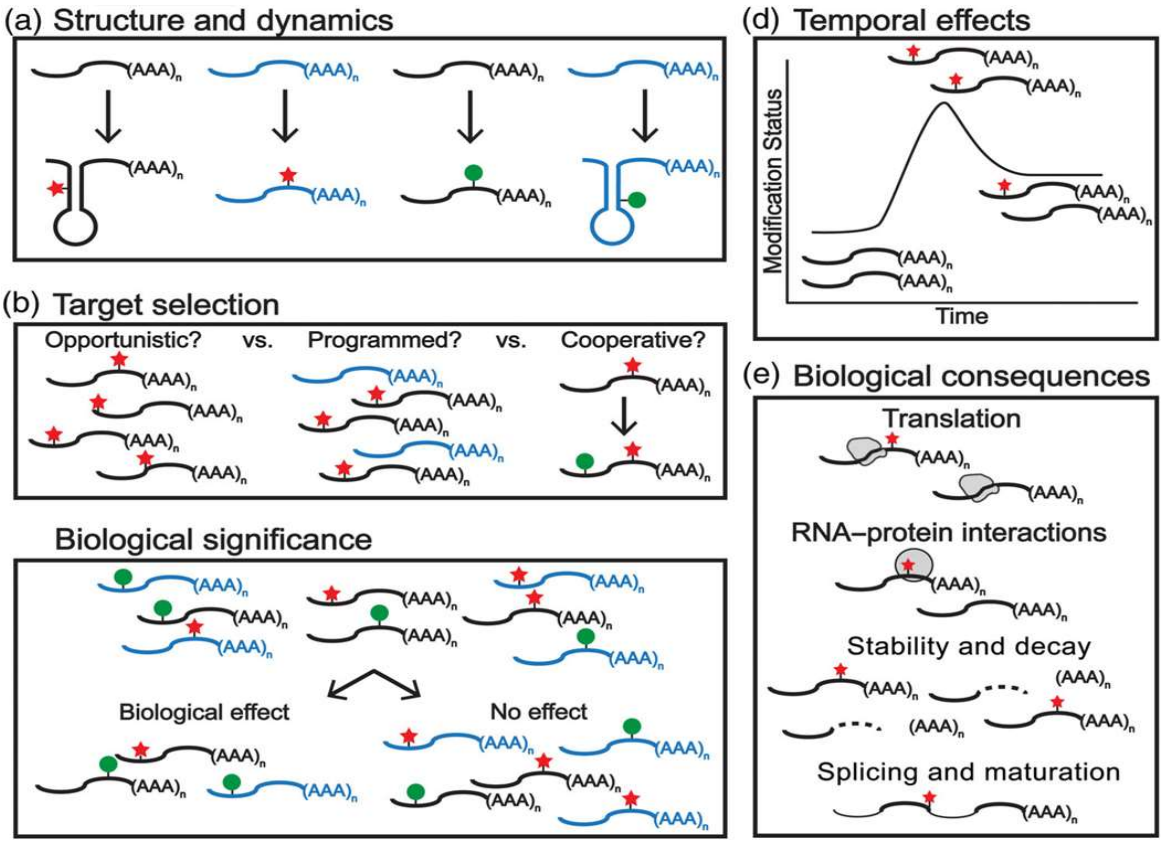

Figure 5 *Knowledge gaps. The implementation of quantitative approaches will allow us to critically assess some of the key questions in the epitranscriptome field and establish a molecular understanding of individual mRNA modificationsHere we present several knowledge gaps that we think can be best filled using quantitative approaches: (**A**) Several mRNA modifications, m6A, m1A, m1G, Ψ and f5C, affect the stability of RNA secondary structure, but limited knowledge is known about the effect of other chemical modifications [67,159–161,163]. High-resolution structural biology and structure-probing techniques are needed to uncover modification mediated structural changes. (**B**) Current transcriptome wide sequencing approaches have uncovered thousands of modification sites, but little is known about the modification insertion is modulated. Modifications could be randomly incorporated on available nucleotides, incorporated on specific locations of target transcripts, or there could be crosstalk between sites on a single transcript (cooperative incorporation). Kinetic and thermodynamic investigations of modifying enzyme selectivity and broad analyses of the contributions of structure to selectivity (as in ([29]), coupled with measurements of the stoichiometry of multiple modifications on individual transcripts can help to distinguish between these models. (**C**) Since most mRNA modifying enzymes incorporated modifications onto ncRNA, targeted approaches will be required to discern which mRNA modification sites are biologically relevant. Measurements of modification stoichiometry, and assessment of how the stoichiometry at individual sites varies as a function of cell cycle, environment and disease are one example of experiments that could be done to identify significant sites of modification. (**D**) Occupancy of individual sites might be temporally controlled and need to be quantitatively assessed as a function of time. Without this information it is likely that biologically relevant sites may be overlooked. (**E**) It is difficult to deconvolute the impact of mRNA modifications on mRNA-protein, mRNA stability, and mRNA translation on protein output in cells (see Figure 1). Reconstituted systems are ideally suited to overcome this challenge by allowing researchers to dissect how each individual interaction is influenced by mRNA modifications. These sorts of studies can help to establish which biological processes are likely more impacted by particular modifications and have the potential to suggest likely consequences of mRNA modifications.*

consider some of the key questions in the emerging epitranscriptome field – including assessing

the potential biological significance/insignificance of individual modifications and modification sites (Figure 3). Here we will discuss the pioneering studies starting to build a molecular foundation basis for characterizing the epitranscriptome. We will focus on studies of modifications other than inosine, as adenosine to inosine (A to I) editing has been extensively reviewed elsewhere [53,73].This review will emphasize the work conducted to quantify modification abundance, frequency of incorporation, and interactions with the cellular machinery.

2.2 Quantitative approaches for studying mRNA modification levels and consequences

We will begin by presenting and contextualizing some of the most quantitative approaches that have been used to characterize mRNA incorporation levels and interactions with the cellular machinery.

2.2.1 Liquid chromatography with tandem mass spectrometry (LC-MS/MS) measures total modification abundance

The overall abundance of modifications is an important metric for gauging how broadly a particular modification might influence mRNAs. Sequencing strategies have provided deep insight into where mRNA modifications can be localized. However, sequencing based approaches cannot reliably report on absolute modification abundances because they rely heavily on the efficiency and specificity of the biochemical workflow as well as the bioinformatic parameters used to analyze the data (peak alignment, peak detection method, etc.) [74] . Direct methods, such as LC-MS/MS, are better suited to measure the overall abundance of modifications in mRNAs. LC-MS/MS is a well-established approach extensively utilized to quantify post-transcriptional

modifications in ncRNAs including tRNAs and rRNAs and is increasingly being applied to study mRNA modifications.

In order to measure modification levels by LC-MS/MS, mRNAs are purified and enzymatically hydrolyzed to mononucleosides [75–79]. The resulting nucleosides are separated using liquid chromatography (LC) and absolutely quantitated by mass spectrometry using multiple reaction monitoring with an internal standard. Early studies used LC-MS/MS to confirm the presence of mRNA modifications found by RNA-seq, but more recently researchers have begun to use LC-MS/MS to identify new modifications and modifying enzymes[36,37,80] . Additionally, high-throughput applications of LC-MS/MS for mRNA modification discovery and characterization are emerging, allowing researchers to rapidly explore a broad chemical space – similar to mass spectrometry studies of tRNA modifications that characterize dozens of nucleosides in parallel [36,37,79]. Nonetheless, the impact of current LC-MS/MS approaches is limited because they do not provide any sequence context for modified nucleosides and require large quantities of highly purified mRNA.

2.3 Approaches for measuring modification occupancy.

Determining the occupancy of discrete mRNA modification sites is imperative for uncovering the contributions of modifications to biological processes. If modifications serve as a gene regulatory mechanism, then the occupancy of controlled modification sites is likely to vary over the lifetime of an mRNA to alter its function (Figure 3). Transcriptome wide methodologies to measure site occupancy will allow us to form hypotheses about which modified sites may influence biological processes. This is especially true in the context of stress or diseased states, under which modification occupancy levels could dramatically fluctuate. Comparison of the absolute abundances of mRNA modifications with the number of possible sites of modification

indicates that the occupancy of most modification sites are likely sub-stoichiometric, similar to protein post-translational modifications [81].

The occupancy of individual sites can be measured using site-specific cleavage and radioactive-labeling followed by ligation-assisted extraction and thin-layer chromatography (SCARLET)[82]. SCARLET uses complementary oligos targeted to known modification sites to investigate the occupancy of the modification at discrete sites. This method takes advantage of the different chemical properties of modified and unmodified nucleosides - using TLC to separate radioactively labeled modified/unmodified RNA species in a manner that enables the quantification of the relative modification frequency (described in detail in Figure 4). Notably, because SCARLET does not rely on the specific recognition of a modification by an antibody or nuclease, it can be applied to all modifications. While SCARLET is a highly accurate method for quantifying the extent of modification incorporation in mRNAs, it requires researchers to know where modification sites exist, can only assess a single site at a time, and is challenging to implement. As such, despite being the first and arguably most reliable method of quantifying mRNA modification occupancy, SCARLET has only been applied to study a handful of m^6A sites, and a single Ψ-modified mRNA [83–88] .

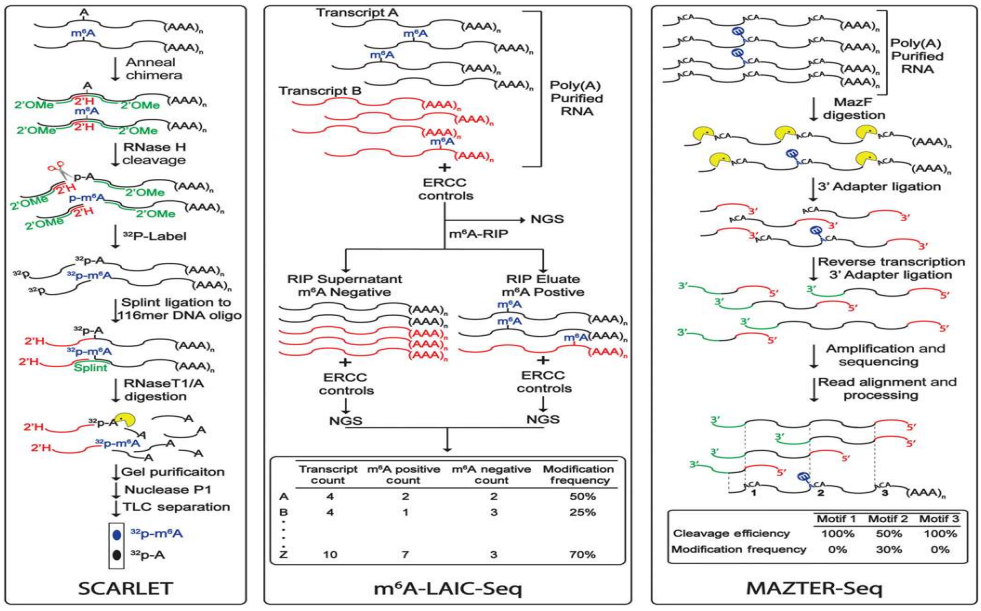

Figure 6 *Methods to quantify messenger RNA (mRNA) m6A modification stoichiometry.* ***(A)*** *Site-specific cleavage and radioactive-labeling followed by ligation-assisted extraction and thin-layer chromatography (SCARLET) is most direct method developed to quantify m^{6}A frequency(N. Liu et al., 2013). During this process, a chimera is annealed to a specific mRNA where the DNA sequence is immediately upstream of the putative modification site. RNase H is used to cleave the mRNA to release an oligonucleotide containing the putative modification at the 5'-end. The 5'-end of the oligonucleotide is ^{32}P-labeled using T4 polynucleotide kinase and is splint ligated to a 116mer DNA oligomer. RNase T1/A is used to digest the resulting chimera to contain a single A or m^{6}A at the 3'-end of the 116mer DNA oligomer. The resulting oligonucleotide is gel purified, digested to nucleosides using nuclease P1, and analyzed using TLC. The stoichiometry is measure based on the relative intensity of the m^{6}A and A phosphorescence.* ***(B)*** *m^{6}A-level and isoform-characterization sequencing (m^{6}A-LAIC-seq)[91] utilizes m^{6}A modified ERCC control RNAs to normalize the measured m^{6}A stoichiometries to increase the accuracy of a standard m^{6}A-RIP assay. ERCC controls are added before and after m^{6}A-RIP to normalize the efficiency of the immunoprecipitation and detection by next generation sequencing, respectively. The relative counts of m^{6}A positive and negative reads of the same transcript determine the stoichiometry. The occupancy levels measured by m^{6}A-LAIC-seq correlate well with modification levels of mRNA standards (R = 0.995) despite the lack of single nucleotide resolution.* ***(C)*** *MAZTER-seq also utilizes RNA-seq to characterize m^{6}A occupancy transcriptome wide (Garcia-Campos et al., 2019). However, MAZTER-seq does not rely on immunoprecipitation to isolate modified mRNAs, and instead identifies sites using the bacterial nuclease MazF to cleave immediately upstream of ACA sequences but not m^{6}ACA sequences. Purified mRNA is digested using MazF, and an adapter is ligated to the 3'-end of the digested products. The resulting oligonucleotides are reverse transcribed, 3' adapter ligated, amplified, and end-pair sequenced. Following read alignment and data processing, the stoichiometry is determined by calculating the cleavage efficiency of MazF at a specific ACA motif. While MAZTER-seq has the advantage of quantifying m^{6}A occupancy at single nucleotide resolution, there are some limitations to this approach. Namely, the lack of quantification at the ~50% of m^{6}A found outside ACA motifs [164]sequences resembling ACA, and the values measured by MAZTER-seq modestly correlate with SCARLET measurements at similar sites (R values = 0.6-0.7)(Garcia-Campos et al., 2019)*

Reliable approaches for measuring the transcriptome wide occupancy of mRNA sites only exist for studying m^{6}A and inosine[89,90] . For the purposes of this review, we will focus on m^{6}A-related methods, m^{6}A-level and isoform-characterization sequencing (m^{6}A-LAIC-seq) and m^{6}A-sensitive RNA digestion and sequencing (MAZTER-seq) (Figure 4), as previously reviewed

inosine methods [46,89,91]. MAZTER-seq and m^{6}A-LAIC-seq use either an antibody or nuclease to identify modified sites in purified cellular RNA and synthetic mRNA controls. RNA-seq is used to measure the abundance of both mRNAs of interest and the controls to determine m^{6}A incorporation frequency. These methods, while powerful, both rely on indirect methods to detect the m^{6}A modification. The recent advent of direct nanopore ion sequencing technology may eventually permit researchers to directly measure the occupancy of all modifications on individual mRNA transcripts, but further advances in the computational analysis of nanopore data will be required before this approach can be widely implemented for this purpose [92].

2.4 Transcriptome wide studies of mRNA translation and half-life.

Sequencing based approaches have been used to assess both the half-life and translation of modified mRNAs transcriptome wide. Ribosome profiling is a powerful technique that allows researchers to take a snap-shot of where every ribosome sits on every mRNA in a cell at a given period of time [93]. This approach enables the identification of well- and poorly-translated sequences *in vivo*, and can even provide insight into how distinct states of translation elongation are modulated [94,95]. Similarly, the half-lives of all cellular mRNAs can be measured in parallel by using RNA-seq to observe the time-dependent reductions in mRNA levels following transcriptional shut-off by small molecules, such as actinomycin, or temperature sensitive RNA Polymerase II mutants[96]. Ribosome profiling and transcriptome wide half-life measurements robustly report on the details of mRNA stability and translation and have greatly advanced our understanding of RNA biology.

Utilizing ribosome profiling and transcriptome wide decay studies to discern the function of a specific modification would ideally involve knocking-out (or knocking-down) an mRNA modifying enzymes and comparing the translation and stability of modified and unmodified

mRNAs. It is important to note that ribosome profiling and transcriptome wide half-life studies report on the average behavior of the overall population of mRNA transcripts containing a given sequence. Therefore, the heterogeneity of modification occupancy introduces challenges for interpreting data collected by these methods. The analysis of such data is further complicated by the fact that most enzymes that catalyze mRNA modification also catalyze the incorporation of the same functional groups into non-coding RNA species essential to protein translation (e.g. tRNAs, ribosomal RNA (rRNA))[28,34,36,37,52,83]. Since translation and decay rates are coupled, these potential perturbations to the translation machinery can make complicate efforts to deconvolute the impacts of modifications on non-coding RNAs from those on mRNAs by these methods (Figure 1)[97,98]. Regardless of their limitations, ribosome profiling and transcriptome wide mRNA half-life studies will be useful for uncovering how mRNA modifications change translation and mRNA stability, and we anticipate that interpretation of transcriptome wide observations will ultimately benefit from synergistic *in vitro* studies.

2.5 In vitro biochemistry and structural biology.

For over seventy years high-resolution structural and functional studies with purified components have proven invaluable for our understanding of how biology controls the production, function and degradation of biomolecules. Relative to proteins, much less is known about the structures of RNAs, as evidenced by the fact that structures of RNA and RNA-protein complexes represent < 5% of the structures deposited in the Protein Data Bank (PDB)[99]. High resolution X-ray crystallography, cryo-EM and NMR studies of modified mRNAs, modified mRNA-protein, and modified mRNA-ribosome complexes will be vital for building a detailed understanding of how modifications can influence mRNA structure[68,100–102]. Additionally, lower resolution RNA-structure mapping studies comparing modified and unmodified mRNAs can provide

additional insights information about how the shape of mRNAs is influenced by modifications[103]. Structural studies will prove useful not only for understanding fundamental properties of mRNA modifications, but also as researchers are seeking to develop therapeutics targeting m^6A-modified transcripts[104].

Changes in mRNA structure, charge, or base-pairing ability can be expected to alter the interaction of these molecules with other biomolecules. Therefore, *in vitro* kinetic and thermodynamic assays will be required to establish how modifications alter mRNA interactions with proteins, other RNAs, or the ribosome [100,101,105] . Such studies are limited in their scale but have the benefit of being readily interpretable. For example, *in vitro* translation assays on modified mRNAs have been used to directly report on how modifications alter the action of the translation machinery in a straightforward manner, without the needing to consider in rRNA or tRNA modification status or mRNA stability. Single molecule and bulk transient kinetic studies will allow us establish how individual functional groups affect specific steps in the translation kinetic pathway[100,101,106]. Given the critical contributions of fundamental biochemical and structural studies to our understanding essential biological processes, including post-translational protein modifications, we anticipate that such studies will be vital as researchers begin to understand the types and extent of consequences of mRNA modifications on biology.

2.6 Current quantitative perspective on mRNA modifications.

To evaluate the significance of post-transcriptional mRNA modifications there are several fundamental questions that remain to be critically investigated (detailed in Figure 3). Here we discuss how quantitative measurements are allowing researchers to begin addressing some of the key gaps in our knowledge of mRNA modifications. We will examine the available quantitative measurements of mRNA modification levels and incorporation frequency and consider these

findings in the context of post-translational protein modification stoichiometries. Additionally, we will discuss the insights into how mRNA modifications impact interactions between mRNAs and the cellular machinery provided by structural biology, *in vitro* biochemistry, and quantitative transcriptome wide studies. Together, these data suggest that several mRNA modifications are reasonably abundant and can influence how proteins and the ribosome interact with transcripts.

2.7 mRNA modification abundance and frequency

As we begin to investigate the consequences and potential biological functions of mRNA modifications it seems reasonable to first consider where and how frequently they are present. The levels of different mRNA modifications vary widely; there is a > 1,000-fold range in concentrations for the mRNA modifications levels measured to date (Table 1 and Figure 5). m^6A is the most abundant modification across all organisms (Table 1), as might be expected given its purported widespread role in the post-transcriptional regulation of a host of mRNAs. SCARLET, m^6A-LAIC-seq and MAZTER-seq established a wide range of m^6A frequencies (0-95%) at mapped sites [46,83–86,88] . Transcriptome wide analyses of m^6A site occupancies revealed a nearly bimodal distribution of m^6A frequency (centered around ~10% and 50-60%), and demonstrate that m^6A modification frequencies differ on the same transcripts between GM12878, HEK293T and hESC cells. m^6A modifications are enriched in mRNA 3' UTRs and near stop codons, and further analysis of the m^6A occupancies of these different mRNA regions might be useful[45,49]. Regardless of where they are localized, these data suggest that m^6A sites are essentially never fully occupied on any given transcript, making it unlikely that modifications serve as a binary switch to dictate the maturation, movement or behavior of the entirety of mRNA molecules of any particular sequence.

Several modifications, Ψ, ac^4C, Cm, and Gm, have abundances approaching those of m^6A[28,36,83,107]. These modifications have been less well studied than m^6A, but their prevalence and localization in mRNA coding regions suggests that they might also play roles in regulating mRNA function[28,29,33,34,83,107–109]. Little is known about how often modifications other than m^6A or inosine are incorporated at particular mRNA sites. However, estimates of Ψ-frequency based on Ψ-seq experiments suggest that Ψ incorporated into mRNA by pseudouridine synthase 7 (Pus 7) is present at high levels; with a distribution occupancy comparable to ribosomal RNA (rRNA) levels[34]. Furthermore, SCARLET measurements of Ψ occupancy in EEF1A1 mRNA are consistent with this conclusion - Ψ is present in 56% of the time in this transcript, a frequency comparable to many of the reported m^6A and inosine sites [83,89]Together these data suggest that the incorporation frequency of Ψ, at least at some sites, is likely to be high.

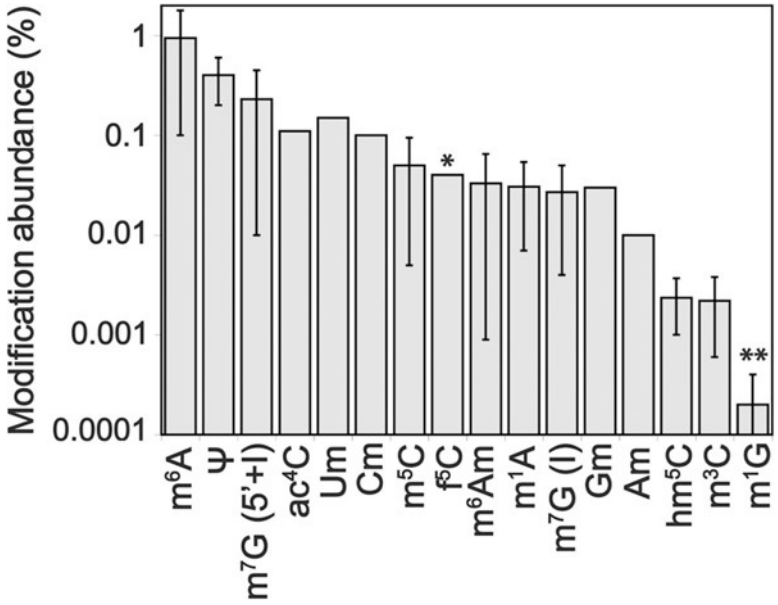

Figure 7 *LC–MS/MS measurements of mRNA modification abundance.LC-MS/MS measurements of modification abundance. All values displayed are the average values for mammals unless indicated otherwise (* f^5C, ** m^1G) (Table 1). The error bars reflect the range of values measured. Modifications without error bars have only one reported value in the literature.*

Most modifications are present at levels 10- to 100-fold less than m^6A, and a handful of modifications (m^3C, m^1G, hm^5C) are even more rare, with levels at least 500-fold lower than m^6A (Figure 5, Table 1). The location of m^5C modifications have been mapped primarily to mRNA 5' UTRs, and the relative occupancy of m^5C sites has also been estimated using a stringent bisulfite

sequencing method[40,110]. While incomplete conversion of cytidine and m^5C during bisulfite treatment limits the accurate quantification and location of m^5C throughout the transcriptome, control RNAs were utilized to tune treatment conditions and approximate m^5C modification frequency ($R^2 = 0.98$) and location. This study suggests that m^5C occupancy at most sites is low (< 20 %) relative to m^6A and Ψ, as might be expected from the modest levels of m^5C measured in mRNAs by LC-MS/MS (Figure 5). The modest levels of the majority of modifications suggest that the enzymes responsible for these modifications likely either target only a handful of specific mRNAs targets, as studies indicate is the case for m^1A, or might modify many different mRNAs at relatively low frequencies[111,112]. Alternatively, it is possible that the levels of these modifications have just not been measured yet under conditions where the modification is most highly incorporated. We expect to find other relatively rare mRNA modifications, such as m^3C and m^1G, may also exhibit low occupancy at many (though perhaps not all) of their sites.

It is important to note that just because sites are not well occupied in a given transcriptome wide snapshot, this does not necessarily mean that they are insignificant. Post-translational modifications (PTMs) are also typically sub-stoichiometric, and their frequency varies from site to site and in response to cellular conditions[81]. For example, protein acetylation occurs at a wide range of stoichiometries (< 1- 98%), with bulk of protein acetylation sites exhibiting very low modification frequencies (< 1%)[113–115]. In contrast, sites of phosphorylation tend to be occupied at a modestly higher levels (> 20%)[116–119], while N-glycosylation sites are frequently occupied (> 60%)[109,120]. Despite the wide distribution of PTM stoichiometries, they each significantly impact the regulation of protein biology. This highlights the need to extensively characterize mRNA modifications despite the sub-stoichiometric modification of sites.

Furthermore, occupancy of sites might be temporally controlled so that they are only impactful at a particular time (Figure 3D). In ncRNAs, nucleoside levels dynamically fluctuate in response to environmental stress, nutrient deprivation, stages in circadian rhythms, and cell cycle progression to alter RNA function[74,121–124]. Analysis of mRNA modification abundances under different conditions may provide insight into modification-mediated mechanisms activated by environmental stress or disease. Consistent with this possibility, both the abundances and distributions of mRNAs modifications are dependent on environmental conditions, cell-type, disease, and organism (Table 1)[18,29,34,36,80,83,85,125]. Nucleoside methylations and acetylation exhibit the largest changes in mRNA modification abundance as a result of shifting cellular environments[36]. In line with this observation, the metabolites used by enzymes to catalyze methyl- and acetyl- modifications (S-adenosylmethionine and acetyl-CoA) also fluctuate significantly in response to cellular conditions[72,126,127]. Comprehensive studies of modification frequency under varied cellular conditions, disease states, and time-points will be necessary to uncover this information and link sites more directly to function (Figure 3C and D).

2.8 Consequences of mRNA modifications on translation

The functional roles of mRNAs in the cell is to serve as blueprints for protein synthesis. As such the translational machinery surely encounters modified mRNAs. Most mRNA modifications have been observed throughout mRNAs, and the preponderance of Ψ, ac^4C and 2'O-methyl modifications are found in mRNA coding regions[8,28,29,34,107,108,128]. Modifications

have the potential to change how the ribosome interprets the mRNA blueprint because

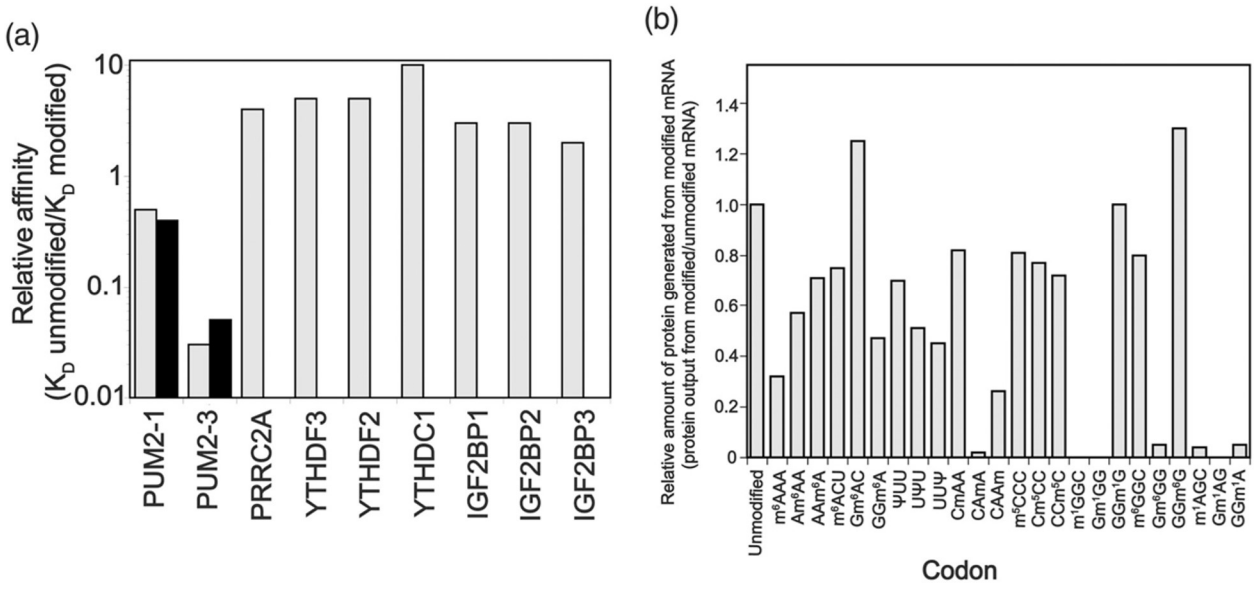

Figure 8 *mRNA-binding protein affinities are modestly altered by nucleoside modifications.* ***(A)*** *The ratio of binding affinities (K_D) for proteins binding to m^6A (gray bars) and Ψ (black bars) modified and unmodified mRNA transcripts binding to a Pumilio proteins (PUM2), and the m^6A binding proteins proline rich coiled-coil 2A (PRRC2A), YTHDF3, YTHDF2, YTHDC1, and insulin-like factor 2 mRNA binding proteins 1,2, and 3 (IGF2BP1, IGF2BP2, IGF2BP3) [95,105,110,165] The affinity of PUM2 was measured for model mRNAs containing 1 (PUM2_1) or 3 (PUM2_3) modifications.* ***(B)*** *Reporter proteins were expressed from mRNAs containing a single nucleotide modification in commercially available fully-reconstituted bacterial translation assays. The plot displays the amount of protein produced in from the modified mRNA relative to an unmodified transcript as a function of codon. The values in this table were from studies by [13,137,140]The magnitude of each modification's effect is depends not only on the identity of the modification, but also on the codon in which it is located, the position of the modification within that codon.*

modifications can alter the hydrogen bonding interactions between codons and aminoacylated-tRNAs. This possibility is supported by decades of observations indicating that tRNA anti-codon nucleobase modifications alter mRNA:tRNA interactions to influence ribosome speed and fidelity[129–134]. However, deciphering the impact of mRNA modifications on translation in biological systems has been challenging for a number of reasons. Foremost amongst these is the fact that most enzymes that catalyze mRNA modification also catalyze the incorporation of the same functional groups into non-coding RNA species essential to protein translation (e.g. tRNAs, ribosomal RNA (rRNA))[28,34,36,83,135]. The shared origin of many coding and non-coding RNA modifications has limited the utility of classical genetics to discern mRNA modification function. Furthermore, the heterogeneity in modification occupancy makes it difficult for

researchers to directly observe translation of modified transcripts *in vivo*. Lastly, it can be problematic to fully deconvolute the impact of translation from protein- and mRNA-stability on protein output in cells. Illustrative of this, reporter-based studies have reached conflicting conclusions regarding how several modifications influence translation[13,31,102,136–138]. Therefore, for the purpose of this review, we will focus on discussing *in vitro* studies with reconstituted translation systems that offer a way to directly assess how modifications impact ribosome function.

Initial *in vitro* studies of varying resolution on a limited set of mRNA modifications indicated that they can alter the overall rate and fidelity of protein synthesis[13,100,101,106,107,137,139]. In fully reconstituted *E. coli* translation systems, naturally occurring nucleoside enzymatic modifications and damaged ribonucleobases appear to change translation to varying degrees (Figure 6A). In the context of reporter peptides containing a single modified nucleobase (m^6A, Ψ, m^5C, m^1G, m^6G, m^1A, Cm, and Am) the overall level of protein production is reduced by 2 to > 50 fold for m^6A, Ψ, Cm, Am, m^1A, m^6G and m^1G, and is essentially unchanged for m^5C [13,140].The severity of the protein expression defect is highly dependent on the location of the modification within a codon, with the effect of modfications on protein output ranging by > 25-fold within a single codon[13,140]. The effects observed in *E. coli* have been recapitulated in eukaryotic wheat germ extract translation assays, where m^6A, m^1A, m^6G and m^1G were shown to reduce the production of a reporter peptide in a position dependent manner[140]. Notably, in contrast to findings in *E. coli*, m^6G also appeared to both impede and enhance protein output in wheat germ extacts depending on where it was localized within a modified codon.

Further elegant bulk and single-molecule mechanistic investigations of 2' O-methyl, m^6A, Ψ and m^6G modifications reveal that they impact multiple steps in the ribosome kinetic pathway, reducing the rate of peptide bond formation and GTP hydrolysis by EF-Tu [100,101,106,139]2' O-methylmodifications and m^6A have been further shown to impede tRNA accomodation – a crucial step in translation elongation[100,106]. Crystal structures of the 30S *T. thermophilus* ribosome bound to m^6A-modified mRNAs, and the 70S ribosome on a Ψ-modified mRNA indicate that m^6A and Ψ can still form watson-crick base-pairs with cognate tRNAs[100,101]. The structure of the 70S ribosome with $tRNA^{Phe}$ bound to ΨUU in the A site further demonstrates that despite the presence of correct mRNA:tRNA base-pairing interactions, the 3' CCA of $tRNA^{Phe}$ is properly positioned in the peptidyl-transfer center (PTC) of the ribosome, consistent with the kinetic observations suggesting that Ψ changes translation[101]. Together, these studies indicate that mRNA modifications tend to slow the ribosome as a result of changing steps in translation where mRNA:tRNA hydrogen bonding interactions are particularly critical. Furthermore, they indicate that the magnitude to which a modification perturbs translation depends strongly on the sequence context of the modification.

Ribosome profiling studies have reached slightly different conclusions regrding how modifications impact translation. These studies suggest that m^1A slows translation, and that m^6A and ac^4C enhance translation efficiency [28]. There could be several reasons for the differing conclusions reached by ribosome profiling and *in vitro* studies including modification reader proteins in the cell altering translation, and, given the substoichiometric occurance of mRNA modifications, the possibility that the population of mRNAs being well-translated might lack the targeted modification. Further work will need to be done to reconcile the relationship between the differing observations between *in vitro* and ribosome profiling studies.

Since modifications can alter the fundamental properties of RNAs, including their secondary structures and base-pairing abilities, it has been proposed that one consequence of mRNA modification could be to promote the incorporation of multiple amino acids on a single codon. Establishing if modifications alter tRNA selection on the ribosome is a timely question given that a wide range of modified nucleosides (Ψ, N1-methyl- Ψ, 2-thiouridine, 5-methyl-cytosine) are being routinely inserted into synthetic mRNAs at high stoichiometric ratios for therapeutic applications[141]. Multiple studies indicate that this is indeed possible for m^5C, m^1G, I, Ψ and m^6G, but not for m^1A and m^6A[13,60,61,101,139]. Similar to their effects on translation rate, the magnitude of the decoding errors is highly dependent on the position of a modified within a codon. Notably, the positions of some modifications appear to be conserved – for example Ψ is most commonly found in the 2nd and 3rd position of UUU and 2nd position of UUC codons in protozoa, plant and human mRNA coding regions[34,108,109]. Additionally, Ψ-containing stop codons have been observed to direct the nonsense suppression of translation termination in both bacteria and yeast [13,137,138,142], though the impact of Ψ in stop codons remains an unresolved question, as a follow-up studies have not recapitulated these effects [101,102,137].

Taken together, there is a growing body of *in vitro* translation and ribosome profiling studies suggesting that mRNA modifications have the ability to influence both the rate and fidelity of translation. How these alterations contribute to biology still remains to be established. Even if mRNA modifications are not used to directly regulate translation, their impact on translation may still have consequences for biological systems, for example under stress conditions where increased levels of amino acid substitution have been shown to increase cellular fitness[129,130,134]. Further work will need to be done to determine the differential effects of individual modifications on the translation mechanism, and identify situations (e.g. times in the

cell cycle, environmental stress, or disease) in which more somewhat subtle impacts on translation could contribute to cellular health.

2.9 mRNA-protein interactions modifications

In addition to understanding how mRNA modifications impact translation, gaining quantitative insight into the extent that modifications modulate mRNA-protein interactions is also important to establish because RNA binding proteins can control the processing, localization, and stability of mRNAs. Modulation of mRNA-protein interactions has the potential to be biologically significant because many RNA binding proteins interact with a multiple mRNA sequences and even small perturbations in affinity have the potential to shift the cellular environment, and thus fate, of a host of mRNAs[70,143–148]. Immunoprecipitation, pull-down, mass-spectrometry and RNA-seq approaches have begun to identify proteins whose interactions with mRNAs are mediated by modifications. These studies reveal that m^6A, m^1A and m^5C are specifically recognized by proteins that can either read or erase modifications to alter mRNA translation, localization, and stabilization (reviewed in [14,15,52,57,82,83,128,149]. To date, no 'readers' or 'erasers' of other mRNA modifications have been reported.

Modifications appear to modulate of mRNA stability, suggesting that they impact, either directly or indirectly, interactions between mRNAs and the RNA degradation machinery. Notably, different modifications fine-tune stability in different directions – m^6A generally decreases stability, while ac^4C, Ψ and m^5C tend to increase mRNA half-life[24,28,65,108,141]. It is not entirely clear precisely how this is accomplished, though the observation that the YTHDC2 m^6A reader interacts with the major 5'→3' exonuclease involved in mRNA decay, Xrn1, suggests that

interactions between modified mRNAs and components of the mRNA degradation pathway may, at least sometimes, be facilitated by modification binding proteins[150].

Despite the discovery of several proteins that interact with modified mRNAs, the extent to which modifications alter mRNA-protein interactions is less clear. Thermodynamic dissociation constants (K_D) have only been measured for a handful of the proteins reported to bind modified mRNAs (examples in Figure 5B). Initial studies of modified mRNA-protein interactions demonstrate that m^6A and Ψ can both enhance and weaken RNA-protein interactions by ~2-20 fold (Figure 6B). Members of the YTH-family of m^6A 'reader' proteins appear to discriminate between methylated/unmethylated transcripts to a higher level (5-20 fold) than other mRNA binding proteins (2-4 fold) (Figure 6B). Interestingly, these studies find modifications only induce relatively modest changes in protein affinities for mRNAs. This suggests that modifications could be more likely to subtly, rather than drastically, shift the balance and identity of cellular mRNA-protein pools.

2.10 Outlook

The epitranscriptome field is quickly opening a new chapter, advancing through modification discovery to investigate the biological roles and mechanisms of a broad set of mRNA modifications. The ground-breaking investigations that established this burgeoning field of study relied heavily on sequencing-based tools to map the location of discrete modifications across all RNAs in a cell. Such studies were a vital first step for the field to establish the existence and pervasiveness of mRNA modifications. More recently, researchers have begun skillfully mining transcriptome wide data sets to infer the biological function of modifications. The next horizon for the emerging mRNA modification field is to establish a molecular level view of how modifications change interactions between mRNAs and the cellular machinery. A detailed understanding of the

consequences of modifications will be greatly enhanced by the biochemical characterization of individual cellular components and how they interact. The quantitative data generated from such experiments (e.g. affinities, on and off rates, reaction rates, etc.) will facilitate the interpretation of existing and future transcriptome wide studies, as they will provide parameters for the mRNA modification community to refine their models of modification function.

Structural biology and reductionist biochemistry approaches will provide more than mechanistic details – they have the potential to generate new insights into the function of modifications that could not be immediately derived by correlative studies. These techniques can answer temporal questions, allow us to identify highly-occupied modification sites, determine how specificity or promiscuity of modifying enzymes determines target selection, and directly assess how they change interactions with the translation and decay machinery (Figure 3). The ability to compare interactions of fully modified/unmodified mRNAs with purified components will be particularly valuable in light of the challenges of interpreting transcriptome wide mapping, half-life and ribosome profiling data for heterogenous populations of sub-stoichiometrically modified mRNAs. Furthermore, the fact that mRNA modifying enzymes also target ncRNAs further complicates these analyses by making it difficult to study the impact of removing an mRNA modification without generally perturbing the cellular protein translation machinery. The initial quantitative studies described in this review demonstrate how biochemistry can reveal aspects of RNA-protein and mRNA-ribosome interactions that are masked by other approaches. The continued integration of quantitative, reductionist approaches combined and transcriptome wide studies will ultimately be required to identify the biological consequences of the epitranscriptome.

2.11 References

[1] Cohn WE, Volkin E. Nucleoside-5′-Phosphates from Ribonucleic Acid. Nature 1951;167:483–4. https://doi.org/10.1038/167483a0.

[2] Davis FF, Allen FW. RIBONUCLEIC ACIDS FROM YEAST WHICH CONTAIN A FIFTH NUCLEOTIDE. Journal of Biological Chemistry 1957;227:907–15. https://doi.org/10.1016/S0021-9258(18)70770-9.

[3] Helm M, Alfonzo JD. Post-transcriptional RNA modifications: Playing metabolic games in a cell's chemical legoland. Chem Biol 2014;21:174–85. https://doi.org/10.1016/j.chembiol.2013.10.015.

[4] Perry RP, Kelley DE. Existence of methylated messenger RNA in mouse L cells. Cell 1974;1:37–42. https://doi.org/10.1016/0092-8674(74)90153-6.

[5] Perry RP, Kelley DE, Friderici K, Rottman F. The methylated constituents of L cell messenger RNA: Evidence for an unusual cluster at the 5′ terminus. Cell 1975;4:387–94. https://doi.org/10.1016/0092-8674(75)90159-2.

[6] Desrosiers R, Friderici K, Rottman F. Identification of Methylated Nucleosides in Messenger RNA from Novikoff Hepatoma Cells. Proc Natl Acad Sci U S A 1974;71:3971–5.

[7] Morse DP, Bass BL. Detection of Inosine in Messenger RNA by Inosine-Specific Cleavage. Biochemistry 1997;36:8429–34. https://doi.org/10.1021/bi9709607.

[8] Nachtergaele S, He C. The emerging biology of RNA post-transcriptional modifications. RNA Biol 2016;14:156–63. https://doi.org/10.1080/15476286.2016.1267096.

[9] Paul MS, Bass BL. Inosine exists in mRNA at tissue-specific levels and is most abundant in brain mRNA. EMBO J 1998;17:1120–7. https://doi.org/10.1093/emboj/17.4.1120.

[10] Frye M, Harada BT, Behm M, He C. RNA modifications modulate gene expression during development. Science 2018;361:1346–9. https://doi.org/10.1126/science.aau1646.

[11] Gilbert WV, Bell TA, Schaening C. Messenger RNA modifications: Form, distribution, and function. Science 2016;352:1408–12. https://doi.org/10.1126/science.aad8711.

[12] Gilbert WV, Bell TA, Schaening C. Messenger RNA modifications – Form, distribution, and function. Science 2016;352:1408–12. https://doi.org/10.1126/science.aad8711.

[13] Hoernes TP, Clementi N, Faserl K, Glasner H, Breuker K, Lindner H, et al. Nucleotide modifications within bacterial messenger RNAs regulate their translation and are able to rewire the genetic code. Nucleic Acids Res 2016;44:852–62. https://doi.org/10.1093/nar/gkv1182.

[14] Peer E, Rechavi G, Dominissini D. Epitranscriptomics: regulation of mRNA metabolism through modifications. Curr Opin Chem Biol 2017;41:93–8. https://doi.org/10.1016/j.cbpa.2017.10.008.

[15] Roundtree IA, Evans ME, Pan T, He C. Dynamic RNA Modifications in Gene Expression Regulation. Cell 2017;169:1187–200. https://doi.org/10.1016/j.cell.2017.05.045.

[16] Saletore Y, Meyer K, Korlach J, Vilfan ID, Jaffrey S, Mason CE. The birth of the Epitranscriptome: deciphering the function of RNA modifications. Genome Biology 2012;13:175. https://doi.org/10.1186/gb-2012-13-10-175.

[17] Angelova MT, Dimitrova DG, Dinges N, Lence T, Worpenberg L, Carré C, et al. The Emerging Field of Epitranscriptomics in Neurodevelopmental and Neuronal Disorders. Front Bioeng Biotechnol 2018;6:46. https://doi.org/10.3389/fbioe.2018.00046.

[18] Cui Q, Shi H, Ye P, Li L, Qu Q, Sun G, et al. m 6 A RNA Methylation Regulates the Self-Renewal and Tumorigenesis of Glioblastoma Stem Cells. Cell Reports 2017;18:2622–34. https://doi.org/10.1016/j.celrep.2017.02.059.

[19] De Jesus DF, Zhang Z, Kahraman S, Brown NK, Chen M, Hu J, et al. m6A mRNA Methylation Regulates Human β-Cell Biology in Physiological States and in Type 2 Diabetes. Nat Metab 2019;1:765–74. https://doi.org/10.1038/s42255-019-0089-9.

[20] Fustin J-M, Kojima R, Itoh K, Chang H-Y, Ye S, Zhuang B, et al. Two Ck1δ transcripts regulated by m6A methylation code for two antagonistic kinases in the control of the circadian clock. Proc Natl Acad Sci U S A 2018;115:5980–5. https://doi.org/10.1073/pnas.1721371115.

[21] Haussmann IU, Bodi Z, Sanchez-Moran E, Mongan NP, Archer N, Fray RG, et al. m6A potentiates Sxl alternative pre-mRNA splicing for robust Drosophila sex determination. Nature 2016;540:301–4. https://doi.org/10.1038/nature20577.

[22] Jia G, Fu Y, Zhao X, Dai Q, Zheng G, Yang Y, et al. N6-Methyladenosine in Nuclear RNA is a Major Substrate of the Obesity-Associated FTO. Nat Chem Biol 2011;7:885–7. https://doi.org/10.1038/nchembio.687.

[23] Lin S, Choe J, Du P, Triboulet R, Gregory RI. METTL3 promotes translation in human cancer cells. Mol Cell 2016;62:335–45. https://doi.org/10.1016/j.molcel.2016.03.021.

[24] Sibbritt T, Patel HR, Preiss T. Mapping and significance of the mRNA methylome. Wiley Interdiscip Rev RNA 2013;4:397–422. https://doi.org/10.1002/wrna.1166.

[25] Yoon K-J, Ringeling FR, Vissers C, Jacob F, Pokrass M, Jimenez-Cyrus D, et al. Temporal Control of Mammalian Cortical Neurogenesis by m6A Methylation. Cell 2017;171:877-889.e17. https://doi.org/10.1016/j.cell.2017.09.003.

[26] Zhang C, Samanta D, Lu H, Bullen JW, Zhang H, Chen I, et al. Hypoxia induces the breast cancer stem cell phenotype by HIF-dependent and ALKBH5-mediated m6A-demethylation of NANOG mRNA. Proc Natl Acad Sci U S A 2016;113:E2047–56. https://doi.org/10.1073/pnas.1602883113.

[27] Zhong X, Yu J, Frazier K, Weng X, Li Y, Cham CM, et al. Circadian Clock Regulation of Hepatic Lipid Metabolism by Modulation of m6A mRNA Methylation. Cell Rep 2018;25:1816-1828.e4. https://doi.org/10.1016/j.celrep.2018.10.068.

[28] Arango D, Sturgill D, Alhusaini N, Dillman AA, Sweet TJ, Hanson G, et al. Acetylation of Cytidine in mRNA Promotes Translation Efficiency. Cell 2018;175:1872-1886.e24. https://doi.org/10.1016/j.cell.2018.10.030.

[29] Carlile TM, Rojas-Duran MF, Zinshteyn B, Shin H, Bartoli KM, Gilbert WV. Pseudouridine profiling reveals regulated mRNA pseudouridylation in yeast and human cells. Nature 2014;515:143–6. https://doi.org/10.1038/nature13802.

[30] Delatte B, Wang F, Ngoc LV, Collignon E, Bonvin E, Deplus R, et al. Transcriptome-wide distribution and function of RNA hydroxymethylcytosine. Science 2016;351:282–5. https://doi.org/10.1126/science.aac5253.

[31] Dominissini D, Nachtergaele S, Moshitch-Moshkovitz S, Peer E, Kol N, Ben-Haim MS, et al. The dynamic N1-methyladenosine methylome in eukaryotic messenger RNA. Nature 2016;530:441–6. https://doi.org/10.1038/nature16998.

[32] Huber SM, van Delft P, Mendil L, Bachman M, Smollett K, Werner F, et al. Formation and Abundance of 5-Hydroxymethylcytosine in RNA. Chembiochem 2015;16:752–5. https://doi.org/10.1002/cbic.201500013.

[33] Lovejoy AF, Riordan DP, Brown PO. Transcriptome-wide mapping of pseudouridines: pseudouridine synthases modify specific mRNAs in S. cerevisiae. PLoS One 2014;9:e110799. https://doi.org/10.1371/journal.pone.0110799.

[34] Schwartz S, Bernstein DA, Mumbach MR, Jovanovic M, Herbst RH, León-Ricardo BX, et al. Transcriptome-wide Mapping Reveals Widespread Dynamic-Regulated Pseudouridylation of ncRNA and mRNA. Cell 2014;159:148–62. https://doi.org/10.1016/j.cell.2014.08.028.

[35] Squires JE, Patel HR, Nousch M, Sibbritt T, Humphreys DT, Parker BJ, et al. Widespread occurrence of 5-methylcytosine in human coding and non-coding RNA. Nucleic Acids Res 2012;40:5023–33. https://doi.org/10.1093/nar/gks144.

[36] Tardu M, Jones JD, Kennedy RT, Lin Q, Koutmou KS. Identification and Quantification of Modified Nucleosides in Saccharomyces cerevisiae mRNAs. ACS Chem Biol 2019;14:1403–9. https://doi.org/10.1021/acschembio.9b00369.

[37] Xu L, Liu X, Sheng N, Oo KS, Liang J, Chionh YH, et al. Three distinct 3-methylcytidine (m3C) methyltransferases modify tRNA and mRNA in mice and humans. Journal of Biological Chemistry 2017;292:14695–703. https://doi.org/10.1074/jbc.M117.798298.

[38] Deng X, Chen K, Luo G-Z, Weng X, Ji Q, Zhou T, et al. Widespread occurrence of N6-methyladenosine in bacterial mRNA. Nucleic Acids Res 2015;43:6557–67. https://doi.org/10.1093/nar/gkv596.

[39] Kennedy EM, Courtney DG, Tsai K, Cullen BR. Viral Epitranscriptomics. J Virol 2017;91:e02263-16. https://doi.org/10.1128/JVI.02263-16.

[40] Amort T, Rieder D, Wille A, Khokhlova-Cubberley D, Riml C, Trixl L, et al. Distinct 5-methylcytosine profiles in poly(A) RNA from mouse embryonic stem cells and brain. Genome Biol 2017;18:1. https://doi.org/10.1186/s13059-016-1139-1.

[41] Motorin Y, Helm M. Methods for RNA Modification Mapping Using Deep Sequencing: Established and New Emerging Technologies. Genes (Basel) 2019;10:E35. https://doi.org/10.3390/genes10010035.

[42] Alon S, Garrett SC, Levanon EY, Olson S, Graveley BR, Rosenthal JJC, et al. The majority of transcripts in the squid nervous system are extensively recoded by A-to-I RNA editing. ELife n.d.;4:e05198. https://doi.org/10.7554/eLife.05198.

[43] Cui X, Liang Z, Shen L, Zhang Q, Bao S, Geng Y, et al. 5-Methylcytosine RNA Methylation in Arabidopsis Thaliana. Molecular Plant 2017;10:1387–99. https://doi.org/10.1016/j.molp.2017.09.013.

[44] Danecek P, Nellåker C, McIntyre RE, Buendia-Buendia JE, Bumpstead S, Ponting CP, et al. High levels of RNA-editing site conservation amongst 15 laboratory mouse strains. Genome Biol 2012;13:r26. https://doi.org/10.1186/gb-2012-13-4-r26.

[45] Dominissini D, Moshitch-Moshkovitz S, Schwartz S, Salmon-Divon M, Ungar L, Osenberg S, et al. Topology of the human and mouse m6A RNA methylomes revealed by m6A-seq. Nature 2012;485:201–6. https://doi.org/10.1038/nature11112.

[46] Garcia-Campos MA, Edelheit S, Toth U, Safra M, Shachar R, Viukov S, et al. Deciphering the "m6A Code" via Antibody-Independent Quantitative Profiling. Cell 2019;178:731-747.e16. https://doi.org/10.1016/j.cell.2019.06.013.

[47] Kim DDY, Kim TTY, Walsh T, Kobayashi Y, Matise TC, Buyske S, et al. Widespread RNA Editing of Embedded Alu Elements in the Human Transcriptome. Genome Res 2004;14:1719–25. https://doi.org/10.1101/gr.2855504.

[48] Levanon EY, Eisenberg E, Yelin R, Nemzer S, Hallegger M, Shemesh R, et al. Systematic identification of abundant A-to-I editing sites in the human transcriptome. Nat Biotechnol 2004;22:1001–5. https://doi.org/10.1038/nbt996.

[49] Meyer KD, Saletore Y, Zumbo P, Elemento O, Mason CE, Jaffrey SR. Comprehensive analysis of mRNA methylation reveals enrichment in 3' UTRs and near stop codons. Cell 2012;149:1635–46. https://doi.org/10.1016/j.cell.2012.05.003.

[50] Sakurai M, Yano T, Kawabata H, Ueda H, Suzuki T. Inosine cyanoethylation identifies A-to-I RNA editing sites in the human transcriptome. Nat Chem Biol 2010;6:733–40. https://doi.org/10.1038/nchembio.434.

[51] Li X, Xiong X, Zhang M, Wang K, Chen Y, Zhou J, et al. Base-resolution mapping reveals distinct m1A methylome in nuclear- and mitochondrial-encoded transcripts. Mol Cell 2017;68:993-1005.e9. https://doi.org/10.1016/j.molcel.2017.10.019.

[52] Yang X, Yang Y, Sun B-F, Chen Y-S, Xu J-W, Lai W-Y, et al. 5-methylcytosine promotes mRNA export — NSUN2 as the methyltransferase and ALYREF as an m5C reader. Cell Res 2017;27:606–25. https://doi.org/10.1038/cr.2017.55.

[53] Wang X, Li Z, Kong B, Song C, Cong J, Hou J, et al. Reduced m^6A mRNA methylation is correlated with the progression of human cervical cancer. Oncotarget 2017;8. https://doi.org/10.18632/oncotarget.22041.

[54] Yuan F, Bi Y, Siejka-Zielinska P, Zhou Y-L, Zhang X-X, Song C-X. Bisulfite-free and base-resolution analysis of 5-methylcytidine and 5-hydroxymethylcytidine in RNA with peroxotungstate †Electronic supplementary information (ESI) available. See DOI: 10.1039/c9cc00274j. Chem Commun (Camb) 2019;55:2328–31. https://doi.org/10.1039/c9cc00274j.

[55] Zhang X, Wei L-H, Wang Y, Xiao Y, Liu J, Zhang W, et al. Structural insights into FTO's catalytic mechanism for the demethylation of multiple RNA substrates. Proc Natl Acad Sci U S A 2019;116:2919–24. https://doi.org/10.1073/pnas.1820574116.

[56] Bajad P, Jantsch MF, Keegan L, O'Connell M. A to I editing in disease is not fake news. RNA Biol 2017;14:1223–31. https://doi.org/10.1080/15476286.2017.1306173.

[57] Schwartz S. Cracking the epitranscriptome. RNA 2016;22:169–74. https://doi.org/10.1261/rna.054502.115.

[58] Bazak L, Haviv A, Barak M, Jacob-Hirsch J, Deng P, Zhang R, et al. A-to-I RNA editing occurs at over a hundred million genomic sites, located in a majority of human genes. Genome Res 2014;24:365–76. https://doi.org/10.1101/gr.164749.113.

[59] Ferreira PG, Oti M, Barann M, Wieland T, Ezquina S, Friedländer MR, et al. Sequence variation between 462 human individuals fine-tunes functional sites of RNA processing. Sci Rep 2016;6:32406. https://doi.org/10.1038/srep32406.

[60] Garrett S, Rosenthal JJC. RNA Editing Underlies Temperature Adaptation in K+ Channels from Polar Octopuses. Science 2012;335:848–51. https://doi.org/10.1126/science.1212795.

[61] Licht K, Hartl M, Amman F, Anrather D, Janisiw MP, Jantsch MF. Inosine induces context-dependent recoding and translational stalling. Nucleic Acids Res 2019;47:3–14. https://doi.org/10.1093/nar/gky1163.

[62] Peng X, Xu X, Wang Y, Hawke DH, Yu S, Han L, et al. A-to-I RNA Editing Contributes to Proteomic Diversity in Cancer. Cancer Cell 2018;33:817-828.e7. https://doi.org/10.1016/j.ccell.2018.03.026.

[63] Ramaswami G, Zhang R, Piskol R, Keegan LP, Deng P, O'Connell MA, et al. Identifying RNA editing sites using RNA sequencing data alone. Nat Methods 2013;10:128–32. https://doi.org/10.1038/nmeth.2330.

[64] Rueter SM, Dawson TR, Emeson RB. Regulation of alternative splicing by RNA editing. Nature 1999;399:75–80. https://doi.org/10.1038/19992.

[65] Ke S, Pandya-Jones A, Saito Y, Fak JJ, Vågbø CB, Geula S, et al. m6A mRNA modifications are deposited in nascent pre-mRNA and are not required for splicing but do specify cytoplasmic turnover. Genes Dev 2017;31:990–1006. https://doi.org/10.1101/gad.301036.117.

[66] Pendleton KE, Chen B, Liu K, Hunter OV, Xie Y, Tu BP, et al. The U6 snRNA m6A Methyltransferase METTL16 Regulates SAM Synthetase Intron Retention. Cell 2017;169:824-835.e14. https://doi.org/10.1016/j.cell.2017.05.003.

[67] Wang R, Luo Z, He K, Delaney MO, Chen D, Sheng J. Base pairing and structural insights into the 5-formylcytosine in RNA duplex. Nucleic Acids Res 2016;44:4968–77. https://doi.org/10.1093/nar/gkw235.

[68] Xiao W, Adhikari S, Dahal U, Chen Y-S, Hao Y-J, Sun B-F, et al. Nuclear m6A Reader YTHDC1 Regulates mRNA Splicing. Molecular Cell 2016;61:507–19. https://doi.org/10.1016/j.molcel.2016.01.012.

[69] Zhao X, Yang Y, Sun B-F, Shi Y, Yang X, Xiao W, et al. FTO-dependent demethylation of N6-methyladenosine regulates mRNA splicing and is required for adipogenesis. Cell Res 2014;24:1403–19. https://doi.org/10.1038/cr.2014.151.

[70] Patil DP, Pickering BF, Jaffrey SR. Reading m6A in the transcriptome: m6A-binding proteins. Trends Cell Biol 2018;28:113–27. https://doi.org/10.1016/j.tcb.2017.10.001.

[71] Rajecka V, Skalicky T, Vanacova S. The role of RNA adenosine demethylases in the control of gene expression. Biochim Biophys Acta Gene Regul Mech 2019;1862:343–55. https://doi.org/10.1016/j.bbagrm.2018.12.001.

[72] Shi H, Wei J, He C. Where, When, and How: Context-Dependent Functions of RNA Methylation Writers, Readers, and Erasers. Mol Cell 2019;74:640–50. https://doi.org/10.1016/j.molcel.2019.04.025.

[73] Nishikura K. A-to-I editing of coding and non-coding RNAs by ADARs. Nat Rev Mol Cell Biol 2016;17:83–96. https://doi.org/10.1038/nrm.2015.4.

[74] Helm M, Motorin Y. Detecting RNA modifications in the epitranscriptome: predict and validate. Nature Reviews Genetics 2017;18:275–91. https://doi.org/10.1038/nrg.2016.169.

[75] Chan CTY, Dyavaiah M, DeMott MS, Taghizadeh K, Dedon PC, Begley TJ. A Quantitative Systems Approach Reveals Dynamic Control of tRNA Modifications during Cellular Stress. PLoS Genet 2010;6:e1001247. https://doi.org/10.1371/journal.pgen.1001247.

[76] Kowalak JA, Pomerantz SC, Crain PF, McCloskey JA. A novel method for the determination of post-transcriptional modification in RNA by mass spectrometry. Nucleic Acids Res 1993;21:4577–85.

[77] Pomerantz SC, McCloskey JA. Analysis of RNA hydrolyzates by liquid chromatography-mass spectrometry. Methods Enzymol 1990;193:796–824. https://doi.org/10.1016/0076-6879(90)93452-q.

[78] Russell SP, Limbach PA. Evaluating the reproducibility of quantifying modified nucleosides from ribonucleic acids by LC–UV–MS. J Chromatogr B Analyt Technol Biomed Life Sci 2013;0:74–82. https://doi.org/10.1016/j.jchromb.2013.02.010.

[79] Su D, Chan CTY, Gu C, Lim KS, Chionh YH, McBee ME, et al. Quantitative analysis of tRNA modifications by HPLC-coupled mass spectrometry. Nat Protoc 2014;9:828–41. https://doi.org/10.1038/nprot.2014.047.

[80] Chu J-M, Ye T-T, Ma C-J, Lan M-D, Liu T, Yuan B-F, et al. Existence of Internal N7-Methylguanosine Modification in mRNA Determined by Differential Enzyme Treatment

Coupled with Mass Spectrometry Analysis. ACS Chem Biol 2018;13:3243–50. https://doi.org/10.1021/acschembio.7b00906.

[81] Prus G, Hoegl A, Weinert BT, Choudhary C. Analysis and Interpretation of Protein Post-Translational Modification Site Stoichiometry. Trends Biochem Sci 2019;44:943–60. https://doi.org/10.1016/j.tibs.2019.06.003.

[82] Liu N, Pan T. Probing N 6-methyladenosine (m6A) RNA Modification in Total RNA with SCARLET. In: Dassi E, editor. Post-Transcriptional Gene Regulation, New York, NY: Springer; 2016, p. 285–92. https://doi.org/10.1007/978-1-4939-3067-8_17.

[83] Li X, Zhu P, Ma S, Song J, Bai J, Sun F, et al. Chemical pulldown reveals dynamic pseudouridylation of the mammalian transcriptome. Nat Chem Biol 2015;11:592–7. https://doi.org/10.1038/nchembio.1836.

[84] Chen K, Lu Z, Wang X, Fu Y, Luo G-Z, Liu N, et al. High-Resolution N6-Methyladenosine (m6A) Map Using Photo-Crosslinking-Assisted m6A Sequencing. Angew Chem Int Ed Engl 2015;54:1587–90. https://doi.org/10.1002/anie.201410647.

[85] Duan H-C, Wei L-H, Zhang C, Wang Y, Chen L, Lu Z, et al. ALKBH10B Is an RNA N6-Methyladenosine Demethylase Affecting Arabidopsis Floral Transition. Plant Cell 2017;29:2995–3011. https://doi.org/10.1105/tpc.16.00912.

[86] Linder B, Grozhik AV, Olarerin-George AO, Meydan C, Mason CE, Jaffrey SR. Single-nucleotide resolution mapping of m6A and m6Am throughout the transcriptome. Nat Methods 2015;12:767–72. https://doi.org/10.1038/nmeth.3453.

[87] Liu N, Parisien M, Dai Q, Zheng G, He C, Pan T. Probing N6-methyladenosine RNA modification status at single nucleotide resolution in mRNA and long noncoding RNA. RNA 2013;19:1848–56. https://doi.org/10.1261/rna.041178.113.

[88] Zhao W, Zhou Y, Cui Q, Zhou Y. PACES: prediction of N4-acetylcytidine (ac4C) modification sites in mRNA. Sci Rep 2019;9:1–7. https://doi.org/10.1038/s41598-019-47594-7.

[89] Sakurai M, Ueda H, Yano T, Okada S, Terajima H, Mitsuyama T, et al. A biochemical landscape of A-to-I RNA editing in the human brain transcriptome. Genome Res 2014;24:522–34. https://doi.org/10.1101/gr.162537.113.

[90] Saletore Y, Meyer K, Korlach J, Vilfan ID, Jaffrey S, Mason CE. The birth of the Epitranscriptome: deciphering the function of RNA modifications. Genome Biol 2012;13:175. https://doi.org/10.1186/gb-2012-13-10-175.

[91] Molinie B, Wang J, Lim K-S, Hillebrand R, Lu Z, Van Wittenberghe N, et al. m6A level and isoform characterization sequencing (m6A-LAIC-seq) reveals the census and complexity of the m6A epitranscriptome. Nat Methods 2016;13:692–8. https://doi.org/10.1038/nmeth.3898.

[92] Jain M, Olsen HE, Paten B, Akeson M. The Oxford Nanopore MinION: delivery of nanopore sequencing to the genomics community. Genome Biol 2016;17:239. https://doi.org/10.1186/s13059-016-1103-0.

[93] Ingolia NT, Ghaemmaghami S, Newman JRS, Weissman JS. Genome-Wide Analysis in Vivo of Translation with Nucleotide Resolution Using Ribosome Profiling. Science 2009;324:218–23. https://doi.org/10.1126/science.1168978.

[94] Lareau LF, Hite DH, Hogan GJ, Brown PO. Distinct stages of the translation elongation cycle revealed by sequencing ribosome-protected mRNA fragments. ELife 2014;3:e01257. https://doi.org/10.7554/eLife.01257.

[95] Wu CC-C, Zinshteyn B, Wehner KA, Green R. High-Resolution Ribosome Profiling Defines Discrete Ribosome Elongation States and Translational Regulation during Cellular Stress. Mol Cell 2019;73:959-970.e5. https://doi.org/10.1016/j.molcel.2018.12.009.

[96] Lugowski A, Nicholson B, Rissland OS. Determining mRNA half-lives on a transcriptome-wide scale. Methods 2018;137:90–8. https://doi.org/10.1016/j.ymeth.2017.12.006.

[97] Presnyak V, Alhusaini N, Chen Y-H, Martin S, Morris N, Kline N, et al. Codon optimality is a major determinant of mRNA stability. Cell 2015;160:1111–24. https://doi.org/10.1016/j.cell.2015.02.029.

[98] Radhakrishnan A, Chen Y-H, Martin S, Alhusaini N, Green R, Coller J. The DEAD-Box Protein Dhh1p Couples mRNA Decay and Translation by Monitoring Codon Optimality. Cell 2016;167:122-132.e9. https://doi.org/10.1016/j.cell.2016.08.053.

[99] Berman H, Henrick K, Nakamura H. Announcing the worldwide Protein Data Bank. Nat Struct Biol 2003;10:980. https://doi.org/10.1038/nsb1203-980.

[100] Choi J, Ieong K-W, Demirci H, Chen J, Petrov A, Prabhakar A, et al. N6-methyladenosine in mRNA disrupts tRNA selection and translation elongation dynamics. Nat Struct Mol Biol 2016;23:110–5. https://doi.org/10.1038/nsmb.3148.

[101] Eyler DE, Franco MK, Batool Z, Wu MZ, Dubuke ML, Dobosz-Bartoszek M, et al. Pseudouridinylation of mRNA coding sequences alters translation. Proc Natl Acad Sci U S A 2019;116:23068–74. https://doi.org/10.1073/pnas.1821754116.

[102] Svidritskiy E, Madireddy R, Korostelev AA. Structural Basis for Translation Termination on a Pseudouridylated Stop Codon. J Mol Biol 2016;428:2228–36. https://doi.org/10.1016/j.jmb.2016.04.018.

[103] Mauger DM, Cabral BJ, Presnyak V, Su SV, Reid DW, Goodman B, et al. mRNA structure regulates protein expression through changes in functional half-life. Proc Natl Acad Sci U S A 2019;116:24075–83. https://doi.org/10.1073/pnas.1908052116.

[104] Cross R. Epitranscriptomics: The new RNA code and the race to drug it. Chemical & Engineering News n.d. https://cen.acs.org/business/start-ups/Epitranscriptomics-new-RNA-code-race/97/i7 (accessed April 21, 2022).

[105] Vaidyanathan PP, AlSadhan I, Merriman DK, Al-Hashimi HM, Herschlag D. Pseudouridine and N6-methyladenosine modifications weaken PUF protein/RNA interactions. RNA 2017;23:611–8. https://doi.org/10.1261/rna.060053.116.

[106] Choi J, Indrisiunaite G, DeMirci H, Ieong K-W, Wang J, Petrov A, et al. 2′-O-methylation in mRNA disrupts tRNA decoding during translation elongation. Nat Struct Mol Biol 2018;25:208–16. https://doi.org/10.1038/s41594-018-0030-z.

[107] You C, Dai X, Wang Y. Position-dependent effects of regioisomeric methylated adenine and guanine ribonucleosides on translation. Nucleic Acids Res 2017;45:9059–67. https://doi.org/10.1093/nar/gkx515.

[108] Nakamoto MA, Lovejoy AF, Cygan AM, Boothroyd JC. mRNA pseudouridylation affects RNA metabolism in the parasite Toxoplasma gondii. RNA 2017;23:1834–49. https://doi.org/10.1261/rna.062794.117.

[109] Sun L, Xu Y, Bai S, Bai X, Zhu H, Dong H, et al. Transcriptome-wide analysis of pseudouridylation of mRNA and non-coding RNAs in Arabidopsis. J Exp Bot 2019;70:5089–600. https://doi.org/10.1093/jxb/erz273.

[110] Huang T, Chen W, Liu J, Gu N, Zhang R. Genome-wide identification of mRNA 5-methylcytosine in mammals. Nat Struct Mol Biol 2019;26:380–8. https://doi.org/10.1038/s41594-019-0218-x.

[111] Khoddami V, Yerra A, Mosbruger TL, Fleming AM, Burrows CJ, Cairns BR. Transcriptome-wide profiling of multiple RNA modifications simultaneously at single-base resolution. Proc Natl Acad Sci U S A 2019;116:6784–9. https://doi.org/10.1073/pnas.1817334116.

[112] Safra M, Sas-Chen A, Nir R, Winkler R, Nachshon A, Bar-Yaacov D, et al. The m1A landscape on cytosolic and mitochondrial mRNA at single-base resolution. Nature 2017;551:251–5. https://doi.org/10.1038/nature24456.

[113] Baeza J, Dowell JA, Smallegan MJ, Fan J, Amador-Noguez D, Khan Z, et al. Stoichiometry of Site-specific Lysine Acetylation in an Entire Proteome♦. J Biol Chem 2014;289:21326–38. https://doi.org/10.1074/jbc.M114.581843.

[114] Hansen BK, Gupta R, Baldus L, Lyon D, Narita T, Lammers M, et al. Analysis of human acetylation stoichiometry defines mechanistic constraints on protein regulation. Nat Commun 2019;10:1055. https://doi.org/10.1038/s41467-019-09024-0.

[115] Weinert BT, Iesmantavicius V, Moustafa T, Schölz C, Wagner SA, Magnes C, et al. Acetylation dynamics and stoichiometry in Saccharomyces cerevisiae. Mol Syst Biol 2014;10:716. https://doi.org/10.1002/msb.134766.

[116] Carpy A, Krug K, Graf S, Koch A, Popic S, Hauf S, et al. Absolute Proteome and Phosphoproteome Dynamics during the Cell Cycle of Schizosaccharomyces pombe (Fission Yeast). Mol Cell Proteomics 2014;13:1925–36. https://doi.org/10.1074/mcp.M113.035824.

[117] Olsen JV, Vermeulen M, Santamaria A, Kumar C, Miller ML, Jensen LJ, et al. Quantitative phosphoproteomics reveals widespread full phosphorylation site occupancy during mitosis. Sci Signal 2010;3:ra3. https://doi.org/10.1126/scisignal.2000475.

[118] Tsai C-F, Wang Y-T, Yen H-Y, Tsou C-C, Ku W-C, Lin P-Y, et al. Large-scale determination of absolute phosphorylation stoichiometries in human cells by motif-targeting quantitative proteomics. Nat Commun 2015;6:6622. https://doi.org/10.1038/ncomms7622.

[119] Wu R, Haas W, Dephoure N, Huttlin EL, Zhai B, Sowa ME, et al. A large-scale method to measure absolute protein phosphorylation stoichiometries. Nat Methods 2011;8:677–83. https://doi.org/10.1038/nmeth.1636.

[120] Zielinska DF, Gnad F, Wiśniewski JR, Mann M. Precision mapping of an in vivo N-glycoproteome reveals rigid topological and sequence constraints. Cell 2010;141:897–907. https://doi.org/10.1016/j.cell.2010.04.012.

[121] Baudin-Baillieu A, Fabret C, Liang X, Piekna-Przybylska D, Fournier MJ, Rousset J-P. Nucleotide modifications in three functionally important regions of the Saccharomyces cerevisiae ribosome affect translation accuracy. Nucleic Acids Res 2009;37:7665–77. https://doi.org/10.1093/nar/gkp816.

[122] Demirci H, Murphy F, Belardinelli R, Kelley AC, Ramakrishnan V, Gregory ST, et al. Modification of 16S ribosomal RNA by the KsgA methyltransferase restructures the 30S subunit to optimize ribosome function. RNA 2010;16:2319–24. https://doi.org/10.1261/rna.2357210.

[123] Maraia RJ, Arimbasseri AG.
Factors That Shape Eukaryotic tRNAomes: Processing, Modification and Anticodon-Codon Use. Biomolecules 2017;7:E26. https://doi.org/10.3390/biom7010026.

[124] Sergiev PV, Aleksashin NA, Chugunova AA, Polikanov YS, Dontsova OA. Structural and evolutionary insights into ribosomal RNA methylation. Nat Chem Biol 2018;14:226–35. https://doi.org/10.1038/nchembio.2569.

[125] Zhou J, Wan J, Gao X, Zhang X, Jaffrey SR, Qian S-B. Dynamic m(6)A mRNA methylation directs translational control of heat shock response. Nature 2015;526:591–4. https://doi.org/10.1038/nature15377.

[126] Anstee QM, Day CP. S-adenosylmethionine (SAMe) therapy in liver disease: A review of current evidence and clinical utility. Journal of Hepatology 2012;57:1097–109. https://doi.org/10.1016/j.jhep.2012.04.041.

[127] Pietrocola F, Galluzzi L, Bravo-San Pedro JM, Madeo F, Kroemer G. Acetyl coenzyme A: a central metabolite and second messenger. Cell Metab 2015;21:805–21. https://doi.org/10.1016/j.cmet.2015.05.014.

[128] Dai Q, Moshitch-Moshkovitz S, Han D, Kol N, Amariglio N, Rechavi G, et al. Nm-seq maps 2′-O-methylation sites in human mRNA with base precision. Nat Methods 2017;14:695–8. https://doi.org/10.1038/nmeth.4294.

[129] Fan Y, Wu J, Ung MH, De Lay N, Cheng C, Ling J. Protein mistranslation protects bacteria against oxidative stress. Nucleic Acids Res 2015;43:1740–8. https://doi.org/10.1093/nar/gku1404.

[130] Fan Y, Evans CR, Barber KW, Banerjee K, Weiss KJ, Margolin W, et al. Heterogeneity of Stop Codon Readthrough in Single Bacterial Cells and Implications for Population Fitness. Mol Cell 2017;67:826-836.e5. https://doi.org/10.1016/j.molcel.2017.07.010.

[131] Pan T. Modifications and functional genomics of human transfer RNA. Cell Res 2018;28:395–404. https://doi.org/10.1038/s41422-018-0013-y.

[132] Phizicky EM, Hopper AK. tRNA processing, modification, and subcellular dynamics: past, present, and future. RNA 2015;21:483–5. https://doi.org/10.1261/rna.049932.115.

[133] Ranjan N, Rodnina MV. Thio-Modification of tRNA at the Wobble Position as Regulator of the Kinetics of Decoding and Translocation on the Ribosome. J Am Chem Soc 2017;139:5857–64. https://doi.org/10.1021/jacs.7b00727.

[134] Schwartz MH, Pan T. Temperature dependent mistranslation in a hyperthermophile adapts proteins to lower temperatures. Nucleic Acids Res 2016;44:294–303. https://doi.org/10.1093/nar/gkv1379.

[135] Xu L, Liu X, Sheng N, Oo KS, Liang J, Chionh YH, et al. Three distinct 3-methylcytidine (m3C) methyltransferases modify tRNA and mRNA in mice and humans. J Biol Chem 2017;292:14695–703. https://doi.org/10.1074/jbc.M117.798298.

[136] Grozhik AV, Jaffrey SR. Distinguishing RNA modifications from noise in epitranscriptome maps. Nat Chem Biol 2018;14:215–25. https://doi.org/10.1038/nchembio.2546.

[137] Hoernes TP, Heimdörfer D, Köstner D, Faserl K, Nußbaumer F, Plangger R, et al. Eukaryotic Translation Elongation is Modulated by Single Natural Nucleotide Derivatives in the Coding Sequences of mRNAs. Genes (Basel) 2019;10:84. https://doi.org/10.3390/genes10020084.

[138] Karijolich J, Yu Y-T. Converting nonsense codons into sense codons by targeted pseudouridylation. Nature 2011;474:395–8. https://doi.org/10.1038/nature10165.

[139] Hudson BH, Zaher HS. O6-Methylguanosine leads to position-dependent effects on ribosome speed and fidelity. RNA 2015;21:1648–59. https://doi.org/10.1261/rna.052464.115.

[140] You C, Dai X, Wang Y. Position-dependent effects of regioisomeric methylated adenine and guanine ribonucleosides on translation. Nucleic Acids Res 2017;45:9059–67. https://doi.org/10.1093/nar/gkx515.

[141] Karikó K, Muramatsu H, Welsh FA, Ludwig J, Kato H, Akira S, et al. Incorporation of Pseudouridine Into mRNA Yields Superior Nonimmunogenic Vector With Increased Translational Capacity and Biological Stability. Mol Ther 2008;16:1833–40. https://doi.org/10.1038/mt.2008.200.

[142] Fernández IS, Ng CL, Kelley AC, Wu G, Yu Y-T, Ramakrishnan V. Unusual base pairing during the decoding of a stop codon by the ribosome. Nature 2013;500:107–10. https://doi.org/10.1038/nature12302.

[143] Castello A, Hentze MW, Preiss T. Metabolic Enzymes Enjoying New Partnerships as RNA-Binding Proteins. Trends Endocrinol Metab 2015;26:746–57. https://doi.org/10.1016/j.tem.2015.09.012.

[144] Gerber AP, Herschlag D, Brown PO. Extensive Association of Functionally and Cytotopically Related mRNAs with Puf Family RNA-Binding Proteins in Yeast. PLoS Biol 2004;2:e79. https://doi.org/10.1371/journal.pbio.0020079.

[145] Moore LD, Le T, Fan G. DNA Methylation and Its Basic Function. Neuropsychopharmacology 2013;38:23–38. https://doi.org/10.1038/npp.2012.112.

[146] Hentze MW, Castello A, Schwarzl T, Preiss T. A brave new world of RNA-binding proteins. Nat Rev Mol Cell Biol 2018;19:327–41. https://doi.org/10.1038/nrm.2017.130.

[147] Lewis CJ, Pan T, Kalsotra A. RNA Modifications and Structures Cooperate to Guide RNA-protein Interactions. Nat Rev Mol Cell Biol 2017;18:202–10. https://doi.org/10.1038/nrm.2016.163.

[148] Jarmoskaite I, Denny SK, Vaidyanathan PP, Becker WR, Andreasson JOL, Layton CJ, et al. A Quantitative and Predictive Model for RNA Binding by Human Pumilio Proteins. Mol Cell 2019;74:966-981.e18. https://doi.org/10.1016/j.molcel.2019.04.012.

[149] Trixl L, Lusser A. The dynamic RNA modification 5-methylcytosine and its emerging role as an epitranscriptomic mark. Wiley Interdiscip Rev RNA 2019;10:e1510. https://doi.org/10.1002/wrna.1510.

[150] Kretschmer J, Rao H, Hackert P, Sloan KE, Höbartner C, Bohnsack MT. The m6A reader protein YTHDC2 interacts with the small ribosomal subunit and the 5′–3′ exoribonuclease XRN1. RNA 2018;24:1339–50. https://doi.org/10.1261/rna.064238.117.

[151] Gromadski KB, Rodnina MV. Kinetic Determinants of High-Fidelity tRNA Discrimination on the Ribosome. Molecular Cell 2004;13:191–200. https://doi.org/10.1016/S1097-2765(04)00005-X.

[152] Steiner RE, Ibba M. Regulation of tRNA-dependent translational quality control. IUBMB Life 2019;71:1150–7. https://doi.org/10.1002/iub.2080.

[153] Kapur M, Ackerman SL. mRNA Translation Gone Awry: Translation Fidelity and Neurological Disease. Trends Genet 2018;34:218–31. https://doi.org/10.1016/j.tig.2017.12.007.

[154] Garrett S, Rosenthal JJC. RNA Editing Underlies Temperature Adaptation in K+ Channels from Polar Octopuses. Science 2012;335:848–51. https://doi.org/10.1126/science.1212795.

[155] Drummond DA, Wilke CO. The evolutionary consequences of erroneous protein synthesis. Nat Rev Genet 2009;10:715–24. https://doi.org/10.1038/nrg2662.

[156] Pan T. Adaptive translation as a mechanism of stress response and adaptation. Annu Rev Genet 2013;47:121–37. https://doi.org/10.1146/annurev-genet-111212-133522.

[157] Jackman JE, Alfonzo JD. Transfer RNA modifications: Nature's combinatorial chemistry playground. Wiley Interdiscip Rev RNA 2013;4:35–48. https://doi.org/10.1002/wrna.1144.

[158] Hudson BH, Zaher HS. Ribosomes Left in the Dust: Diverse Strategies for Peptide-Mediated Translation Stalling. Mol Cell 2014;56:345–6. https://doi.org/10.1016/j.molcel.2014.10.023.

[159] Eyler DE, Franco MK, Batool Z, Wu MZ, Dubuke ML, Dobosz-Bartoszek M, et al. Pseudouridinylation of mRNA coding sequences alters translation. Proc Natl Acad Sci U S A 2019;116:23068–74. https://doi.org/10.1073/pnas.1821754116.

[160] Hoernes TP, Clementi N, Juen MA, Shi X, Faserl K, Willi J, et al. Atomic mutagenesis of stop codon nucleotides reveals the chemical prerequisites for release factor-mediated peptide release. Proc Natl Acad Sci USA 2018;115:E382–9. https://doi.org/10.1073/pnas.1714554115.

[161] Dunkle JA, Dunham CM. Mechanisms of mRNA frame maintenance and its subversion during translation of the genetic code. Biochimie 2015;114:90–6. https://doi.org/10.1016/j.biochi.2015.02.007.

[162] Jones JD, Monroe J, Koutmou KS. A molecular-level perspective on the frequency, distribution, and consequences of messenger RNA modifications. WIREs RNA 2020;11:e1586. https://doi.org/10.1002/wrna.1586.

[163] Andries O, Mc Cafferty S, De Smedt SC, Weiss R, Sanders NN, Kitada T. N1-methylpseudouridine-incorporated mRNA outperforms pseudouridine-incorporated mRNA by providing enhanced protein expression and reduced immunogenicity in mammalian cell lines and mice. Journal of Controlled Release 2015;217:337–44. https://doi.org/10.1016/j.jconrel.2015.08.051.

[164] Sahin U, Karikó K, Türeci Ö. mRNA-based therapeutics — developing a new class of drugs. Nature Reviews Drug Discovery 2014;13:759–80. https://doi.org/10.1038/nrd4278.

[165] Pardi N, Hogan MJ, Porter FW, Weissman D. mRNA vaccines — a new era in vaccinology. Nat Rev Drug Discov 2018;17:261–79. https://doi.org/10.1038/nrd.2017.243.

[166] Karikó K, Muramatsu H, Welsh FA, Ludwig J, Kato H, Akira S, et al. Incorporation of Pseudouridine Into mRNA Yields Superior Nonimmunogenic Vector With Increased Translational Capacity and Biological Stability. Mol Ther 2008;16:1833–40. https://doi.org/10.1038/mt.2008.200.

[167] Nirenberg MW, Matthaei JH. The dependence of cell-free protein synthesis in E. coli upon naturally occurring or synthetic polyribonucleotides. PNAS 1961;47:1588–602. https://doi.org/10.1073/pnas.47.10.1588.

[168] Rodnina MV, Wintermeyer W. Fidelity of Aminoacyl-tRNA Selection on the Ribosome: Kinetic and Structural Mechanisms. Annu Rev Biochem 2001;70:415–35. https://doi.org/10.1146/annurev.biochem.70.1.415.

[169] Dever TE, Dinman JD, Green R. Translation Elongation and Recoding in Eukaryotes. Cold Spring Harb Perspect Biol 2018;10. https://doi.org/10.1101/cshperspect.a032649.

[170] Pape T, Wintermeyer W, Rodnina MV. Complete kinetic mechanism of elongation factor Tu-dependent binding of aminoacyl-tRNA to the A site of the E. coli ribosome. EMBO J 1998;17:7490–7. https://doi.org/10.1093/emboj/17.24.7490.

[171] Frye M, Jaffrey SR, Pan T, Rechavi G, Suzuki T. RNA modifications: what have we learned and where are we headed? Nat Rev Genet 2016;17:365–72. https://doi.org/10.1038/nrg.2016.47.

[172] Nachtergaele S, He C. The emerging biology of RNA post-transcriptional modifications. RNA Biol 2016;14:156–63. https://doi.org/10.1080/15476286.2016.1267096.

[173] Roundtree IA, Evans ME, Pan T, He C. Dynamic RNA modifications in gene expression regulation. Cell 2017;169:1187–200. https://doi.org/10.1016/j.cell.2017.05.045.

[174] Zhao X, Yang Y, Sun B-F, Shi Y, Yang X, Xiao W, et al. FTO-dependent demethylation of N6-methyladenosine regulates mRNA splicing and is required for adipogenesis. Cell Res 2014;24:1403–19. https://doi.org/10.1038/cr.2014.151.

[175] Ke S, Pandya-Jones A, Saito Y, Fak JJ, Vågbø CB, Geula S, et al. m6A mRNA modifications are deposited in nascent pre-mRNA and are not required for splicing but do specify cytoplasmic turnover. Genes Dev 2017;31:990–1006. https://doi.org/10.1101/gad.301036.117.

[176] Martinez NM, Su A, Burns MC, Nussbacher JK, Schaening C, Sathe S, et al. Pseudouridine synthases modify human pre-mRNA co-transcriptionally and affect pre-mRNA processing. Molecular Cell 2022;82:645-659.e9. https://doi.org/10.1016/j.molcel.2021.12.023.

[177] Jonkhout N, Tran J, Smith MA, Schonrock N, Mattick JS, Novoa EM. The RNA modification landscape in human disease. RNA 2017;23:1754–69. https://doi.org/10.1261/rna.063503.117.

[178] Sloan KE, Warda AS, Sharma S, Entian K-D, Lafontaine DLJ, Bohnsack MT. Tuning the ribosome: The influence of rRNA modification on eukaryotic ribosome biogenesis and function. RNA Biology 2017;14:1138–52. https://doi.org/10.1080/15476286.2016.1259781.

[179] Pan T. Modifications and functional genomics of human transfer RNA. Cell Res 2018;28:395–404. https://doi.org/10.1038/s41422-018-0013-y.

[180] RNA modifications and cancer n.d. https://www.ncbi.nlm.nih.gov/pmc/articles/PMC7567502/ (accessed December 15, 2021).

[181] Jackman JE, Alfonzo JD. Transfer RNA modifications: nature's combinatorial chemistry playground. WIREs RNA 2013;4:35–48. https://doi.org/10.1002/wrna.1144.

[182] Jones JD, Monroe J, Koutmou KS. A molecular-level perspective on the frequency, distribution, and consequences of messenger RNA modifications. Wiley Interdiscip Rev RNA 2020;11:e1586. https://doi.org/10.1002/wrna.1586.

[183] Gilbert WV, Bell TA, Schaening C. Messenger RNA modifications: Form, distribution, and function. Science 2016;352:1408–12. https://doi.org/10.1126/science.aad8711.

[184] Hoernes TP, Hüttenhofer A, Erlacher MD. mRNA modifications: Dynamic regulators of gene expression? RNA Biol 2016;13:760–5. https://doi.org/10.1080/15476286.2016.1203504.

[185] Zhao BS, Roundtree IA, He C. Post-transcriptional gene regulation by mRNA modifications. Nat Rev Mol Cell Biol 2017;18:31–42. https://doi.org/10.1038/nrm.2016.132.

[186] Motorin Y, Helm M. Methods for RNA Modification Mapping Using Deep Sequencing: Established and New Emerging Technologies. Genes 2019;10:35. https://doi.org/10.3390/genes10010035.

[187] Limbach PA, Paulines MJ. Going global: the new era of mapping modifications in RNA. WIREs RNA 2017;8:e1367. https://doi.org/10.1002/wrna.1367.

[188] Li X, Xiong X, Yi C. Epitranscriptome sequencing technologies: decoding RNA modifications. Nat Methods 2017;14:23–31. https://doi.org/10.1038/nmeth.4110.

[189] Helm M, Motorin Y. Detecting RNA modifications in the epitranscriptome: predict and validate. Nat Rev Genet 2017;18:275–91. https://doi.org/10.1038/nrg.2016.169.

[190] Grozhik AV, Jaffrey SR. Distinguishing RNA modifications from noise in epitranscriptome maps. Nat Chem Biol 2018;14:215–25. https://doi.org/10.1038/nchembio.2546.

[191] Finet O, Yague-Sanz C, Kruger LK, Migeot V, Ernst FGM, Lafontaine DLJ, et al. Transcription-Wide Mapping of Dihydrouridine (D) Reveals that mRNA Dihydrouridylation is Essential for Meiotic Chromosome Segregation. Rochester, NY: Social Science Research Network; 2020. https://doi.org/10.2139/ssrn.3569550.

[192] Monroe JG, Smith TJ, Koutmou KS. Investigating the consequences of mRNA modifications on protein synthesis using in vitro translation assays. Methods in Enzymology, Academic Press; 2021. https://doi.org/10.1016/bs.mie.2021.06.011.

[193] Arango D, Sturgill D, Alhusaini N, Dillman AA, Sweet TJ, Hanson G, et al. Acetylation of Cytidine in mRNA Promotes Translation Efficiency. Cell 2018;175:1872-1886.e24. https://doi.org/10.1016/j.cell.2018.10.030.

[194] Schwartz S, Bernstein DA, Mumbach MR, Jovanovic M, Herbst RH, León-Ricardo BX, et al. Transcriptome-wide Mapping Reveals Widespread Dynamic-Regulated Pseudouridylation of ncRNA and mRNA. Cell 2014;159:148–62. https://doi.org/10.1016/j.cell.2014.08.028.

[195] Tardu M, Jones JD, Kennedy RT, Lin Q, Koutmou KS. Identification and Quantification of Modified Nucleosides in Saccharomyces cerevisiae mRNAs. ACS Chem Biol 2019;14:1403–9. https://doi.org/10.1021/acschembio.9b00369.

[196] Xu L, Liu X, Sheng N, Oo KS, Liang J, Chionh YH, et al. Three distinct 3-methylcytidine (m3C) methyltransferases modify tRNA and mRNA in mice and humans. Journal of Biological Chemistry 2017;292:14695–703. https://doi.org/10.1074/jbc.M117.798298.

[197] Franco MK, Koutmou KS. Chemical modifications to mRNA nucleobases impact translation elongation and termination. Biophysical Chemistry 2022;285:106780. https://doi.org/10.1016/j.bpc.2022.106780.

[198] Eyler DE, Franco MK, Batool Z, Wu MZ, Dubuke ML, Dobosz-Bartoszek M, et al. Pseudouridinylation of mRNA coding sequences alters translation. PNAS 2019;116:23068–74. https://doi.org/10.1073/pnas.1821754116.

[199] Licht K, Hartl M, Amman F, Anrather D, Janisiw MP, Jantsch MF. Inosine induces context-dependent recoding and translational stalling. Nucleic Acids Res 2019;47:3–14. https://doi.org/10.1093/nar/gky1163.

[200] You C, Dai X, Wang Y. Position-dependent effects of regioisomeric methylated adenine and guanine ribonucleosides on translation. Nucleic Acids Res 2017;45:9059–67. https://doi.org/10.1093/nar/gkx515.

[201] Meyer KD, Jaffrey SR. The dynamic epitranscriptome: N6-methyladenosine and gene expression control. Nat Rev Mol Cell Biol 2014;15:313–26. https://doi.org/10.1038/nrm3785.

[202] Agrawal S. RNA Therapeutics Are Stepping Out of the Maze. Trends Mol Med 2020;26:1061–4. https://doi.org/10.1016/j.molmed.2020.08.007.

[203] Zhou L-Y, Qin Z, Zhu Y-H, He Z-Y, Xu T. Current RNA-based Therapeutics in Clinical Trials. Curr Gene Ther 2019;19:172–96. https://doi.org/10.2174/1566523219666190719100526.

[204] Sergeeva OV, Koteliansky VE, Zatsepin TS. mRNA-based therapeutics–Advances and perspectives. Biochemistry Moscow 2016;81:709–22. https://doi.org/10.1134/S0006297916070075.

[205] Gao M, Zhang Q, Feng X-H, Liu J. Synthetic modified messenger RNA for therapeutic applications. Acta Biomater 2021;131:1–15. https://doi.org/10.1016/j.actbio.2021.06.020.

[206] Nance KD, Meier JL. Modifications in an Emergency: The Role of N1-Methylpseudouridine in COVID-19 Vaccines. ACS Cent Sci 2021. https://doi.org/10.1021/acscentsci.1c00197.

[207] Parr CJC, Wada S, Kotake K, Kameda S, Matsuura S, Sakashita S, et al. N 1-Methylpseudouridine substitution enhances the performance of synthetic mRNA switches in cells. Nucleic Acids Research 2020;48:e35–e35. https://doi.org/10.1093/nar/gkaa070.

[208] Svitkin YV, Cheng YM, Chakraborty T, Presnyak V, John M, Sonenberg N. N1-methyl-pseudouridine in mRNA enhances translation through eIF2α-dependent and independent mechanisms by increasing ribosome density. Nucleic Acids Res 2017;45:6023–36. https://doi.org/10.1093/nar/gkx135.

[209] Karikó K, Muramatsu H, Welsh FA, Ludwig J, Kato H, Akira S, et al. Incorporation of Pseudouridine Into mRNA Yields Superior Nonimmunogenic Vector With Increased Translational Capacity and Biological Stability. Mol Ther 2008;16:1833–40. https://doi.org/10.1038/mt.2008.200.

[210] Karikó K, Buckstein M, Ni H, Weissman D. Suppression of RNA Recognition by Toll-like Receptors: The Impact of Nucleoside Modification and the Evolutionary Origin of RNA. Immunity 2005;23:165–75. https://doi.org/10.1016/j.immuni.2005.06.008.

[211] Svitkin YV, Gingras A-C, Sonenberg N. Membrane-dependent relief of translation elongation arrest on pseudouridine- and N1-methyl-pseudouridine-modified mRNAs. Nucleic Acids Res 2021:gkab1241. https://doi.org/10.1093/nar/gkab1241.

[212] Hoernes TP, Clementi N, Faserl K, Glasner H, Breuker K, Lindner H, et al. Nucleotide modifications within bacterial messenger RNAs regulate their translation and are able to rewire the genetic code. Nucleic Acids Res 2016;44:852–62. https://doi.org/10.1093/nar/gkv1182.

[213] Levi O, Arava YS. Pseudouridine-mediated translation control of mRNA by methionine aminoacyl tRNA synthetase. Nucleic Acids Research 2020. https://doi.org/10.1093/nar/gkaa1178.

[214] Kurland CG. Translational accuracy and the fitness of bacteria. Annu Rev Genet 1992;26:29–50. https://doi.org/10.1146/annurev.ge.26.120192.000333.

[215] Wohlgemuth I, Pohl C, Rodnina MV. Optimization of speed and accuracy of decoding in translation. EMBO J 2010;29:3701–9. https://doi.org/10.1038/emboj.2010.229.

[216] Sitron CS, Brandman O. Detection and Degradation of Stalled Nascent Chains via Ribosome-Associated Quality Control. Annu Rev Biochem 2020;89:417–42. https://doi.org/10.1146/annurev-biochem-013118-110729.

[217] Ramakrishnan V. Ribosome Structure and the Mechanism of Translation. Cell 2002;108:557–72. https://doi.org/10.1016/S0092-8674(02)00619-0.

[218] Jobe A, Liu Z, Gutierrez-Vargas C, Frank J. New Insights into Ribosome Structure and Function. Cold Spring Harb Perspect Biol 2019;11:a032615. https://doi.org/10.1101/cshperspect.a032615.

[219] Zaher HS, Green R. Quality control by the ribosome following peptide bond formation. Nature 2009;457:161–6. https://doi.org/10.1038/nature07582.

[220] Hetrick B, Lee K, Joseph S. Kinetics of Stop Codon Recognition by Release Factor 1. Biochemistry 2009;48:11178–84. https://doi.org/10.1021/bi901577d.

[221] Svidritskiy E, Madireddy R, Korostelev AA. Structural Basis for Translation Termination on a Pseudouridylated Stop Codon. Journal of Molecular Biology 2016;428:2228–36. https://doi.org/10.1016/j.jmb.2016.04.018.

[222] Pardi N, Tuyishime S, Muramatsu H, Kariko K, Mui BL, Tam YK, et al. Expression kinetics of nucleoside-modified mRNA delivered in lipid nanoparticles to mice by various routes. J Control Release 2015;217:345–51. https://doi.org/10.1016/j.jconrel.2015.08.007.

[223] Karijolich J, Yu Y-T. Converting nonsense codons into sense codons by targeted pseudouridylation. Nature 2011;474:395–8. https://doi.org/10.1038/nature10165.

[224] Weixlbaumer A, Murphy FV, Dziergowska A, Malkiewicz A, Vendeix FAP, Agris PF, et al. Mechanism of expanding the decoding capacity of tRNAs by modification of uridines. Nat Struct Mol Biol 2007;14:498–502. https://doi.org/10.1038/nsmb1242.

[225] Murphy FV, Ramakrishnan V, Malkiewicz A, Agris PF. The role of modifications in codon discrimination by tRNA(Lys)UUU. Nat Struct Mol Biol 2004;11:1186–91. https://doi.org/10.1038/nsmb861.

[226] Rodnina MV, Wintermeyer W. Fidelity of Aminoacyl-tRNA Selection on the Ribosome: Kinetic and Structural Mechanisms. Annual Review of Biochemistry 2001;70:415–35. https://doi.org/10.1146/annurev.biochem.70.1.415.

[227] Eyler DE, Franco MK, Batool Z, Wu MZ, Dubuke ML, Dobosz-Bartoszek M, et al. Pseudouridinylation of mRNA coding sequences alters translation. Proc Natl Acad Sci U S A 2019;116:23068–74. https://doi.org/10.1073/pnas.1821754116.

[228] Andries O, Mc Cafferty S, De Smedt SC, Weiss R, Sanders NN, Kitada T. N1-methylpseudouridine-incorporated mRNA outperforms pseudouridine-incorporated mRNA by providing enhanced protein expression and reduced immunogenicity in mammalian cell lines and mice. Journal of Controlled Release 2015;217:337–44. https://doi.org/10.1016/j.jconrel.2015.08.051.

[229] Choi J, Ieong K-W, Demirci H, Chen J, Petrov A, Prabhakar A, et al. N6-methyladenosine in mRNA disrupts tRNA selection and translation elongation dynamics. Nat Struct Mol Biol 2016;23:110–5. https://doi.org/10.1038/nsmb.3148.

[230] Gromadski KB, Rodnina MV. Kinetic Determinants of High-Fidelity tRNA Discrimination on the Ribosome. Molecular Cell 2004;13:191–200. https://doi.org/10.1016/S1097-2765(04)00005-X.

[231] Pape T. Induced fit in initial selection and proofreading of aminoacyl-tRNA on the ribosome. The EMBO Journal 1999;18:3800–7. https://doi.org/10.1093/emboj/18.13.3800.

[232] Charette M, Gray MW. Pseudouridine in RNA: What, Where, How, and Why. IUBMB Life 2000;49:341–51. https://doi.org/10.1080/152165400410182.

[233] Kierzek E, Malgowska M, Lisowiec J, Turner DH, Gdaniec Z, Kierzek R. The contribution of pseudouridine to stabilities and structure of RNAs. Nucleic Acids Res 2014;42:3492–501. https://doi.org/10.1093/nar/gkt1330.

[234] Davis DR, Veltri CA, Nielsen L. An RNA Model System for Investigation of Pseudouridine Stabilization of the Codon-Anticodon Interaction in tRNALys, tRNAHis and tRNATyr. Journal of Biomolecular Structure and Dynamics 1998;15:1121–32. https://doi.org/10.1080/07391102.1998.10509006.

[235] Davis DR. Stabilization of RNA stacking by pseudouridine. Nucleic Acids Res 1995;23:5020–6. https://doi.org/10.1093/nar/23.24.5020.

[236] Lucas X, Bauzá A, Frontera A, Quiñonero D. A thorough anion–π interaction study in biomolecules: on the importance of cooperativity effects. Chemical Science 2016;7:1038–50. https://doi.org/10.1039/C5SC01386K.

[237] Westhof E. Pseudouridines or how to draw on weak energy differences. Biochemical and Biophysical Research Communications 2019;520:702–4. https://doi.org/10.1016/j.bbrc.2019.10.009.

[238] Li S, Mason CE. The Pivotal Regulatory Landscape of RNA Modifications. Annu Rev Genom Hum Genet 2014;15:127–50. https://doi.org/10.1146/annurev-genom-090413-025405.

[239] Muramatsu T, Nishikawa K, Nemoto F, Kuchino Y, Nishimura S, Miyazawa T, et al. Codon and amino-acid specificities of a transfer RNA are both converted by a single post-transcriptional modification. Nature 1988;336:179–81. https://doi.org/10.1038/336179a0.

[240] Satpati P, Bauer P, Åqvist J. Energetic Tuning by tRNA Modifications Ensures Correct Decoding of Isoleucine and Methionine on the Ribosome. Chemistry – A European Journal 2014;20:10271–5. https://doi.org/10.1002/chem.201404016.

[241] Durant PC, Bajji AC, Sundaram M, Kumar RK, Davis DR. Structural effects of hypermodified nucleosides in the Escherichia coli and human tRNALys anticodon loop: the effect of nucleosides s2U, mcm5U, mcm5s2U, mnm5s2U, t6A, and ms2t6A. Biochemistry 2005;44:8078–89. https://doi.org/10.1021/bi050343f.

[242] Shi H, Chai P, Jia R, Fan X. Novel insight into the regulatory roles of diverse RNA modifications: Re-defining the bridge between transcription and translation. Mol Cancer 2020;19:78. https://doi.org/10.1186/s12943-020-01194-6.

[243] Boccaletto P, Machnicka MA, Purta E, Piątkowski P, Bagiński B, Wirecki TK, et al. MODOMICS: a database of RNA modification pathways. 2017 update. Nucleic Acids Research 2018;46:D303–7. https://doi.org/10.1093/nar/gkx1030.

[244] Garcia DM, Campbell EA, Jakobson CM, Tsuchiya M, Shaw EA, DiNardo AL, et al. A prion accelerates proliferation at the expense of lifespan. Elife 2021;10:e60917. https://doi.org/10.7554/eLife.60917.

Chapter 3 Assessing the Consequences of mRNA Modifications on Protein Synthesis using *In Vitro* Translation Assays

Chapter 3 is reprinted from with permission from Methods Enzymol. 2021;658:379-406.

Manuscript was written by Jeremy Monroe, Tyler Smith, and Dr. Kristin Koutmou. Tyler Smith wrote the ribosome purification and initiation complex formation and amino acid addition sections and created the quantification and kinetic analysis figure (Figure 10). Kristin Koutmou participated as editor of the manuscript.

3.1 Introduction

Translation of the genetic code into functional protein molecules is accomplished by the ribosome. The ribosome uses messenger RNAs (mRNAs) as molecular blueprints to direct the rapid and accurate synthesis of proteins. The ability of the cell to faithfully express its genetic code is essential for cellular survival. However, the speed and fidelity of the ribosome is not uniform. Even in healthy cells, amino acids unspecified by the mRNA are incorporated into growing polypeptide chains every 1,000 to 10,000 codons [1]. While most miscoding events are inconsequential for protein function, reductions in translational fidelity can have biological consequences – both perturbing and promoting cellular health. Increases in amino acid substitution levels are deleterious to cellular health and to linked a variety of neurological disorders (Kapur & Ackerman, 2018)[2,3]. However, under some conditions temporary, modest increases in miscoding transcriptome side enhance cellular fitness under environmental stress [4–6].

Many factors, including the availability of aminoacyl-tRNAs and the post-transcriptional modification status of RNAs in the translational machinery, influence the how accurately ribosomes decode mRNAs [7–11]. Evaluating the impact of individual RNA modifications on translational fidelity is challenging in the context of a cell because modifications are often incorporated into multiple RNAs important for protein synthesis (tRNAs, rRNAs and mRNAs) by the same enzyme. This makes it difficult to deplete RNA modifying enzymes and confidently assign observed changes in protein output to a distinct RNA species. Determining the influence of mRNA modifications on translational fidelity is becoming an important question with the discovery of modifications in mRNA codons, and the incorporation of modified nucleosides into mRNAs in emerging mRNA-based vaccine and therapeutic platforms [12–16].

In vitro and cell free systems to study translation date back to the 1960's when they were used to reveal the triplet codon pattern of the genetic code [17]. Here we discuss the application of a fully reconstituted *E. coli in vitro* translation system to investigate how chemically modified mRNA codons impact ribosome fidelity at the molecular level. This approach has long been used by researchers to discover how the ribosome decodes mRNA codons [18–20]. We present how to purify the individual

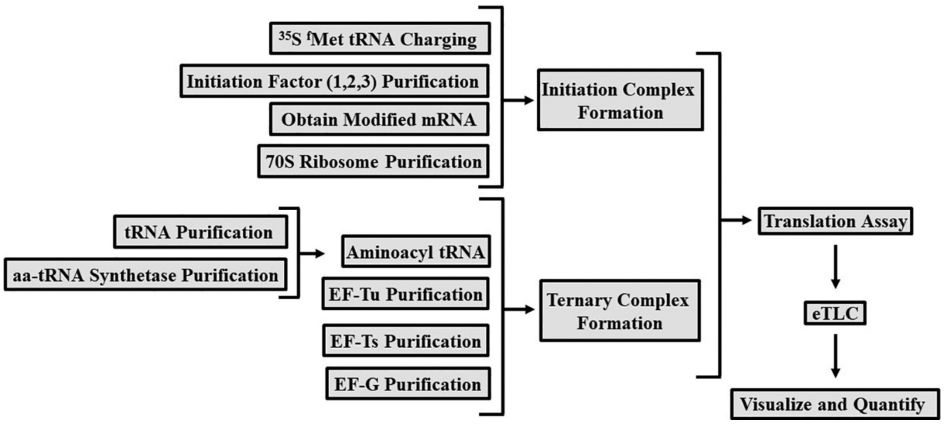

Figure 9 *Experimental flowchart for in vitro translation assays*

components required for translation (ribosomes, mRNAs, tRNAs and translation factors), reconstitute active translation complexes from purified components, and perform single turnover assays to assess amino acid incorporation (and misincorporation) by the ribosome (Figure 1).

While these experiments focus on investigating modifications in mRNAs, the approaches we discuss can also be applied to other aspects of translation.

3.2 In vitro System Chemicals and Equipment and Buffers

Chemicals	Equipment
Tris Base	HPLC (+ Fraction collector)
Luria-Base (LB) Broth	FPLC (+ Fraction collector)
Luria-Base (LB) Agar	Waters XBridge BEH C18 OBD Prep wide pore HPLC column
Luria-Base (LB) Agar	HisTrap FF column, 5 mL
Acetic Acid	Resource Q Column, 5 mL
Magnesium Chloride ($MgCl_2$)	Beckman Coulter Optima XE-90 Ultracentrifuge with zonal setting
Ammonium Chloride (NH_4Cl_2)	Ti-15 Zonal Rotor
Sucrose	Type 45 Ti Fixed-Angle Titanium Rotor
Beta-mercaptoethanol (BME)	Ti45 Polycarbonate Ultracentrifuge tubes
Terrific Base (TB) Broth	Beckman TLA 100 Benchtop Ultracentrifuge (or similar able to spink at 69,000 RPM)
Ethylenediaminetetraacetic acid (EDTA)	TLA-100 Rotor (or comparable)
Pyridine	5 mL polycarbonate Ultracentrifuge tubes
Stoddard Solvent	Teledyne ISCO UA-6 UV/Vis Detector and Type 6 Optical Unit Attachment
Ethanol (EtOH)	French press/Microfluidizer
Liquid Nitrogen	Large Shaking Incubator
Ampicillin	CO8000 Cell Density Meter
E. coli cells with a pUC57 plasmid over expressing tRNA of interest	4 L Erlenmeyer Flasks
E. coli strain MRE600	50 mL conical centrifuge tubes
GTP	15 mL conical centrifuge tubes
Iron (III) Chloride ($FeCl_3$)	Ultracentrifuge tubes
Glycerol	Bio-Rad P6 Spin Columns
Acetic Acid	Micropipettes and filter tips (2, 20, 200, and 1000 µL)

Table 1 *A table of needed materials both chemical and instrumental in order to prepare and assess miscoding in an prokaryotic in vitro system*

Buffer R-D:

Reagent	Final Concentration
Tris HCl, pH 7.5	20 mM
NH4Cl	500 mM
MgCl2	10 mM
EDTA	0.5 mM
Sucrose	1.1 M

Buffer R-60:

Reagent	Final Concentration
Buffer R-O (10X)	1X
Sucrose	60% (w/v)
BME	3mM

Buffer R-10: 1X Buffer R-O, 10% w/v sucrose, 3 mM BME

Reagent	Final Concentration
Buffer R-O (10X)	1X
Sucrose	10% (w/v)
BME	3mM

Buffer R-O (10X):

Reagent	Final Concentration
Tris HCl, pH 7.5	200 mM
NH4Cl	600 mM
MgCl2	52.5 mM
EDTA	2.5 mM

Buffer R-50:

Reagent	Final Concentration
Buffer R-O (10X)	1X
Sucrose	50% (w/v)
BME	3mM

Buffer R-40:

Reagent	Final Concentration
Buffer R-O (10X)	1X
Sucrose	40% (w/v)
BME	3mM

Buffer R-A

Reagent	Final Concentration
Tris HCl, pH 7.5	20 mM
NH4Cl	100 mM
MgCl2	10 mM
EDTA	0.5 mM
BME	6 mM

Table 2 *Ribosome buffers needed for the purification of 70S ribosomes*

tRNA Growth Media

Reagent	Concentration
Terrific Broth (TB)	25 g/L
Glycerol	5 g/L
NH_4Cl	50 mM
$MgSO_4$	2 mM
$FeCl_3$	0.1 mM
Glucose	0.05% (w/v)
Lactose (if using autoinduction)	0.2% (w/v)

Buffer A (IEX)

Regent	Final Concentration
NH_4OAc	50 mM
NaCl	300 mM
$MgCl_2$	10 mM

Buffer B (IEX)

Regent	Final Concentration
NH_4OAc	50 mM
NaCl	800 mM
$MgCl_2$	10 mM

HPLC Buffer A, pH 5

Reagent	Final Concentration
NH_4OAc	20 mM
$MgCl_2$	10 mM
NaCl	400 mM

HPLC Buffer B, pH 5

Reagent	Final Concentration
NH_4OAc	20 mM
$MgCl_2$	10 mM
NaCl	400 mM
Methanol	60%

5x KF Buffer

Reagent	Final Concentration
HEPES	0.5 M
KCl	0.05 M
$MgCl_2$	0.1 M
H_2O	to 1 mL

Extraction Buffer, pH 7

$Mg(OAc)_2$	20 mM
Tris-HCl	20 mM

Table 3 *Buffers required to purify native tRNA*

5x Charging Buffer

Reagent	Final Concentration
HEPES	0.5 M
KCl	0.05 M
$MgCl_2$	0.1 M
H_2O	to 1 mL

10x Translation Buffer

Reagent	Final Concentration
Tris-Cl pH 7.5	0.5 M
NH_4Cl	0.7 M
KCl	0.3 M
MgCl2	0.07 M
BME	0.05 M
H_2O	to 1 mL

Table 4 *Buffers needed for miscoding assays*

eTLC Buffers		
pH	**Contents**	**Volume in 3L (final volume)**
1.9	formic acid/acetic acid	60mL/240mL
2	formic acid	80 mL
2.5	acetic acid	200 mL
2.8	pyridine/acetic acid	15 mL /600 mL
3.5	pyridine/acetic acid	6.6 mL/66 mL
3.6	ammonium formate/formic acid	6.3g/10ml
3.7	2M citric acid/1N sodium hydroxide	40 mL/67 mL
4.5	acetic acid/sodium acetate/EDTA	9.4 mL /10.3g/1.3g
5.3	pyridine/acetic acid	20mL/8mL
6	acetic acid/pyridine	14mL/136mL
6.4	pyridine/acetic acid	200mL/8mL
8.6	barbitone/sodium diethylbarbitone	3.3g/25.5g
9.2	sodium borate	38g

Table 5 *Possible buffers conditions for proper separation in an eTLC system*

3.3 Section 1: Ribosome Purification

Zonal centrifugation of crude *E. coli* cell lysate yields fractions of 30S and 50S ribosomal subunits, 70S ribosomes and polysomes. We use a linear sucrose gradient to purify coupled 70S ribosomes and separate the 30S and 50S subunits. We find that standard double pelleting ribosomes yields materials of insufficient purity for our assays [21].

3.3.1 Protocol

Day 1

1. Streak MRE 600 cells onto an LB-agar plate without antibiotic and incubate overnight at 37°C. *E. coli* MRE 600 is the strain of choice ribosome growth because it lacks Ribonuclease I and has negligible nuclease activity [22].

Day 2

2. Inoculate 50 mL of LB media with a single MRE600 colony. Grow overnight (~16 hours) in a shaker-incubator at 37ºC, 220 rpm.

Day 3

3. Prewarm 6 x 4L flasks containing 1L of LB media. Add 5 mL of the MRE600 overnight culture to each flask. Shake and incubate at 37°C, 220 rpm.

4. While the cultures grow, prepare an ice bath for the 4 L flasks.

5. Once the cultures reach an OD600 of 0.6, transfer them to the ice bath for 20 minutes.

6. Spin the chilled cultures at in a JLA-8.100 rotor at 4,000 RPM, 4ºC for 15 minutes. Combine the cell pellets in a 50 mL conical tube. Either store at -80°C, or continue to step 7.

7. Resuspend pellet in ~50 mL of cold Buffer R-A. Lyse cells by microfluidizer or French-Press.

8. Clarify lysate by centrifugation. Spin in a JA-20 rotor at 16,000 RPM, 4º C for 30 minutes.

9. While the lysate spins, prepare sucrose cushions by filling 4-6 Ti45 ultracentrifuge tubes with 35 mL of Buffer R-D. Chill on ice.

10. Discard the pellet. Filter supernatant through a 0.22 μM PES syringe filter.

11. Add cold Buffer R-A to bring the filtered supernatant volume to 100 mL.

12. Slowly pour (layer) 25 mL of the supernatant onto the pre-chilled Buffer R-D in Ti45 ultracentrifuge tubes. Balance centrifuge tubes with Buffer R-A.

13. Centrifuge tubes in a Ti45 Ultracentrifuge rotor at 37,000 x RPM, 4°C for 18 hours. Use the slowest acceleration and deceleration setting available on the centrifuge.

Day 4

14. Remove supernatant and rinse each pellet with ~50 □L of cold Buffer R-A.

15. Add 400 μL of Buffer R-A and resuspend pellets in the centrifuge bottles by orbital shaking at 120 rpm, 4°C for 2 hours.

16. Prepare, filter (0.22 μM PES) and chill (store at 4°C) Buffer R-O, Buffer R-5, Buffer R-10, Buffer R-40, Buffer R-50, and Buffer R-60. Add BME only after filtering.

**Note*: make enough R-10 and R-40 to fill your zonal rotor (~1.85 L for the Ti-15 zonal rotor used here).

17. While the pellets resuspend, generate a sucrose gradient in the chilled Ti-15 zonal rotor. Using a gradient maker, begin slowly loading Buffer R-10 via the loading/unloading device (rotor specific). A peristaltic pump can be used to automate buffer loading. After adding ~250 mL of Buffer R-10, begin slowly adding Buffer R-40 into Buffer R-10 to create a 10-40%

sucrose gradient. Keep stirring to ensure proper mixing of sucrose to form desired gradient. After R-40 is loaded, add Buffer R-50 (~100 mL) until sucrose solution begins coming out of the top of the rotor or loading device to ensure rotor is completely filled. Keep the rotor and centrifuge chilled at 4°C and 3,000 RPM.

18. Clarify resuspended pellets (from step 15) by centrifuging in a benchtop microfuge at 14,800 RPM for 1 minute.

19. Combine the ribosome-containing supernatants in a 50 mL conical tube on ice. Make a 1:1,000 dilution of the supernatant and measure (in triplicate) the absorbance readings at 260 nm.

20. Dilute supernatant to ~ 30 mL in cold Buffer R-5. Load onto the top of the sucrose gradient in the zonal rotor (step 17) via the loading/unloading device. For best results, load using a 50 mL syringe.

21. Use a 50 mL syringe to slowly add 30 mL of cold Buffer R-O to the top of the gradient in the zonal rotor via the loading/unloading device. This will fully displace the ribosome suspension onto the sucrose gradient.

22. Spin the zonal rotor at 28,000 RPM, 4°C for 19 hours. After 19 hours the centrifuge should not stop, but be programmed to transition to spin at 3,000 RPM, 4°C.

Note: check if your zonal rotor has different cap components for loading/unloading and higher speed centrifugation, as these caps may need to be changed.

Day 5

23. Attach a UA-6 UV spectrophotometer to the loading/unloading device for the zonal rotor to follow ribosome unloading at 260 nM.

24. Slowly unload the rotor by adding Buffer R-50 (as described in step 17). After adding ~250 mL, begin mixing Buffer R-60. Collect 15-50 mL fractions in conical tubes when UV peaks are observed. Label tubes with fraction number, place on ice.

25. Take 100 μL of each fraction of interest and extract with 500 μL Buffer R-Extraction. Phenol-chloroform extract the solution and ethanol precipitate the aqueous phase samples with 2.5 volumes of ethanol for 15 minutes on ice.

26. Centrifuge samples for 15 minutes in a benchtop microfuge at maximum speed. Remove supernatant and wash pellets with 70% ethanol. Resuspend pelleted fractions in 25 μL of MilliQ H_2O.

27. Mix up to 2 μg from extracted samples with 2X formamide RNA loading dye and heat denature at 95°C for 10 minutes. Run samples on a 5% denaturing PAGE gel and visualize by UV shadowing or methylene blue staining. Fractions containing 70S ribosomes will have 2 predominant bands corresponding to the 16S and 23S rRNA.

28. Pool the fractions (from step 24) that contain 70S ribosomes. Measure and record the absorbance of the pooled sample at 260 nm.

29. Place 70S ribosomes into chilled Ti-45 centrifuge tubes. Balance tubes with Buffer R-A and spin at 37,000 X RPM, 4°C for 18 hours. Use the slowest possible acceleration and deceleration settings.

Day *6*

30. Remove the supernatant from tubes, taking care because the ribosome pellet is glassy and not well attached. Gently resuspend the pellets using a total of 2-5 mL of Buffer R-A. Do not pull the ribosome pellet up into the pipette tip, instead repeatedly (~50 times) rinse over the pellet buffer until resuspended.

31. Measure the absorbance of the pooled ribosomes at 260 nm and calculate the concentration ($\varepsilon = 6.94 \times 10^7\ M^{-1}cm^{-1}$). Aliquot (50-100 μL) ribosomes and flash freeze in liquid nitrogen and store at -80°C.

3.4 Section 2: Translation Factor Purification

A single round of translation involves a host of translation factor proteins. At a minimum, initiation factors 1, 2, and 3 (IF1, IF2, IF3), ^{f}methionyl-tRNA formyltransferase (MTF), aminoacyl-tRNA synthetases (AA-RSs) and elongation factor-Tu (EF-Tu) are required for the reconstituted bacterial translation system to function. Additional protein factors, including elongation factor thermal stable (EF-Ts) and elongation factor -G (EF-G), are needed if more than one round of amino acid addition is desired. We purify translation factor proteins from His-tagged plasmids available from AddGene. Multiple expression and purification protocols for translation factors can be found in the literature, and are therefore not included here [9] [23] [24] [25] [26] [27].

3.5 Section 3: Purification of Natively Modified tRNA

Transfer RNAs (tRNAs) contain multiple post-transcriptional modifications important for their function. While T7 transcribed tRNAs can be used for reconstituted translation assays, these tRNAs often exhibit reduced speeds and accuracy in translation reactions compared to their natively modified counterparts. [7] [11]. Below we describe the large-scale purification of individual natively modified *E. coli* tRNAs.

3.5.1 Protocol

Day 1 – Transform tRNA plasmid

1. Transform a pUC57 plasmid containing an *E. coli* tRNA sequence of interest (e.g. $tRNA^{Phe}$) into HB101 cells. Grow overnight on an LB-ampicillin agar plate at 37°C.

Day 2 – Overnight culture

2. Inoculate 5 mL of LB-ampicillin media with a single tRNA-expressing colony. Shake for ~16 hours at 37ºC and 220 rpm.

Day 3 – Large scale expression of tRNA

3. Add 400 µg/mL ampicillin to 1 L of enriched TB media. Inoculate TB media with 5 mL of the starter culture from Day 2 (see for details see [28]).

4. Grow cells ~ 16-18 hours in a shaker incubator at 37 °C and 220 rpm.

Day 4 – Isolate tRNA from cells

5. Harvest cells by spinning in a JLA-8.100 rotor at 4,000 RPM, 4 °C for 30 minutes.

6. Pour off supernatant and weigh the cell pellet(s). Pellets can be stored at -80 °C, or extracted as described below.

7. For each cell pellet gather 2 x 250 mL Teflon centrifuge bottles with ETFE O-rings. Label the centrifuge bottles A, B.

8. Resuspend each cell pellet in extraction buffer (200 mL buffer / 25 g cells).

9. Place resuspended cells in Teflon centrifuge bottle A.

10. Add a 1:1 volume ratio of RNase free acid phenol: chloroform (5:1), pH 4.3.

11. Tape centrifuge bottle A horizontally in a shaker-incubator. Shake at 4°C and 200 rpm for 1 hour.

12. Remove the cells from the shaker-incubator. Separate the aqueous and phenol layer by centrifuging the bottles in an A-4-44 swinging bucket rotor with 250 mL bottle adaptors at 5,000 RPM for 1 hour, 4 °C. There will be three layers: brown (bottom, cell debris), thin white (middle, lipids), and transparent (top, aqueous).

13. Use a 25 mL glass pipette to transfer the aqueous layer from tube A to tube B, avoiding the lipid the layer. Add 1:1 ratio of chloroform.

14. Add 100 mL of tRNA extraction buffer to solution remaining in tube A. Shake the tubes for 30 seconds in a fume hood.

15. Spin tubes A and B at A-4-44 swinging bucket rotor at 5,000 RPM, 4° C for 1 hour.

16. Transfer the top layer from tube B to a collection tube. Move the top layer of tube A to tube B.

17. Shake tube B for 30 seconds by hand in a fume hood, then spin in a A-4-44 swinging bucket rotor at 5,000 RPM, 4 °C for 1 hour.

18. Collect the top layer from tube B and combine with the top layer from tube A in a 500 mL JA-10 centrifuge tube.

19. To the contents of the JA-10 tube, add NaOAc, pH 5.2 to 0.3 M (final) and 100% Isopropanol to 20% (final volume). Shake for 30 seconds.

20. Centrifuge in a JA-10 rotor at 9,000 RPM, 4 °C for 1 hour. A small DNA pellet will be visible following centrifugation.

21. Transfer the supernatant to another 500 mL JA-10 tube. Increase the amount of isopropanol in the solution from 20% to 60% (final). Mix by shaking.

22. Precipitate tRNA at -20° C for at least 2 hours.

Day 4 – Deacylated tRNA

23. Centrifuge the tRNA precipitant solution in a JA-10 rotor at 9,000 RPM, 4° C for 1 hour.

24. Discard the supernatant and resuspend the pellet in 10 mL of 200 mM Tris-Acetate, pH 8.0.

25. De-acylate tRNA by taping centrifuge bottles horizontally in a shaker-incubator at 37 °C and 220 rpm for at least 30 minutes.

26. Adding NaOAc to 0.3 M (final concentration) and 2.1 volumes of 100% ethanol to the deacylated tRNA and precipitate overnight at -20°C.

Day 5 – FPLC purification

27. Spin precipitated deacylated tRNA in a JA-10 rotor at 9,000 RPM, 4°C for 1 hour.

28. Wash the pellets with 70% ethanol. Resuspend tRNA in 5 mL of MilliQ H_2O.

29. Filter tRNA with a 0.22 μm syringe filter.

30. Load the filtered tRNA onto 5 mL ResourceQ ion exchange column equilibrated with Buffer A on an FPLC.

31. Monitor column flow through at multiple absorbance readings (A260, A280 and A230) if possible because the tRNA may saturate the detector. Wash the column with Buffer A until the A260 reading returns to zero.

32. Elute over a linear gradient to 100% Buffer B with >15 column volumes, collecting 1.5 mL fractions.

33. Ethanol precipitate the fractions of interest overnight at -20 °C by adding 1 □L glycoblue/1.5 mL of fraction, 0.3 M NaOAc (final) and 2.1V 100% ethanol.

Day 6 – Selecting tRNA fraction

34. Spin down the ethanol precipitated tRNA at maximum speed in a refrigerated micro-centrifuge set 4°C for 45 minutes.

35. Wash the pellets with 70% ethanol and resuspend in ~20-50 □L MilliQ H_2O.

36. Estimate the tRNA concentration via absorbance at 260 nm (□ = 76,000 $M^{-1} \cdot cm^{-1}$).

37. Since tRNA can distributed throughout the peak, the ability of the components of each fraction to be aminoacylated with the amino acid of interest should be evaluated. An example of a test aminoacylation reaction is given in Table 1 for $tRNA^{Phe}$. A control (null) aminoacylation reaction with no tRNA included should be performed in parallel. Aminoacylation reactions should be run for 30 minutes at 37°C.

Reagent	Final concentration
H_2O	to 20 µL
Charging Buffer	1 ×
DTT	1 mM
ATP	10 mM
^{14}C-Phe	19.7 µM
Phe	80 µM
tRNA in fraction (estimated from A260)	5 µM
Phe-RS	1 ×

Table 6 *$tRNA^{Phe}$ aminoacylation reaction*

38. While the aminoacylation reaction is running, chill 50 mL of 10% TCA and 50 mL of 100% ethanol for 30 minutes.

39. After the reactions are complete, remove 1 µL from each reaction and spot on a piece of Whatman paper. Measure the input cpms by scintillation counting.

40. To the reaction mixtures Add 5 µL of heat denatured 10 mg/µL carrier DNA (e.g. calf thymus DNA).

41. Add 500 µL of chilled 10% TCA and pipette to mix. Place the TCA/reaction mixture on ice for 10 minutes.

42. While the TCA/aminoacyl-tRNA reaction mixtures incubate, set up a vacuum flask apparatus with microfiber glass filter paper.

43. After 10 minutes pre-wet the filter with 1 mL of cold 10% TCA and add the TCA/aminoacyl-tRNA reaction mixture to the filter.

44. Wash the precipitated aminoacyl-tRNA twice with 1.5 mL cold 10% TCA.

45. Rinse the filter with 2 mL of cold 100% ethanol.

46. Dry the filter and wash the edges of the filter paper with ethanol to remove any residual contaminates.

47. Remove the filter and measure the output counts (cpms) in a scintillation counter.

48. Use the input cpms and the concentration of unlabeled amino acid (e.g. Phe) added to the reaction to calculate the cpm/pmol for each fraction, in Equation 1.

$$cpm/_{pmol} = \frac{Input\ cpm}{Input\ amino\ acid\ concentration\ (uM)} \quad (1)$$

49. Next determine the pmols of Phe in the output, in Equation 2.

$$pmols\ amino\ acid\ output = \frac{(Output\ cpm - Null\ output\ cpm)}{\left(cpm/_{pmol}\right)} \quad (2)$$

50. Calculate the concentration of amino acid output by using Equation 3:

$$amino\ acid\ output\ (uM): \frac{pmol\ amino\ acid\ output}{reaction\ volume\ (19\ uL)} \quad (3)$$

51. Determine the percent charging with Equation 4:

$$\frac{Output\ amino\ acid\ concentration\ (uM)}{Input\ tRNA\ concentration\ (uM)} \times 100\% \quad (4)$$

52. Fractions with greater than 50% charging should be pooled and further purified.

Day 7- HPLC purification

53. Pre-equilibrate a Waters XBridge BEH C18 OBD Prep wide pore column with Buffer A.

54. Inject filtered tRNA sample onto the column on an HPLC.

55. Elute purified tRNA by setting the HPLC to run the program below. Monitor tRNA elution at 260 nm and 280 nm. Set the fraction collector to collect peaks (peak defined as a change of 50 mAU).

- **a)** Flow rate: 3.75 mL/min
- **b)** Inject
- **c)** Linear gradient to 35% buffer B over 35 minutes
- **d)** Linear gradient to 100% B over 5 minutes
- **e)** Hold 100% buffer B for 10 minutes
- **f)** Linear gradient to 0% buffer B over 1 minute

56. Pool the fractions of interest and buffer exchange into water with a 15 mL Amicon Ultra centrifugal filter (10K MWCO).

57. Ethanol precipitate pooled fractions of interest.

58. Estimate concentration via absorbance at A260 (ε = 76,000 $M^{-1} \cdot cm^{-1}$). Concentrate tRNA to ~100 µM by spinning in a 15 mL Amicon Ultra centrifugal filter (10K MWCO) if necessary.

59. Measure the absorbance of 1 µL of purified tRNA at 260 nm – this the A260/µL value required later for the calculation of acceptor activity.

Day 8 – Calculating tRNA acceptor activity

60. Prepare three reactions (Null, S100, and AA-RS) in triplicate to determine the purified tRNA acceptor activity. An acceptor activity greater than 1000 pmols/A260 unit is desired. An A260 unit is the amount of nucleic acid contained in 1 mL and producing an OD of 1 at 260 nm.

RS Charging reaction		S100 Charging reaction		Null charging reaction	
Reagent	**Final concentration**	**Reagent**	**Final concentration**	**Reagent**	**Final concentration**
H_2O	to 20 µL	H_2O	to 20 µL	H_2O	to 20 µL
Charging Buffer	1 ×	Charging Buffer	1 ×	Charging Buffer	1 ×
DTT	1 mM	DTT	1 mM	DTT	1 mM
ATP	10 mM	ATP	10 mM	ATP	10 mM
^{14}C-Phe	19.7 µM	^{14}C-Phe	19.7 µM	^{14}C-Phe	19.7 µM
Phe	80 µM	Phe	80 µM	Phe	80 µM
Phe tRNA fraction	5 µM	Phe tRNA fraction	5 µM	Phe tRNA fraction	0 µM
Phe RS	1 ×	S100	1 ×	Phe RS	1 ×

Table 7 *tRNA acceptor activity assays. Assays should include a positive control (S100) and a Null control.*

Follow the same reaction steps and calculation as a test charging reaction (steps 37-51)

60. Determine aminoacylation acceptor activity for the S100 and RS reactions with Equation 5.

$$Acceptor\ Activity\ = \frac{Average\ pmols\ of\ Phe\ output}{\left(uL\ of\ tRNA\ used\ in\ reaction \times \frac{A260}{1\ uL\ of\ tRNA}\right)} \times 1000 \qquad (5)$$

61. Compare extent of the aminoacylation in the RS and S100 reaction. Use the higher value of acceptor activity as the measure of tRNA purity.

3.6 Section 4: Preparing Aminoacylated tRNAs and mRNA

Aminoacylated-tRNAs are prepared using purified aminoacyl-tRNA synthetases (AA-RS) as previously described [29]. mRNAs used in these studies have the following sequence: 5' – GGUGUCUUGCGAGGAUAAGUGCAUUAUGXXXUAA GCCCUUCUGUAGCCA– 3' with XXX denoting the codons positioned in the ribosome A site. Unmodified mRNAs are generated by transcription with T7 polymerase. Chemically modified mRNA can be purchased from Dharmacon, Keck and IDT, or prepared by ligation as previously described [30]. UHPLC MS/MS can be used to verify the abundance but not the position of mRNA modification incorporation in commercially prepared mRNAs [9].

3.7 Section 5: Initiation complex formation and Amino Acid Addition reactions

The first step in assembling active *in vitro* translating ribosomes is to form initiation complexes (ICs). ICs consist of 70S ribosomes bound to mRNA with ^{35}S-^{f}Met-tRNA^{fMet} in the P site and can be stored at -80°C for ~3-6 months. To perform reactions, the ICs are mixed with ternary complexes (TCs) assembled immediately before the translation reactions are started. Reactions can be performed either by hand, or on a rapid quenching device (quench-flow) depending on the time-frame of the experiment. When planning experiments note that different quenching methods consume varying amounts material per timepoint (i.e. ~1 μL of IC/TC mixture per timepoint for benchtop assays vs. ~15 μL per timepoint for quench-flow).

3.7.1 Protocol

Before forming ICs and carrying out translation reactions have following components available: 1M KOH, 10X translation buffer, 10 mM GTP, 70S ribosomes, ^{35}S-^{f}Met-tRNA^{fMet}, aminoacyl-tRNA of interest, IF-1, IF-2, IF-3, EF-Tu, EF-G and mRNAs (see sections 1-4).

Part 1 - Assemble 70S E. coli Initiation Complexes (ICs)

1. Prepare a 10X mix of Initiation Factors (IFs) containing 20 μM (each) of IF-1, IF-2, and IF-3 in 1X Translation buffer. Place the IF mixture on ice.

2. Assemble ICs by mixing components and *gently* pipetting up and down: 1X Translation Buffer, 1 mM GTP, 1X IF mixture, 2 μM mRNA, 1 μM 70S Ribosomes and 2.5 μM ^{35}S-methionine-tRNA^{f}Met. Add ^{35}S-^{f}Met-tRNA^{fMet} and 70S ribosomes to the tube last.

3. Incubate IC mixture at 37ºC for 30 minutes. Pellet ICs for higher concentrations as described below and store at -80°C, or proceed directly to Part 3 – Ternary Complex Formation. Pelleting removes unbound ^{35}S-^{f}Met-tRNA^{fMet} and is recommended.

4. If pelleting ICs, pre-chill TLA 100.3 rotor and benchtop ultracentrifuge (such as a TLA-100) to 4°C. Additionally, add 1 mL cold Buffer R-D to 5 mL polycarbonate ultracentrifuge tubes and chill on ice.

Part 2 (recommended optional step) - Pellet ICs

5. After IC formation, remove 1 μL of IC and dilute in 9 μL of H_2O. Spot 1 μL of the dilution onto Whatman filter paper and measure the ^{35}S counts (cpm) by scintillation counting. This

measurement is needed to eventually calculate the final concentration of the pelleted, resuspended ICs.

6. Stabilize ICs for pelleting by raising the final concentration of Mg^{2+} to 12 mM using $MgCl_2$. Remember that 1X Translation Buffer already contains 7 mM Mg^{2+}.

7. Layer IC onto chilled Buffer R-D prepared in step 4. Place tubes in a cold TLA 100.3 rotor and spin at 69,000 X RPM, 4º C for 2 hours in a benchtop ultracentrifuge.

8. Immediately following centrifugation, place the tubes on ice.

9. Gently remove the supernatant. The pellet is glassy, fragile, and often poorly attached to the tube.

10. Resuspend each pellet in the minimum amount of 1x Translation Buffer possible (~20-100 µL). For best results, resuspend pellet by *gently* pipetting the Translation Buffer up and down slowly (up to 50 times). Avoid making the ribosome suspension bubbly.

11. Spot 1 µL of the resuspended IC onto Whatman filter paper and measure the ^{35}S counts (cpm) by scintillation counting. Aliquot the remaining pelleted IC into 5-50 µL samples, freeze in liquid N_2 and store at -80ºC.

12. Calculate percent yield, Equation , for IC formation and pelleting the equation below. A good efficiency to aim for is ≥ 60%.

$$Percent\ Yield = \frac{\left(\frac{cpm\ of\ resuspende\ \ pellet}{vol.of\ pellet\ counted\ by\ scintillation}\right) * vol.of\ resuspended\ pellet}{\left(\frac{cpm\ of IC\ formation\ reaction}{vol.of\ IC\ counted\ by\ scintillation}\right) * vol.used\ in\ IC\ formation} \quad (6)$$

13. Calculate the IC concentration using the following equation:

$$[IC] = \frac{[70S\ Ribosomes]}{\left(\frac{cpm\ of\ IC\ formation\ reaction}{vol.of\ IC\ counted\ by\ scintillation}\right)} * \left(\frac{cpm\ of\ resuspended\ pellet}{vol.of\ pellet\ counted\ by\ resuspension}\right) \quad (7)$$

Part 3 - Ternary complex (TC) formation

In contrast to ICs, TCs cannot be preassembled and frozen. The previously prepared protein and nucleic acid component of TCs (EF-Tu, EF-G and aminoacylated tRNAs) should be thawed on ice.

14. Prepare an "EFTu mix" containing final concentrations of 1X translation buffer, 10 mM GTP and 20 μM EFTu. Incubate EFTu mix at 37°C for 15 minutes. The volume of EFTu mix required will vary depending on the scale of the experiment and should be ~1/3 of the total volume of the planned translation assay.

15. While the EF-Tu mix is incubating, prepare a "tRNA mix" containing final concentrations of 1X translation buffer, 10 mM GTP, 10-20 μM aa-tRNA^{aa}. If your investigations involve the formation of more than a single peptide bond, include 24 μM EFG in the tRNA mix to enable translocation. Keep tRNA mix on ice for 10-15 minutes. The volume of tRNA mix required will vary depending on the scale of the experiment and should be ~1/3 of the total volume of the planned translation assay.

16. Form ternary complexes (TCs) by combining equal volumes of the EFTu mix and tRNA mixes and incubating at 37°C for 10 minutes.

Part 4 - Amino acid addition time courses

17. Before running reactions decide on a set of 8-12 timepoints. If your reaction is are slow enough to stop timepoints by hand (3 seconds or longer) prepare a series of quench tubes containing 1 μL KOH prior to beginning assays. If the timepoints are fast enough to need a quench-flow apparatus (e.g. KinTek Model RQF-3) load 1M KOH as the quench.

18. If using frozen ICs, thaw on ice. Make a 160-180 nM solution of ICs in 1X translation buffer for use in your reaction. Immediately freeze any remaining thawed IC.

19. Initiate translation reactions by mixing equal volumes of ICs and TCs. For reactions performed on the benchtop that is quenched by hand, this usually means mixing 4-6 □L of ICs with TCs to make a 8-12 μL reaction. Much larger volumes (> 120 μL of IC and TC) are required for experiments conducted on the quench flow. Reactions can be carried out at room temperature or 37°C.

20. For slower reactions performed on the bench-top, transfer 1 μL of translation reaction to a KOH quench tube prepared in step 17 at each of the pre-selected time points. Review your quench-flow manual for information about how to quench time points 3 seconds or faster.

22. Quenched timepoints can be stored at -20°C or worked up as described in section 7.

Note: If storing samples for extended periods of time, consider neutralizing timepoints with acetic acid.

3.8 : Miscoding Screening Assays

Miscoding screening assays use the endpoint level of overall miscoded dipeptide product to evaluate if a modification alters the fidelity of amino acid incorporation. Screening assays are much like the general translation assays described in section 5, only TCs are formed with a mixture of aminoacylated total-tRNA. Controls should be run concurrently to confidently identify the miscoded dipeptide products. Specifically, make sure to include: 1) a null reaction performed with TCs formed without any aminoacyl-total tRNA, 2) a positive control with the correctly charged aminoacyl-tRNA, and 3) a reaction with ICs formed on mRNA with an unmodified codon. These assays only provide qualitative insights and results should be verified with the careful kinetic assays presented in section 6.2.

3.8.1 Protocol

Part 1- Aminoacylate total tRNA

1. Aminoacylate total tRNA by combining, in order, the following reagents (final concentrations given) on ice: MilliQ H_2O, 1X buffer KF, 0.1 mM amino acid mixture (each amino acid is present at 0.1 mM), 3 mM ATP, 8 mM total RNA, 1 X S100.

2. Incubate at 37° C for 20 minutes.

3. Add NaOAc pH 5.2 to a final concentration of 0.3 M.

4. Perform two sequential acid phenol extraction and a chloroform extraction.

5. Desalt the final aqueous layer using a Bio-Rad P6 spin column or equivalent.

6. To precipitate tRNA, add NaOAc to 0.3 M final and 2.3 volumes of 100% ethanol for at least two hours at - 20ºC.

7. Spin the ethanol precipitation at maximum speed in a refrigerated microfuge for 30 minutes at 4°C. Remove the supernatant and resuspend pellet in ~20 μL 20mM KOAc, pH 5.2.

8. Approximate the overall concentration of aminoacyl-total tRNA by absorbance at 260 nm (ε = 76,000 M^{-1} •cm^{-1})

Note: This is an *estimated* concentration, there is no way to determine the charging efficiency of the S100 or acceptor activity of each tRNA.

9. Aliquot aminoacyl-total tRNA and store at -80°C.

Note: Select aliquot sizes keeping in mind that aminoacyl-total tRNA samples can become significantly deacylated after three or more freeze/thaw cycles.

Part 2- Perform miscoding screening assay

10. Assemble total-TCs by combining, in order, the following reagents (final concentrations given) on ice: water, 1X translation buffer, 8 mM GTP, 4 □M aminoacyl-total tRNA, 30 μM EF-Tu. Incubate total-TC reaction at 37 °C for 15 min.

11. While the total-TCs incubate, prepare ICs as in Section 5. If using frozen ICs, thaw on ice. Make a 200 nM solution of ICs in 1X translation buffer for use in your reaction. Immediately freeze any remaining thawed IC.

12. Initiate miscoding screening reaction by mixing equal volumes of total-TCs with ICs (final concentration 100 nM ribosomes, 2 μM aminoacylated-total tRNA). Typically, small volumes (~1-2 μL of total-TC and IC) are used in these reactions. Incubate at 37 °C for 15 minutes. The control reactions discussed above should be set up in parallel.

13. Quench each reaction by adding 1 μL of 1 M KOH. Visualize the resulting peptide products by eTLC as described in section 8.

3.9 . Measuring Rate constants for Miscoding

To develop an understanding of how different modifications impact miscoding, single turnover kinetic assays should be employed. Due to the ribosome's stringent proofreading mechanisms an energy regeneration mix is used to produce multiple rounds of accommodation, while remaining single turnover with respect to peptidyl transfer, thus producing measurable amounts of miscoded dipeptide product. The energy regeneration mix consists of the ternary complex with the addition of EFTs, pyruvate kinase (PK) and phosphoenolpyruvate (PEP). This protocol is adapted from previous work [18]. Before starting this miscoding assay, it is important to ensure saturating levels aminoacyl-tRNA are being used (typically 5-10 μM). These reactions have a $t_{1/2}$ of ~2 minutes, permitting reactions to manually quenched.

3.9.1 Protocol

1. As in section 5, determine a time-course and set-up a series of tubes containing 5 μL 1 M KOH.

2. Prepare 1 μM ICs in 1X-translation buffer as described in section 5.

3. Assemble the EF-Tu/Ts mixture by combining the following reagents on ice:

Reagent	Concentration in mixture	Final reaction concentration
Water	–	to 500 µL
10 × Translation Buffer	1.1 ×	1 ×
GTP	1.11 mM	1 mM
$MgCl_2$	7.77 mM	7 mM
EF-Tu	44.44 µM	40 µM
EF-Ts	11.11 µM	10 µM
PEP	3.33 mM	3 mM
PK	0.11 mM	0.1 mM

Table 8 *EF-Tu/Ts mixture for miscoding kinetic assays*

4. Incubate the EFTu/Ts mixture at 37 °C for 15 min.
5. Add 1.11 µM of the aminoacyl-tRNA of interest. Incubate at 37 °C for 10 minutes to form miscoding ternary complexes (MC-TCs).
6. Initiate translation reactions by adding the MC-TC to IC in a 10:1 ratio at room temperature.
7. For each timepoint, transfer 1 µL of the reaction to a tube containing 1µL 1 M KOH.
8. After approximately 5 minutes, add 2 µL of 5 M acetic acid to each quenched tube.
9. Spot 1 µL of the quenched and neutralized reaction in 0.8-1 cm increments on a cellulose TLC plate to visualize reactions as described in section 8.

3.10 : Quantification and Kinetic Analysis

Electrophoretic thin layer chromatography (eTLC) separates small charged species by size and charge, similar to isoelectric focusing. Below we describe how to use this method to visualize the unreacted ^{f}Met and small peptide products in the translation reactions generated in sections 5-7. Following separation, the different ^{35}S-labeled species can be detected via scintillation counting or phosphorescence (as is used in this protocol). Volatile buffers are used for separation so that the TLC plates are dry prior to exposure to phosphorscreens. Different peptide compositions and charge states affect separation and resolution. Consider the pI of potential peptides to be synthesized and choose an appropriate pH and composition for your eTLC buffer. An example set-up with buffer system is shown in Figure 2A.

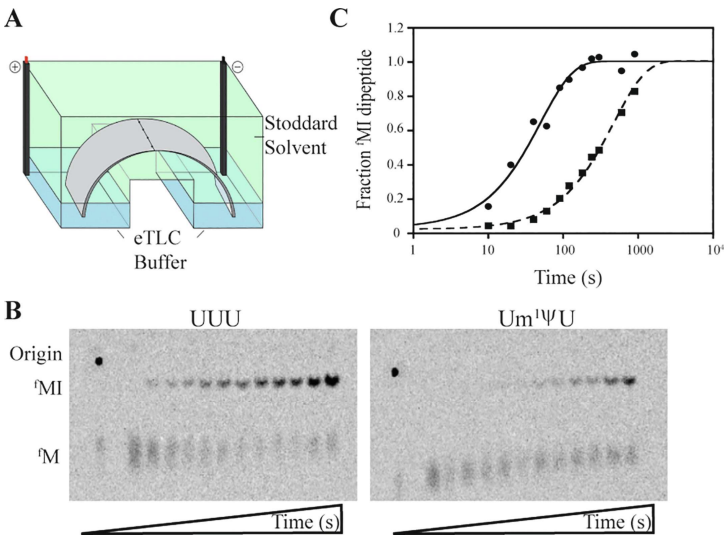

Figure 10 *Visualizing translation products by electrophoretic thin-layer chromatography (eTLC).(**A**) TLC electrophoresis tank used in this protocol. (**B**) Example eTLC plate after separation and phosphorimaging. Time courses of miscoding product formed when Ile-tRNA^{Ile} TCs are mixed with ICs programmed with phenylalanine codons (UUU and Um^{1}ΨU) in the A site. (**C**) Representative curves fit of MI dipeptide formed during experiment shown in (**B**). Data from Ile added on UUU [circle] or Um^{1}ΨU [square] are fit with the equation* $[MI]_{Eq} = [M]_0 * e^{-(k_{obs})t}$ *to determine the observed rate constants (k_{obs}).*

3.10.1 Protocol

1. Spot 1.0 µL of each timepoint onto a cellulose eTLC plate, leaving ~1 cm between spots.

3. Wet TLC plate with the selected buffer (most commonly pyridine acetate buffer, pH 2.8).

4. Run TLC for 10-50 minutes in an electrophoresis tank pyridine acetate buffer in the cathode and anode reservoirs and an organic, nonpolar solvent – such as Stoddard Solvent – as a liquid stationary phase (Figure 2A). Peptide charge state and pI affect separation in this system and longer times may be needed for full separation and resolution of peptide products.

5. Remove TLCs from the tank and dry completely with a heat gun.

6. Once dry, wrap TLCs in plastic wrap and expose them against a phosphorscreen for 1-48 hours. The specific activity of the radiolabel and dilution state of samples will dictate exposure time.

7. Scan phosphorscreen in an instrument capable of imaging in a phosphorescence mode, scanning at a voltage of 4000 PMT and a resolution of 100 μm.

8. Using the image analysis software of your choice (e.g. ImageQuant or ImageJ) quantify phosphorescence signals to obtain percent and volume of peptide species at each time point in the assay.

3.11 References

[1] Gromadski KB, Rodnina MV. Kinetic Determinants of High-Fidelity tRNA Discrimination on the Ribosome. Molecular Cell 2004;13:191–200. https://doi.org/10.1016/S1097-2765(04)00005-X.

[2] Steiner RE, Ibba M. Regulation of tRNA-dependent translational quality control. IUBMB Life 2019;71:1150–7. https://doi.org/10.1002/iub.2080.

[3] Kapur M, Ackerman SL. mRNA Translation Gone Awry: Translation Fidelity and Neurological Disease. Trends Genet 2018;34:218–31. https://doi.org/10.1016/j.tig.2017.12.007.

[4] Garrett S, Rosenthal JJC. RNA Editing Underlies Temperature Adaptation in K+ Channels from Polar Octopuses. Science 2012;335:848–51. https://doi.org/10.1126/science.1212795.

[5] Drummond DA, Wilke CO. The evolutionary consequences of erroneous protein synthesis. Nat Rev Genet 2009;10:715–24. https://doi.org/10.1038/nrg2662.

[6] Pan T. Adaptive translation as a mechanism of stress response and adaptation. Annu Rev Genet 2013;47:121–37. https://doi.org/10.1146/annurev-genet-111212-133522.

[7] Jackman JE, Alfonzo JD. Transfer RNA modifications: Nature's combinatorial chemistry playground. Wiley Interdiscip Rev RNA 2013;4:35–48. https://doi.org/10.1002/wrna.1144.

[8] Hudson BH, Zaher HS. Ribosomes Left in the Dust: Diverse Strategies for Peptide-Mediated Translation Stalling. Mol Cell 2014;56:345–6. https://doi.org/10.1016/j.molcel.2014.10.023.

[9] Eyler DE, Franco MK, Batool Z, Wu MZ, Dubuke ML, Dobosz-Bartoszek M, et al. Pseudouridinylation of mRNA coding sequences alters translation. Proc Natl Acad Sci U S A 2019;116:23068–74. https://doi.org/10.1073/pnas.1821754116.

[10] Hoernes TP, Clementi N, Juen MA, Shi X, Faserl K, Willi J, et al. Atomic mutagenesis of stop codon nucleotides reveals the chemical prerequisites for release factor-mediated peptide release. Proc Natl Acad Sci USA 2018;115:E382–9. https://doi.org/10.1073/pnas.1714554115.

[11] Dunkle JA, Dunham CM. Mechanisms of mRNA frame maintenance and its subversion during translation of the genetic code. Biochimie 2015;114:90–6. https://doi.org/10.1016/j.biochi.2015.02.007.

[12] Jones JD, Monroe J, Koutmou KS. A molecular-level perspective on the frequency, distribution, and consequences of messenger RNA modifications. WIREs RNA 2020;11:e1586. https://doi.org/10.1002/wrna.1586.

[13] Andries O, Mc Cafferty S, De Smedt SC, Weiss R, Sanders NN, Kitada T. N1-methylpseudouridine-incorporated mRNA outperforms pseudouridine-incorporated mRNA by providing enhanced protein expression and reduced immunogenicity in mammalian cell lines and mice. Journal of Controlled Release 2015;217:337–44. https://doi.org/10.1016/j.jconrel.2015.08.051.

[14] Sahin U, Karikó K, Türeci Ö. mRNA-based therapeutics — developing a new class of drugs. Nature Reviews Drug Discovery 2014;13:759–80. https://doi.org/10.1038/nrd4278.

[15] Pardi N, Hogan MJ, Porter FW, Weissman D. mRNA vaccines — a new era in vaccinology. Nat Rev Drug Discov 2018;17:261–79. https://doi.org/10.1038/nrd.2017.243.

[16] Karikó K, Muramatsu H, Welsh FA, Ludwig J, Kato H, Akira S, et al. Incorporation of Pseudouridine Into mRNA Yields Superior Nonimmunogenic Vector With Increased Translational Capacity and Biological Stability. Mol Ther 2008;16:1833–40. https://doi.org/10.1038/mt.2008.200.

[17] Nirenberg MW, Matthaei JH. The dependence of cell-free protein synthesis in E. coli upon naturally occurring or synthetic polyribonucleotides. PNAS 1961;47:1588–602. https://doi.org/10.1073/pnas.47.10.1588.

[18] Rodnina MV, Wintermeyer W. Fidelity of Aminoacyl-tRNA Selection on the Ribosome: Kinetic and Structural Mechanisms. Annu Rev Biochem 2001;70:415–35. https://doi.org/10.1146/annurev.biochem.70.1.415.

[19] Dever TE, Dinman JD, Green R. Translation Elongation and Recoding in Eukaryotes. Cold Spring Harb Perspect Biol 2018;10. https://doi.org/10.1101/cshperspect.a032649.

[20] Pape T, Wintermeyer W, Rodnina MV. Complete kinetic mechanism of elongation factor Tu-dependent binding of aminoacyl-tRNA to the A site of the E. coli ribosome. EMBO J 1998;17:7490–7. https://doi.org/10.1093/emboj/17.24.7490.

[21] Rivera MC, Maguire B, Lake JA. Isolation of Ribosomes and Polysomes. Cold Spring Harb Protoc 2015;2015:pdb.prot081331. https://doi.org/10.1101/pdb.prot081331.

[22] Cammack KA, Wade HE. The sedimentation behaviour of ribonuclease-active and -inactive ribosomes from bacteria. Biochem J 1965;96:671–80.

[23] Rodnina MV, Wintermeyer W. GTP consumption of elongation factor Tu during translation of heteropolymeric mRNAs. Proc Natl Acad Sci U S A 1995;92:1945–9.

[24] Soffientini A, Lorenzetti R, Gastaldo L, Parlett JH, Spurio R, La Teana A, et al. Purification procedure for bacterial translational initiation factors IF2 and IF3. Protein Expr Purif 1994;5:118–24. https://doi.org/10.1006/prep.1994.1018.

[25] Dahlquist KD, Puglisi JD. Interaction of translation initiation factor IF1 with the E. coli ribosomal A site. J Mol Biol 2000;299:1–15. https://doi.org/10.1006/jmbi.2000.3672.

[26] Shimizu Y, Inoue A, Tomari Y, Suzuki T, Yokogawa T, Nishikawa K, et al. Cell-free translation reconstituted with purified components. Nat Biotechnol 2001;19:751–5. https://doi.org/10.1038/90802.

[27] Studer SM, Joseph S. Binding of mRNA to the Bacterial Translation Initiation Complex. Methods in Enzymology, vol. 430, Elsevier; 2007, p. 31–44. https://doi.org/10.1016/S0076-6879(07)30002-5.

[28] Studier FW. Protein production by auto-induction in high density shaking cultures. Protein Expr Purif 2005;41:207–34. https://doi.org/10.1016/j.pep.2005.01.016.

[29] Walker SE, Fredrick* K. Preparation and evaluation of acylated tRNAs. Methods 2008;44:81–6. https://doi.org/10.1016/j.ymeth.2007.09.003.

[30] Keedy HE, Thomas EN, Zaher HS. Decoding on the ribosome depends on the structure of the mRNA phosphodiester backbone. PNAS 2018;115:E6731–40. https://doi.org/10.1073/pnas.1721431115.

Chapter 4 N1-Methylpseudouridine and Pseudouridine Modifications Impact Amino Acid Misincorporation during Translation

Work presented in this chapter is included in a manuscript of the same title by Jeremy Monroe, Lili Mitchell, Indrajit Deb, Bijoyita Roy, Aaron Frank, Kristin Koutmou. Jeremy Monroe performed the *in vitro* translation system experiments, analyzed the data and wrote the paper, Lili Mitchell and Bijoyita Roy contributed the *in cellular* work in HEK293 cells as well as the mass spectrum analysis of the luciferase protein miscoding events. Indrajit Deb and Aaron Frank performed the molecular modeling calculations and help in analyzing the results. Aaron Frank created Figure 4D. Kristin Koutmou helped with experiment design and editing the manuscript drafts. Kristin Koutmou contributed Figure 4 A,B,C.

4.1 Introduction

Chemically modified nucleosides are present in all organisms, often playing essential roles in key cellular processes including splicing and translation [1–6]. Defects in ribosomal RNA (rRNA) and transfer RNA (tRNA) modifying enzymes are linked to a host of deleterious human health issues, illustrating the importance of RNA modifications in protein synthesis [7–10]. There are over 150 unique modifications reported in RNAs that range in size and complexity from isomerized or protonated nucleosides (e.g. pseudouridine and dihydrouridine) to large chemically diverse functional groups (e.g. NAD^+, N(6)-threonylcarbamoyladenosine, glycan and farnesyl) [1,2,11,12]. RNA modifications have been widely studied for almost three quarters of a century and until recently were thought to be almost exclusively incorporated into non-coding RNA species (ncRNAs). However, the transcriptome wide mapping of 13 RNA modifications revealed that protein coding messenger RNAs (mRNAs) can also contain modifications at thousands of

sites [13–22]. This discovery has raised the possibility that mRNA modifications might play a previously underappreciated role in post-transcriptionally regulating gene expression [2,13,14].

The majority of enzymes that modify mRNAs also catalyze their incorporation into ncRNAs central to protein synthesis [23]. Like their protein post-translational counterparts, mRNA post-transcriptional modifications are generally present at sub-stoichiometric levels, with transcripts existing in a mixed population of modified and unmodified states [18,24–27] . Together these circumstances make ascertaining the impact of mRNA modifications on translation challenging. In cells, any changes to protein output observed when RNA modifying enzymes are removed cannot be directly attributed to alterations in a particular mRNA's modification status. Therefore, studies using reconstituted translation systems, where it is possible to uniformly change the modification status of mRNAs without impacting that of ncRNAs, have been particularly useful for assessing the consequences of mRNA modifications on translation [28]. Initial studies reveal that modifications commonly slow the ribosome, though some only do so only in particular mRNA sequence contexts [28]. Additionally, a handful of mRNA modifications, including pseudouridine (Ψ) and inosine (I), also impact the accuracy of mRNA decoding [29–32]. These findings suggest that there is a broad range of possible consequences when the ribosome encounters an mRNA modification. Developing a framework for understanding how individual modifications impact translation in differing sequence contexts will be crucial as researchers seek to uncover which of the thousands of chemically modified positions reported in mRNA codons are the most likely to have consequences for protein synthesis in cells.

In addition to being present in naturally occurring RNA molecules, modifications are also heavily incorporated in RNA-based therapeutics and mRNA vaccines [33–36]. Indeed, the mRNA transcripts that form the basis of the currently available COVID-19 mRNA vaccines substitute

every uridine nucleoside with N1-methylpseudouridine ($m^1\Psi$) [37]. The addition of $m^1\Psi$ reduces the cellular innate immune response to dramatically stabilize the mRNA transcript, and ultimately increase the amount of protein synthesized [38–41]. Recent studies in a lysate-based translation system suggests that $m^1\Psi$ slows the ribosome in a manner that can be alleviated by the addition of membranes [42]. However, there is limited information available directly measuring how $m^1\Psi$ influences the rate and accuracy of amino acid addition. This is an important question to ask because $m^1\Psi$ shares much of its structure with pseudouridine (Ψ) (Figure 1A), a modification that has been shown to change translation speed and tRNA selection [29,43,44]. Even subtle changes in translation rates or fidelity have the potential to impact protein folding or function [45–47]. Therefore, establishing if there are situations in which $m^1\Psi$ can alter translation will be critical for the continued development of mRNA-based therapeutics and vaccines in addition to understanding how different types of chemical moieties impact translation.

To establish the molecular level consequences of Ψ and $m^1\Psi$ codon modifications on ribosome decoding, we compared the translation of unmodified, Ψ- and $m^1\Psi$- modified codons in both a fully reconstituted *E. coli in vitro* translation system and HEK293 cells. Our studies reveal that in contrast to Ψ, $m^1\Psi$ does not reduce the rate constant for cognate amino acid addition. However, $m^1\Psi$ does influence the accuracy of amino acid addition. We demonstrate that Ψ and $m^1\Psi$ can either reduce or enhance non-cognate tRNA selection depending on the surrounding sequence context. Our computational modeling approaches suggest that changes in the enthalpy of mRNA:tRNA interactions likely account for the observed context dependent effects of these modifications. Additionally, they reveal a potential interplay between tRNA and mRNA modifications; with tRNA hypermodifications adjacent to the anti-codon sequence contributing to changes in how the ribosome reads modified mRNA codons. The dynamic modulation of the

ribosome decoding by modifications within the coding region of mRNA transcripts has implications for the translation speed and accuracy of the ribosome and its successful use in mRNA therapeutics.

4.2 Results

4.2.1 $m^1\Psi$ modestly impacts the rate constant for Phe addition and $K_{1/2}$ for peptide release

We used a fully reconstituted *E. coli in vitro* translation system to evaluate the consequences of incorporating $m^1\Psi$ into mRNA codons on translation elongation and termination. In contrast to reporter-based studies in cells and lysates, the *in vitro* system we implemented is not influenced by extra-translational factors that can change observed protein levels (e.g. RNases and proteases) and allows us to directly examine individual steps along the translation pathway with high resolution [23]. This system is particularly well suited to studying translation elongation because tRNA binding sites and ribosome peptidyl-transfer center are highly conserved between eukaryotic and prokaryotic ribosomes [48,49].

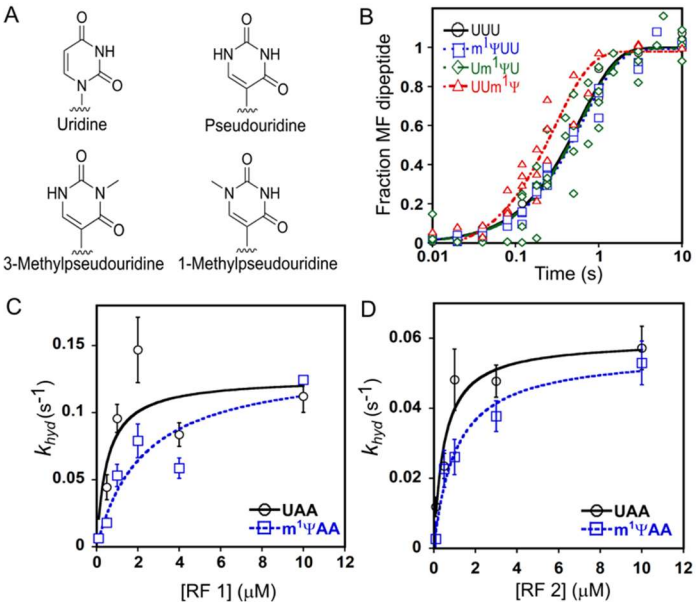

Figure 11 *$m^1\Psi$ modestly increases cognate amino acid addition in a position dependent manner.* ***(A)*** *The chemical structure of the nucleotide bases investigated.* ***(B)*** *The rates of amino acid addition for a phenylalanine (UUU) codon modified at either the first, second, or third position with N1-methylpseudourine.* ***(C)*** *The K ½ curve of RF1 on an UAA or $m^1\Psi$ modified codon.* ***(D)*** *The K ½ curve of RF2 on an UAA or $m^1\Psi$ modified codon.*

The rate constants for amino acid addition were measured on unmodified (UUU) and $m^1\Psi$ modified ($m^1\Psi$UU, Um$^1\Psi$U, and UUm$^1\Psi$) Phe codons (Figure 1A). We chose to first evaluate amino acid incorporation rates on a UUU codon because the kinetics of Phe addition on UUU is well established, and UUU codons are present in the mRNA COVID-19 vaccines [37]. Our translation reactions are initiated by mixing *E. coli* 70S ribosome initiation complexes (ICs; ^{35}S-labeled formylmethionine-tRNA^{fMet} bound to an AUG in the P site and Phe codon in the A site) with an excess of ternary complexes (TCs; Phe-tRNA^{Phe}•EF-Tu•GTP). They are subsequently quenched at select time points, and the unreacted ^{35}S-^{f}Met and ^{35}S-^{f}MetPhe products are visualized by electrophoretic TLC (eTLC) (SI Figure 1A). These studies reveal that cognate Phe incorporation on $m^1\Psi$ modified codons is largely unchanged, though we observe a slight (2 ± 0.3 -fold) increase in the rate constant for Phe addition when $m^1\Psi$ is in the third position in the codon (Figure 1B, SI Figure 1B, SI Table 1).

All three stop codons begin with uridine (UAA, UAG, UGA) ensuring that modified stop codons will be present in synthetic mRNA-based vaccines and therapeutics. We evaluated the ability of class I release factors (RF1 and RF2) to hydrolyze peptidyl-tRNA bonds and terminate translation on $m^1\Psi$ modified stop codons. To accomplish this, we reacted termination complexes

(*E. coli* 70S ribosomes with ^{35}S-labeled formylmethionine-tRNA^{fMet} bound to an AUG in the P site, and a universal stop codon positioned in the A site (UAA, m^{1}ΨAA)) with varying concentrations of the class I release factors RF1 and RF2 (0.1-10 μM). The reactions were quenched at a range of time points and ^{35}S-^{f}Met hydrolyzed by RFs was detected on an eTLC (SI Figures 2 and 3). At saturating levels of the RF1and RF2 the rate constants for peptide release ($k_{hyd,max}$) on UAA and m^{1}ΨAA codons are equivalent (~ 0.1 s^{-1}) and comparable previously published termination rates on an unmodified UAA codon (SI Tables 2 and 3) [50,51]. However, this was not the case at sub-saturating conditions, as reflected by the 2- to 4-fold increase in $K_{1/2}$ values obtained for peptidyl-tRNA hydrolysis by RF1 and RF2 on a m^{1}ΨAA (Figure 1C-D, SI Tables 2 and 3). The re-distribution of the electronegativity around the pyrimidine ring in m^{1}Ψ can weaken the hydrogen bonding network between the first two nucleotides of the stop codon and release factors, perhaps accounting for this observation [51,52]. Nonetheless, because $k_{hyd,max}$ is unperturbed we do not expect m^{1}Ψ to impede translation termination in cells unless the concentration of release factors becomes severely limited. This supposition is supported by numerous observations that reporter peptides generated from fully m^{1}Ψ-substituted mRNAs yield protein products of the expected length [38,53].

We also examined how the ribosome treats modifications at the P-site, using a previously described P-site surveillance mechanism[50]. We observed that the ribosome surveils modified mismatched codon-anticodon interactions at the P-stie in the same manner as unmodified mismatches (SI Figure 4).

4.2.2 m^{1}Ψ alters aminoacyl-tRNA selection by the ribosome in a context dependent manner

Chemical modifications to nucleobases can increase the propensity of the ribosome to incorporate alternative amino acids into a growing polypeptide chain [28–31,54–56]. Relative to

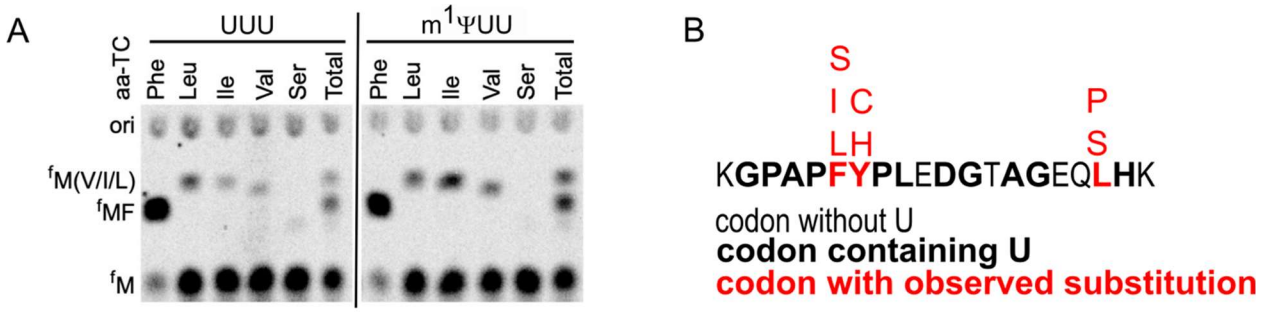

Figure 12 *m1Ψ impacts amino acid selectivity. Amino acids from near-cognate and noncognate tRNA are incorporated into $m^1\Psi$ containing codons. **(A)** A representative electrophoretic TLC displaying dipeptide products from an unmodified UUU and $m^1\Psi$ modified codon $m^1\Psi$UU. **(B)** Summary of amino acid substitutions observed by mass spectrometry in a luciferase peptide incorporated on $m^1\Psi$-containing mRNAs translated in HEK293 cells.*

uridine, $m^1\Psi$ possesses a repositioned, methylated nitrogen in its pyrimidine ring (Figure 1A). The modifications provide $m^1\Psi$ the opportunity to change both the conformational fit of an mRNA in the ribosome, and the variety of mRNA:tRNA base pairing interactions possible. Consistent with this idea, Ψ, which shares a repositioned nitrogen with $m^1\Psi$, was previously shown to enhance the reaction of near-cognate tRNAs on UUU codons *in vitro* and in HEK293 cells [29,30]. To determine if $m^1\Psi$ similarly influences aa-tRNA selection, we presented 70S *E. coli* initiation complexes formed with unmodified (UUU) and modified ($m^1\Psi$UU, U$m^1\Psi$U, and UU$m^1\Psi$) codons in the A site with EF-Tu containing ternary complexes formed using a mixture of total tRNA aminoacylated with a single aminoacyl tRNA synthetase and amino acid for each respective tRNA (Ser-$tRNA^{Ser}$, Leu-$tRNA^{Leu}$, Ile-$tRNA^{Ile}$ and Val-$tRNA^{Val}$). We observed a 2- to 3- fold enhancement in the levels of miscoded Met-Ile (MI) and Met-Ser (MS) peptides formed on $m^1\Psi$UU and UU$m^1\Psi$ codons relative to an unmodified UUU codon (Figure 2A and SI Figure 4).

Subsequently, we measured the single-turnover rate constants (k_{obs}) for amino acid mis-incorporation on unmodified and $m^1\Psi$ substituted Phe (UUU) codons at saturating concentrations of individually purified charged aa-tRNA (Figure 3, SI Figures 5 and 6). An energy regeneration mix was added to our reactions to permit the reformation of ternary complexes (aa-tRNA:EF-Tu:GTP) after an aa-tRNA is rejected by the ribosome [57]. Based on our endpoint results (Figure

2A) we selected three near-cognate native tRNAs to study ($tRNA^{Ile(UAG)}$, $tRNA^{Leu(GAC)}$ and $tRNA^{Ser(UGA)}$). We find that tRNA identity and the position of $m^1\Psi$ within a codon influence the rate constants for amino acid substitution (SI Table 4). $m^1\Psi$ substitution at the first position in the Phe codon ($m^1\Psi UU$) does not change the k_{obs} values for Leu or Ser incorporation but increases rate constant for Ile addition by 3 ± 0.3-fold (Figure 3A-D, SI Table 4). This differs markedly from what we observed on $Um^1\Psi U$-modified codons, which have a much larger effect on tRNA selection. The k_{obs} values are significantly reduced for Ile (6.5 ± 0.5-fold) and Leu (4 ± 1-fold) addition, while the rate constant for Ser mis-incorporation is conversely increased by 6 ± 1.6-fold (Figure 3A-D, SI Table 4). Substitution at the wobble position ($UUm^1\Psi$) generally had modest impacts on the rate constants for amino acid incorporation; decreasing the k_{obs} for Leu addition (2 ± 0.5-fold), while marginally increasing the k_{obs} values for Ile and Ser addition by 1.5 ± 0.25-fold and 2 ± 0.5 -fold, respectively (Figure 3, SI Table 4).

4.2.3 Uridine isomerization largely accounts for observed changes in amino acid substitution on $m^1\Psi$ containing codons

We sought to determine the contributions of uridine isomerization and methylation to $m^1\Psi$ mediated changes in the rate constants for amino acid mis-incorporation. To approach this question, we measured the rate constants for Leu, Ile and Ser mis-incorporation on Ψ modified Phe codons (ΨUU, UΨU and UUΨ) (SI Figure 8). Ψ was selected for study because it contains the same isomerization as $m^1\Psi$, but lacks the methylation a N1 (Figure 1A). The impact of Ψ on Ile and Leu insertion was similar to what we observed when $m^1\Psi$ is present in codons (Figure 3B, F). For example, the rate constant for Ile is significantly decreased (11 ± 6-fold) when Ψ is incorporated at the second codon position (UΨU), while Leu is added more slowly when Ψ is at

all three positions in the codon (Figure 3B,F, SI Table 5). In contrast to what we observed on $m^1\Psi$, Ser incorporation occurs with a 6 to 7-fold faster rate constants when Ψ is at the first and second positions in the codon, and is not influenced by Ψ substituted at the wobble position (UUΨ). Our findings suggest that uridine isomerization accounts for changes in how the ribosome decode some tRNAs ($tRNA^{Ile(UAG)}$, $tRNA^{Leu(GAC)}$), but that other changes induced by the methylation to N1 likely make larger contributions to changes to others ($tRNA^{Ser\ (UGA)}$) (Figure 4A).

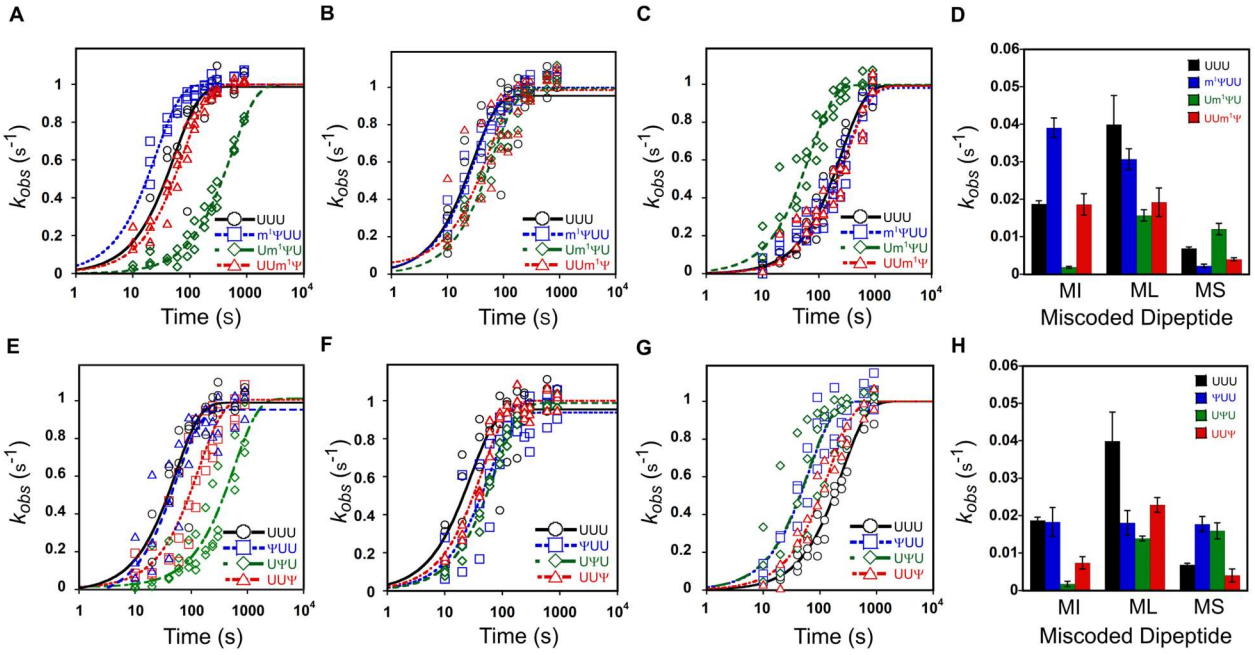

Figure 13 *Ψ and m1Ψ impact the rates of the ribosome reacting with near-cognate tRNAs in a sequence context dependent manner. The rates of miscoded dipeptide formed on phenylalanine (UUU) codon modified with either at first, second, or third position with N1-methylpseudouridine or pseudouridine. (**A**) The rate of MI dipeptide from a $m^1\Psi$ modified UUU codon when presented with a UAG anticodon. (**B**) The rate of ML dipeptide from a $m^1\Psi$ modified UUU codon when presented with a GAC anticodon. (**C**) The rate of MS dipeptide from a $m^1\Psi$ modified UUU codon when presented with a AGU anticodon. (**D**) A comparison of misincorporation rates for isoleucine, leucine, and serine amino acids on a $m^1\Psi$ modified and unmodified UUU codon. (**E**) The rate of MI dipeptide from a Ψ modified UUU codon when presented with a UAG anticodon. (**B**) The rate of ML dipeptide from a Ψ modified UUU codon when presented with a GAC anticodon. (**C**) The rate of MS dipeptide from a Ψ modified UUU codon when presented with a AGU anticodon. (**D**) A comparison of misincorporation rates for isoleucine, leucine, and serine amino acids on a Ψ modified and unmodified UUU codon.*

4.2.4 Amino acid substitution increased on some $m^1\Psi$ containing codons observed in HEK293 cells

Our *in vitro* translation data reveal that $m^1\Psi$ and Ψ can alter tRNA selection by *E. coli* ribosomes in different ways depending on sequence context. We next asked if $m^1\Psi$ has similar effects on amino acid selection in eukaryotic cells when synthetic mRNAs are completely substituted with $m^1\Psi$ and translated in HEK293 cells. We transfected HEK293 cells with luciferase encoding mRNA transcribed *in vitro* with either uridine or $m^1\Psi$. The base composition of the unmodified and modified mRNAs was assessed by liquid chromatography-mass spectrometry (LC-MS), and is consistent between the unmodified and modified mRNA species we generated (SI Figure 9). We observed an increase in luciferase protein expression in the $m^1\Psi$-substituted mRNAs, consistent with previous reports (SI Figure 10-11) [29]. The luciferase proteins generated from both unsubstituted and $m^1\Psi$-substituted mRNAs were purified and analyzed by mass spectrometry to identify amino acid substitutions. The mass spectrometry data analyses focused on a specific luciferase peptide with favorable ionization characteristic [58]. Total amino acid substitution observed within this peptide from the $m^1\Psi$ mRNAs equated to ~0.8% of the observed peptides. Serine, isoleucine, and leucine amino acid substitutions were observed on two Phe codons (UUU and UUC), with an increased frequency of substitution over peptide from unmodified mRNA. Additionally, the likelihood of substitutions occurring was not uniform across $m^1\Psi$ containing codons. The levels of miscoding that we detect are consistent with what we would predict from our *in vitro* studies, as is the heterogeneity of amino acid substitution on $m^1\Psi$-modified codons. Furthermore, the lack of uniformity in amino acid substitution was also seen in our previous findings indicating that Ψ also increases the levels of amino acid misincorporation in the same luciferase reporter peptide [58]. Our results collectively suggest that the extent of misincorporation on any codon containing a C5-glyocside uridine isomer largely depends on the sequence context in which the modification is present.

4.2.5 Modifications change the energetics of interactions between mRNA nucleosides and mRNAs with tRNAs in a position dependent manner

We sought to understand how Ψ and $m^1Ψ$ modifications change the interactions between mRNAs and tRNAs during translation in a position dependent manner (Figures 1-3). To approach this question we used molecular modeling (MM) and quantum mechanical calculations to examine unmodified and Ψ-, $m^1Ψ$- and 3-methylpseudouridine ($m^3Ψ$–) modified UUU mRNA codons interacting with cognate ($tRNA^{Phe}$, UUU:AAG) and near-cognate ($tRNA^{Ile}$,UUU:UAG) tRNAs in a portion of the ribosome active site (Figure 1A). Although we did not investigate the translation of $m^3Ψ$-containing codons, we included $m^3Ψ$ in our computational studies as a positive control for a modification that will abolish mRNA:tRNA interactions; methylation at the uridine N3 position removes the ability of uridine to donate a hydrogen bond and should severely limit tRNA binding. Our MM studies were conducted using models developed based on previously published crystal structures of the 70S *E. coli* ribosome bound with $tRNA^{Phe}$ bound to a ΨUU codon [58]. The MM studies were designed to examine how the location of the modification impacts the pairwise tRNA:mRNA interaction energies. Each modification was placed in either the first, second, or third codon position and the energetics of tRNA:mRNA interactions on modified codons were compared those on an unmodified UUU codon. These calculations suggest that methylations ($m^1Ψ$ and $m^3Ψ$)

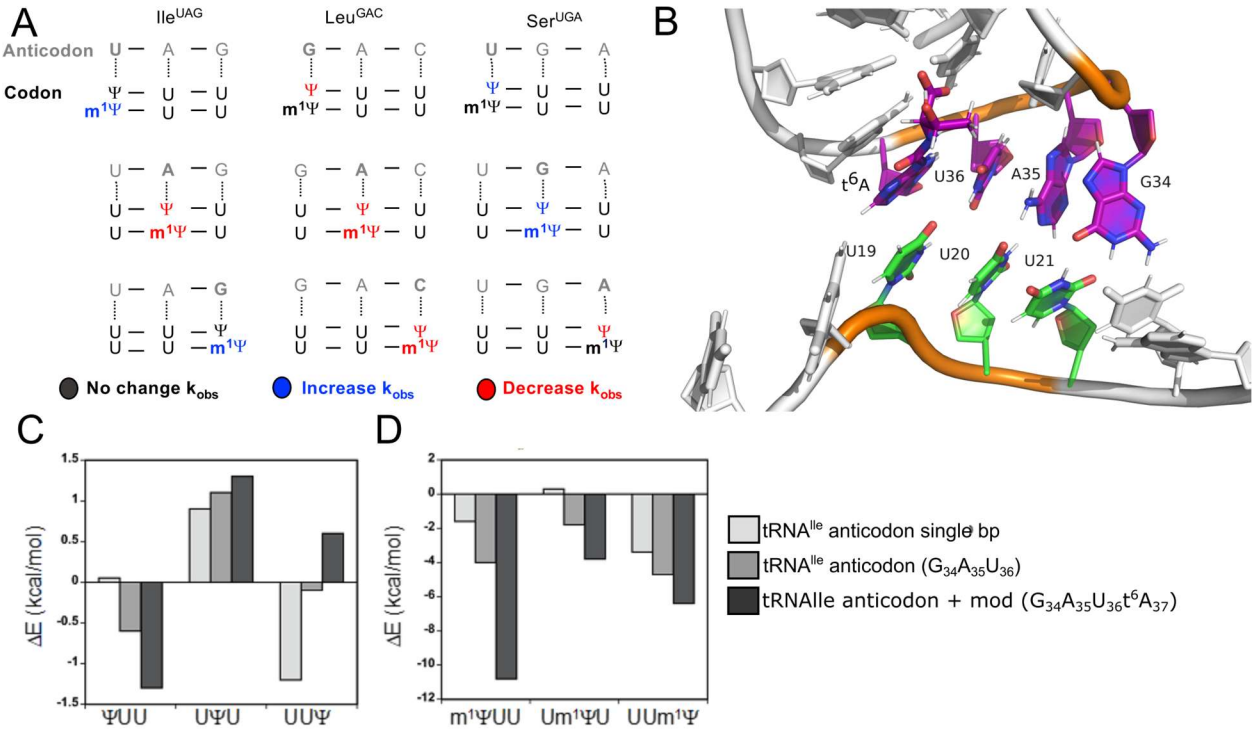

Figure 14 *Consequence of Ψ and m[1] Ψ on Ile misincorporation result from changes in the energetics of mRNA:tRNA interactions.* ***(A)*** *Summary of data in Supplementary Tables 4 and 5 displaying how a Ψ and m1Ψ impact the rate constants for the reaction of near cognate tRNAs with modified codons.* ***B and C.*** *The change in energetics between the residues in the mRNA and between the codon : anticodon residues when a Ψ* ***(B)*** *or m[1] Ψ* ***(C)*** *modification is present at the first, second, or wobble position of the codon.* ***(D)*** *Molecular modeling of an unmodified sequence coding for a Phe UUU codon and a noncognate isoleucine tRNA with an AUG anticodon. The hypermodification t[6]A is present at position 37 in the tRNA.*

have larger impact on the energetics of tRNA:mRNA interactions than isomerization at the C5-position alone (Ψ), and indicate that tRNA hypermodifications adjacent to the anticodon are predicted to make large contributions to the energetics (Figure 4, SI Figure 4.5.12). Our computational analyses generally support our experimental findings that Ψ-derived modifications differentially affect the interactions between codons and both cognate and near cognate tRNAs in context dependent manner (Figure 4, Supplemental Figure 11-13 and Supplemental table X). We see that the strongest predicted interactions between the $tRNA^{Ile}$ anticodon and Ψ and $m^1Ψ$ modified codons occurs when these modifications are in the first and third position of the codon (Figure 4D-E). For example, we observe a decrease in strength of predicted intermolecular interactions observed in Figure 4. This finding could help rationalize our observation that $tRNA^{Ile}$

interacts more rapidly with codons containing Ψ and $m^1Ψ$ in the first and third position of a codon than in the second position (Figures 3, 4A). Furthermore, our calculations also indicate that differences in enthalpy account for the effects of these codon modifications on tRNA interactions. Together with our *in vitro* and cell-based translation assays, these findings indicate that Ψ and $m^1Ψ$ can impact the strength of interactions between mRNAs and near-cognate tRNAs in the context of the ribosome.

4.3 Discussion and Conclusions

During the selection of aminoacylated-tRNAs the ribosome must compromise between the speed and accuracy of decoding. The chemical modification of the RNAs involved in decoding (e.g. mRNA and tRNA) permit the fine tuning of this balancing act. mRNA-based therapeutics and vaccines are emerging as a powerful new platform for treating and preventing disease. Many of these emerging technologies include $m^1Ψ$ as a key component of their RNA biologics [33,37]. As such, it is important to understand how the presence $m^1Ψ$ modifications in mRNA transcripts might impact translation. Our studies indicate that, depending on where it was located within a codon, $m^1Ψ$ either has no effect or modestly increases the rate constant (k_{obs}) for cognate amino acid incorporation (Figure 1B). Similarly, the rate constants (k_{hyd}) for translation termination are not perturbed when sufficient concentrations of release factors are present (Figure 1C-D). Although faster elongation rates might help to partially explain greater protein yield from $m^1Ψ$ containing transcripts in cells (SI Figures 9-10), the preponderance of the increased yields in protein are likely due to $m^1Ψ$-induced enhancements in mRNA stability and avoidance of the cell's innate immune system [40,41,53,59].

In our studies, $m^1Ψ$ altered not only cognate tRNA interactions with the ribosome, but also the propensity of ribosomes to react with near-cognate tRNAs. We find that $m^1Ψ$, and the related

naturally occurring Ψ modification, impact the rate constants for Ile, Leu and Ser amino acid substitution on Phe (UUU) codons. Our kinetic studies reveal that both $m^1\Psi$ and Ψ modifications can either enhance or limit amino acid substitution depending on aa-tRNA identity and the position of the modification within the codon (Figures 3 and 4A). $m^1\Psi$ and Ψ similarly impact the k_{obs} values for both the Ile and Ser mis-incorporation. These *in vitro* observations are supported by cellular reporter studies (Figure 2B, SI Figures 10-11) indicating that $m^1\Psi$ can induce miscoding events when included in full-length transcripts expressed in human cells. Our findings in cells are similar to the increase in miscoding we previously observed on Ψ-containing mRNAs in the same experimental system [58]. These observations are consistent with previous work indicating that naturally occurring mRNA modifications elicit different responses depending on their location within a codon or mRNA sequence [29,30,60]. Comparison of the rates of miscoding on $m^1\Psi$ and Ψ-containing codons suggests that the addition of a methyl group, and altered ring electronics resulting from the exchange of the nitrogen, play distinct positional and codon specific roles in the modulation of miscoding. The changes in translation on $m^1\Psi$-modified codons that we observed both *in vitro* and in cell-based reporters depend strongly on the sequence context of the modification.

The ribosome discriminates between cognate tRNA and near/non cognates with several different interactions: steric fit and correct geometry between the codon:anticodon duplex in the A-site of the ribosome and base-pair stability between the codon:anticodon [57,61,62]. Our modeling data supports our biochemical findings that $m^1\Psi$ alters mRNA:tRNA interactions in the ribosome decoding center (Supplementary Figure 6) [63–68]. This is in line with how modified nucleobases in tRNAs, in both the anticodon and the anticodon loop, have been observed to impact mRNA decoding by the ribosome [9,11,69–71]. For example, the bacterial $tRNA^{Lys}$ and eukaryotic

$tRNA^{Lys3}$ UUU species of tRNA often contain derivatives of hyper-modification 5-methyl-2-thiouridine at position 34 to facilitate the decoding of a degenerate codon (AAG) by stabilizing the non-Watson-Crick base pairing interaction, U:G. In bacteria this is achieved through hydrogen bonding while in eukaryotes changes in conformational stability facilitate the increased stability [72,73]. The modification of adenosines (t^6A, ms^2t^6A,ct^6A) located at tRNA position 37 can also improve the stability of A:U codon:anticodon duplex through enhanced base stacking ability between the mRNA and the tRNA (30, 41, 56, 57). Consistent with the idea that tRNA anticodon step loop (ASL) hypermodifications influence ribosome decoding our miscoding rates (**Figure 3A,E,C,G)** for tRNA with hypermodifications (t^6A in $tRNA^{Ile}$, $ms2i^6A$ and cmo^5Uin $tRNA^{Ser}$) both had the largest alterations in decoding behavior while the $tRNA^{Leu(GAC)}$ (**Figure B,F**) with only has a methylation at position 37 (m^1G), displayed only modestly (maximum 2-fold) reduction in k_{obs} regardless of modification position [74]. Together, our biochemical amino acid misincorporation and modeling data suggest that tRNA hypermodifications may play an important role in mediating the interactions between near cognate tRNAs and modified codons during the decoding process (Figure 4D,E and SI Figure 7).

The ability of $m^1\Psi$ and Ψ to change the decoding behavior of the ribosome while only modestly altering amino acid addition and termination have several implications. Given that Ψ is included into mRNA at increased levels under cellular stress conditions, these findings support the possibility that Ψ–derived modifications can provide the cells with a way to transiently increase the diversity of the proteome under stress to increase fitness [25,75]. Furthermore, this could potentially help to explain the high-efficacy of the mRNA vaccines COVID-19 relative to traditional vaccine platforms; there are possibly *very* low levels of a wider variety of antigens (spike protein mutants) being produced that result in a greater diversity of antibodies being

generated. Our findings raise the possibility of using modification sequence context to modulate the fidelity of the proteins produced from mRNA vaccines to optimize the efficacy of vaccines using this emerging technology.

4.4 Materials and Methods

4.4.1 In vitro amino acid addition assays

E. coli MRE600 tight coupled 70S ribosome were prepared as previously described [23]. Unmodified mRNA were prepared by run-off T7 transcription of DNA oligonucleotides. mRNA containing modified nucleotides were synthesized and HPLC purified by Dharmacon. mRNA sequences were generally of the form GGUGUCUUGCGAGGAAUAAGUGCAUU AUG UUU UAA GCCCUUCUGUAGCCA; the coding sequence is underlined. Modified mRNA had either the first, second, third position of the Phe (UUU) codon modified with $m^1\Psi$ (SI Figure 15). Dharmacon verified quality control via ESI-MS data (SI Figure 16). *E. coli* translation factor constructs were gifted from the laboratory of Dr. Rachel Green unless otherwise noted. Translation Factors and Release Factors were purified according to previously published methods [23,58]. Native tRNA was purified HB101 *E. coli* as previously published [76]. The acceptor activity of the tRNA was validated via triplicate aminoacylation assays with both the appropriate synthetase and S100 lysate.

E. coli initiation complexes (ICs) were prepared in 1x 219 – Tris Buffer (50 mM Tris pH 7.5, 70 mM NH_4Cl, 30 mM KCl, 7 mM $MgCl_2$, 5 mM β-ME) with 1 mM GTP and as previously published [58,76]. Ternary complexes (TCs) were similarly formed as previously published [58]. Amino acid addition reactions were conducted at final concentrations of 1 μM aminoacylated tRNA, 20 μM EF-Tu, 70 nM pre-formed ICs in buffer 1X 219 at 37 °C. Reactions were quenched with 500

mM KOH (final) on a KinTek quench-flow apparatus. eTLCs were visualized by phosophorimaging and then quantified with ImageQuant software. Data was fit to the following Equation 1, where *A* is the amplitude of the signal.

$$FractionProduct = A \circ (1 - e^{k_{obs}t}) \quad (8)$$

4.4.2 In vitro translation termination assays

Pre-termination complexes (pre-TCs) was prepared by forming ICs on a mRNA containing the coding sequence AUG-UAA or AUG-m$^1\Psi$AA. Release assays were performed by mixing 70 nM pre-TCs with release factors (RF1 or RF2; 50 nM to 10 μM) at room temperature (~20 °C). Reaction time points were quenched in 5% formic acid. The fraction of released of f-[^{35}S]-Met-tRNA was fit to Equation 1 and $K_{1/2}$ values were obtained by fitting to Equation 2.

$$k_{hyd} = k_{max} \bullet [RF] / (K_{1/2} + [RF]) \quad (9)$$

4.4.3 In vitro amino acid misincorporation

Assays performed with total aa-tRNA^{aa} were conducted by reacting ICs (70 nM final) with TCs (1 μM total tRNA aminoacylated with either S100 enzymes or specific synthetases, 40 μM EF-Tu and 10 mM GTP) at 37° C for 15 minutes. Reactions were quenched with 500 mM KOH (final). The reactants and products were separated by eTLC and visualized using ImageQuant software. For assays with high-kinetic resolution, ICs were reacted with Ternary complexes (40 μM EF-Tu:10 μM EF-Ts: 10 μM of aminoacylated tRNA (either Ile, Leu, Ser)). These reactions were prepared and conducted as previously published [76].

4.4.4 P site mis-match surveillance assays

Assays were performed as previously described. mRNA transcripts used in IC formation were unmodified T7 transcripts of the form 5'-GGUGUCUUGCGAGGAUAAGUGCAUU-**AUG-UAA**-GUUGCCCUUCUGUAGCCA-3' or synthetic mRNA purchased from Dharmacon of the form 5'-GGUGUCUUGCGAGGAUAAGUGCAUU-**AUG-m**^{1}**ΨAA**GUUGCCCUUCUGUAGCCA-3'. Mismatched initiation complexes were formed as previously described.[50,58] P site mis-match surveillance assays were performed by mixing RNCs (70 nM final) with RF2 (30 μM final) or (RF2/RF3 30 μM mixture).

***In vitro* preparation of luciferase mRNA.**

The template for *in vitro* synthesis of luciferase mRNA consists of: the T7 RNA polymerase promoter, followed by an N-terminal 3× Hemagglutinin (HA) tag fused in-frame with the firefly luciferase gene, in-frame C-terminal StrepII and FLAG tags. The open reading frame spans from the 3xHA tag to the FLAG tag enabling the purification of full-length luciferase protein and not translation truncated products. The luciferase mRNA was transcribed using T7 RNA polymerase (New England Biolabs) as previously published [58].

4.4.5 Luciferase mRNA transfection and expression analyses.

Synthesized, purified mRNAs were transfected into 293H cells using TransIT-mRNA transfection kit as recommended by the manufacturer (Mirus). Tandem purification of the luciferase translation products was performed using the FLAG tag followed by selection for the N-terminal HA tag as described previously [58,77,78] Three independent transfections were performed for uridine/ N1-methylpseudouridine -containing mRNAs. The purified products were analyzed on 8% SDS-PAGE, gels were then silver stained (ProteoSilver, Sigma) and processed

for mass spectrometry. For western blot analyses of the luciferase protein, proteins were separated by SDS- PAGE and blotted as previously described [58].

4.4.6 In-gel Digestion and LC-MS/MS Analysis.

In-gel digestion and LC-MS/MS analysis were performed as previously published [58]. Raw data files were peak picked by Proteome Discoverer (version 2.1), and preliminary searches were performed using the MASCOT search engine (version 2.4) against the SwissProt Human FASTA file (downloaded 05/2018) modified to include the luciferase protein sequence. Search parameters included Trypsin/P specificity, up to 2 missed cleavages, a fixed modification of carbamidomethyl cysteine, and variable modifications of oxidized methionine, pyroglutamic acid for Q, and N-terminal acetylation. The processed peak list was then re-searched in MASCOT against luciferase only as described previously [58]. The final search, with confirmed variable modifications, was analyzed as previously described [58] The sum of the top 3 isotopes were then exported for each modification for further analysis.

4.4.7 Modeling work.

Fragment molecular orbital (FMO) calculations were used to quantify the pairwise Phe UUU codon anti-codon interaction energies[79,79–81]. First, the initial coordinates of the Phe UUU codon: isoleucine tRNA complex were taken from the X-ray crystal of the Thermus thermophilus 70S ribosome in complex with mRNA (PDB ID: 6UO1). Next, starting from these coordinates, we generated six additional codons:tRNA complexes with the UUU codon changed to $^{1}\Psi$UU, U$^{1}\Psi$ U, UU$^{1}\Psi$, ΨUU, UΨ U, and UUΨ, respectively. The codon:tRNA complexes were then processed through CHARMM-GUI webserver add hydrogens, patch the terminal 5' and 3' residues, and prepare the input files for energy minimization[82,83]. Each complex was energy

minimized with 50 steps of steepest descent (SD) and 200 steps of adopted basis Newton-Raphson (ABNR) method with a gradient tolerance of 0.001. During energy minimization, the non-bonded list was generated at a cutoff of 15.0 Å and updated heuristically; and the Lennard-Jones and electrostatic interactions were treated with the switching function. Energy minimization was carried out using the CHARMM36 nucleic force field for the RNAs and solvation effects were models using the Generalized Born using Molecular Volume (GBMV) implicit solvent[84–86]. The energy minimized coordinates of the complexes were used as the starting geometries for FMO calculations.

All calculations were carried out at the Møller-Plesset perturbation theory (MP2)/6-31G* level of theory[87–90]. Solvation effects were modeled using the polarizable continuum model (PCM) interfaced with the FMO method[91]. For the FMO-MP2/6-31G*/PCM calculations, each RNA residue was treated as a single fragment. Input files for FMO calculations we generated from the energy minimized coordinates of the codon:tRNA complexes using an in-house fragment script (https://github.com/atfrank/RNAFMO). Briefly, fragmentation was performed at the C5'-O5' bond of the RNA residues following the approach used in the computational chemistry software Facio (version 22.1.1.32) [92,93]. All FMO calculations were carried out using the *ab initio* quantum chemistry package, general atomic and molecular electronic structure system (GAMESS) (September 2018, R3)[94]. The Pair interaction energy decomposition analysis (PIEDA) facility in GAMESS was used to compute and decompose the pairwise interaction energies between individual fragments (nucleotides) in the mRNA:tRNA complexes[95].

4.5 Supplemental Figures

Dipeptide Formation on an Unmodified and m$^1\Psi$ Modified Phenylalanine Codon

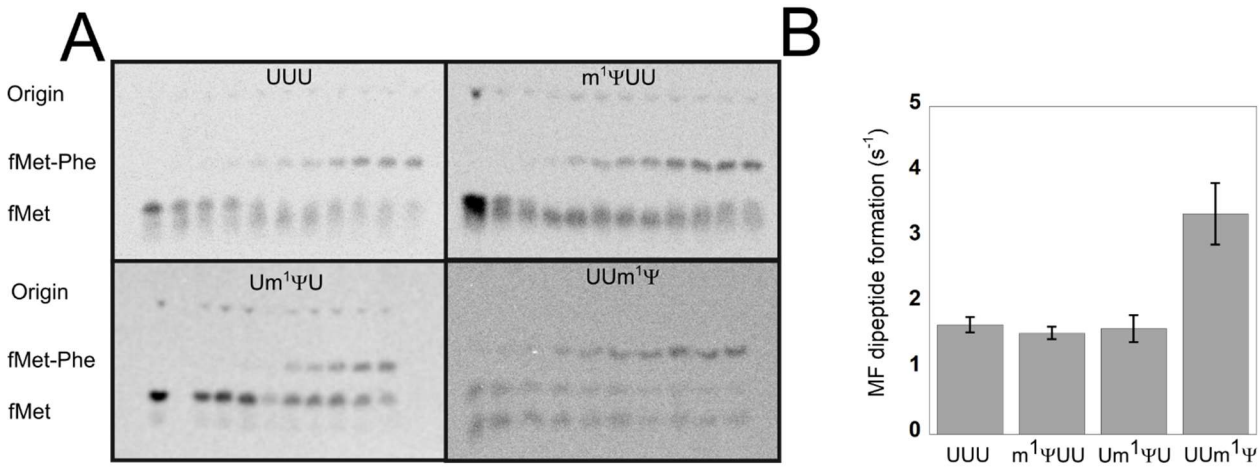

Figure 15 *Dipeptide Formation on an Unmodified and m$^1\Psi$ Modified Phenylalanine Codon (**A**) Comparison of rates of dipeptide formation on a positionally m$^1\Psi$ modified Phe codon (UUU). (**B**) N-formyl-[35S]- methionine-labeled peptides are separated by electrophoresis on a cellulose TLC in a volatile, acidic buffer, and detected by phosphorimaging. Representative images of dipeptide formation acid addition assays, displaying the UUU control, m$^1\Psi$UU Um$^1\Psi$U UUm$^1\Psi$ are shown. The brightness and contrast of these images have been adjusted to clearly show all bands and the background, and as a consequence pixel intensity is no longer linear with signal.*

Rate of Termination by Release Factor 1 on Unmodified and $m^1\Psi$ Modified Stop Codon

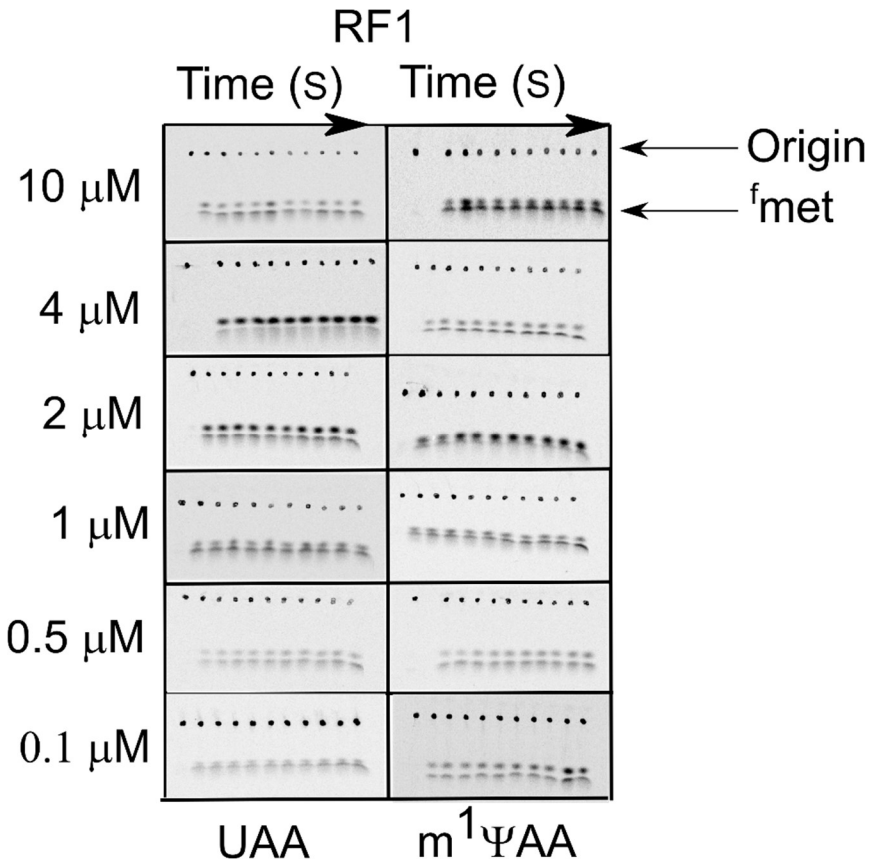

Figure 16 *Representative images of time courses for release factor 1 are shown. The brightness and contrast of these images have been adjusted to clearly show all bands and the background, and as a consequence pixel intensity is no longer linear with signal.*

Rate of Termination by Release Factor 2 on Unmodified and $m^1\Psi$ Modified Stop Codon

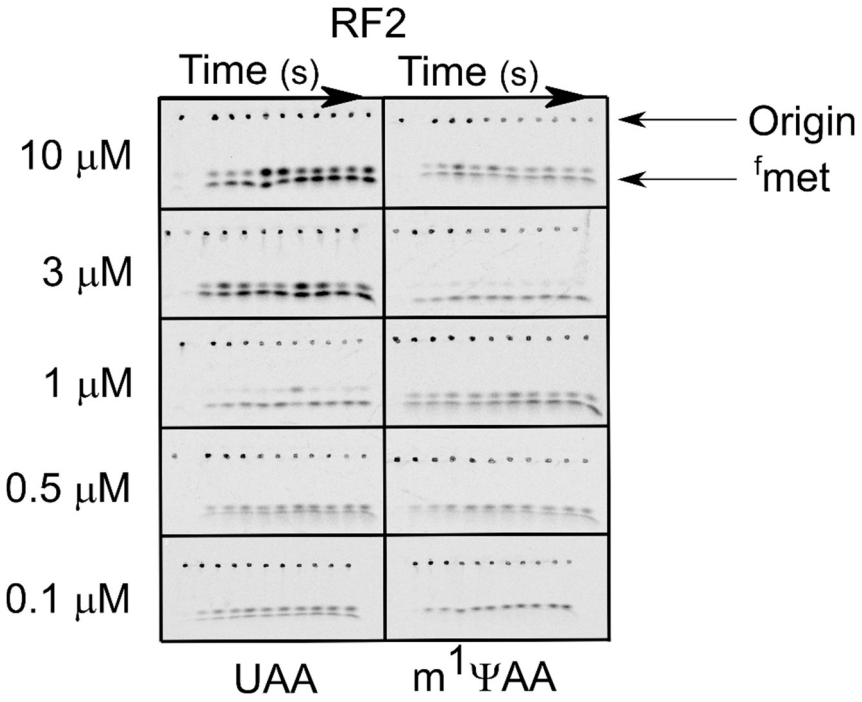

Figure 17 *Representative images of time courses for release factor 2 are shown. The brightness and contrast of these images have been adjusted to clearly show all bands and the background, and as a consequence pixel intensity is no longer linear with signal.*

Fold change in Endpoint Miscoding levels from total tRNA

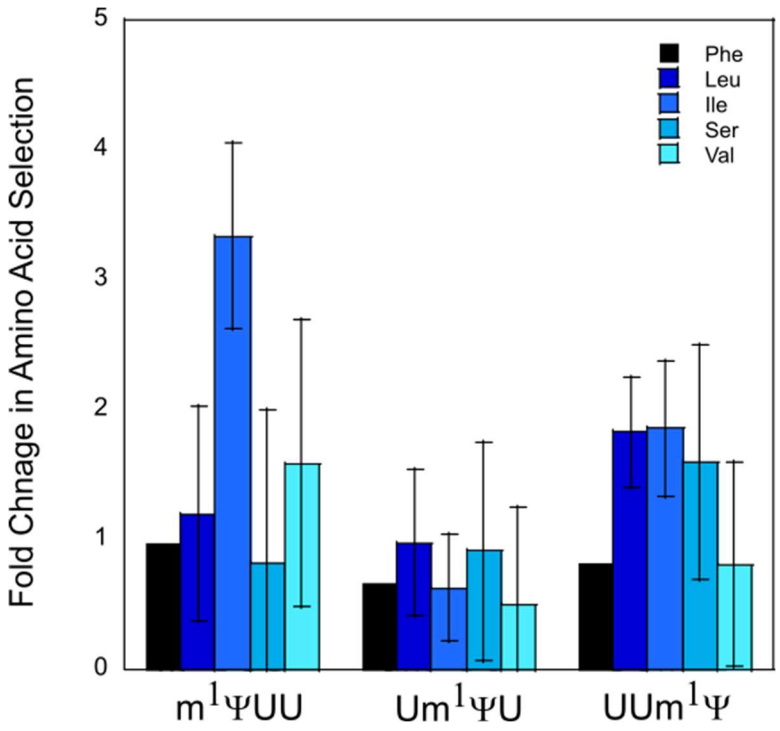

Figure 18 *The endpoint mis-incorporation defects of a m1Ψ positionally modified UUU codon. The miscoded dipeptide was separated via eTLC and the miscoded products identified by size and charge.*

Titration of Ile tRNA on a Phenylalanine Codon

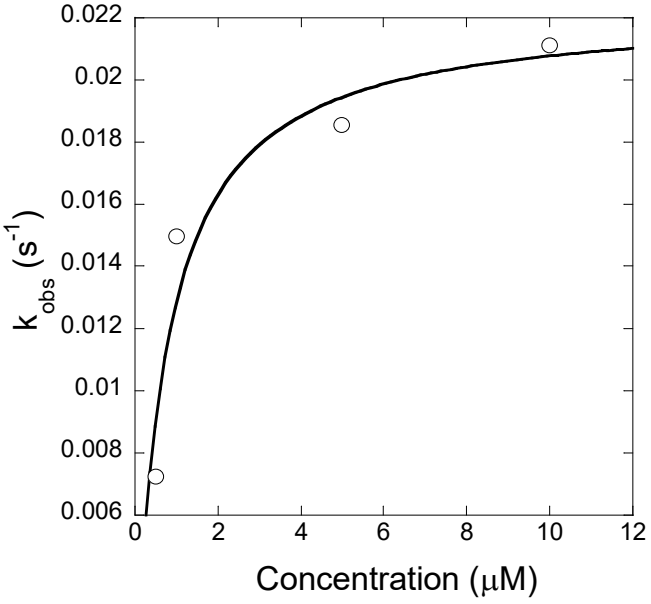

Figure 19 *In order to ensure that the rates of miscoding reactions were carried out under saturating conditions the K1/2 of Ile miscoding by tRNAIle (UAG) was determined. A K1/2 of approximately 0.73 μM was determined, so a final of concentration of 10 μM aa-tRNA in the miscoding assays will be at saturation.*

Representative Images of Misincorporated Dipeptide Products an Unmodified and m1Ψ

Modified Phenylalanine Codon

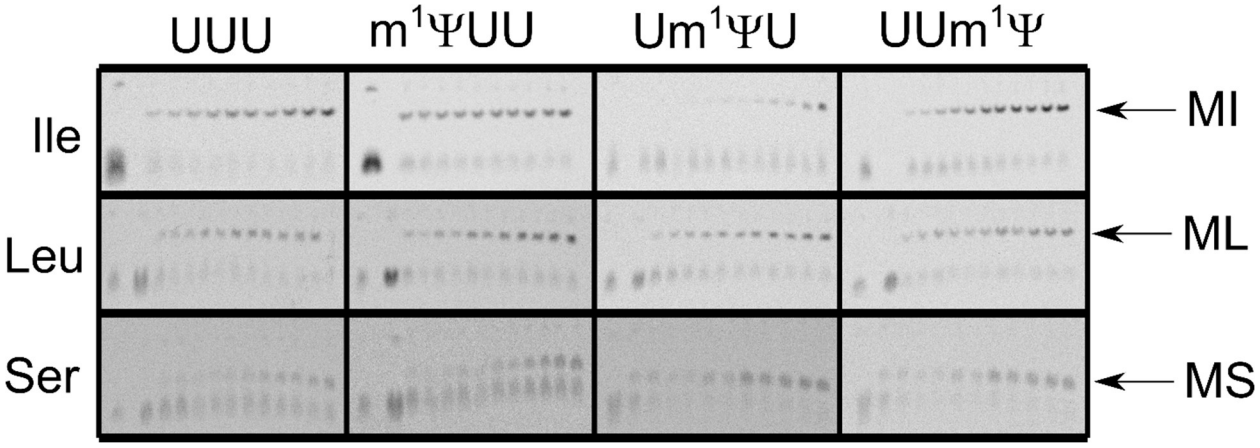

Figure 20 *Representative eTLCs images of dipeptide formation acid addition assays, displaying the UUU control, $m^1ΨUU$ $Um^1ΨU$ $UUm^1Ψ$ miscoding assays performed. Note the reduced formation of the MI dipeptide when the second is modified with $m^1Ψ$.*

Representative Images of Misincorporated Dipeptide Products an Unmodified and Ψ Modified Phenylalanine Codon

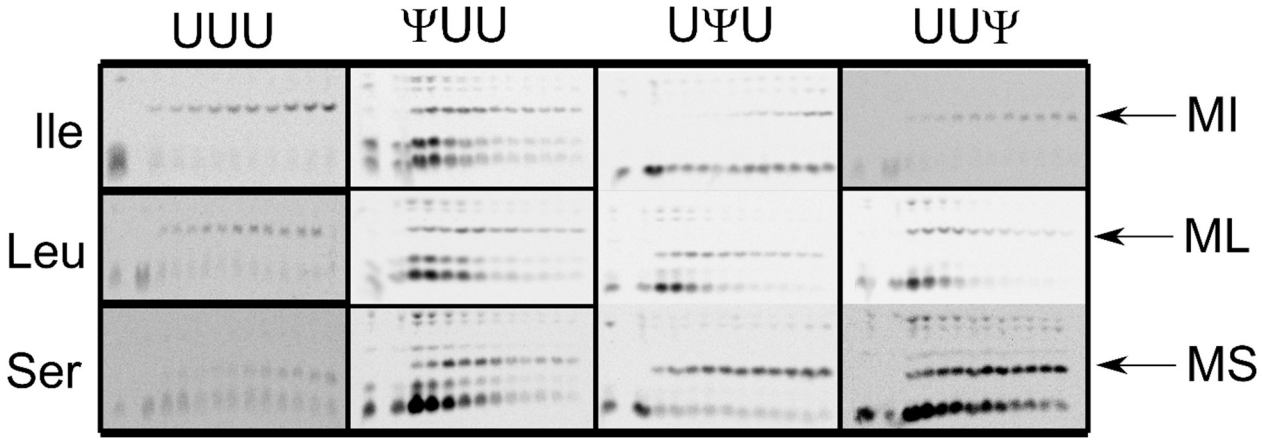

Figure 21 *Representative eTLCs images of dipeptide formation acid addition assays, displaying the UUU control, m1ΨUU Um1ΨU UUm1Ψ miscoding assays performed. Note the reduced formation of the MI dipeptide when the second position is modified with Ψ*

Mass Spectrum Analysis of RNA Bases and Incorporation Efficiency

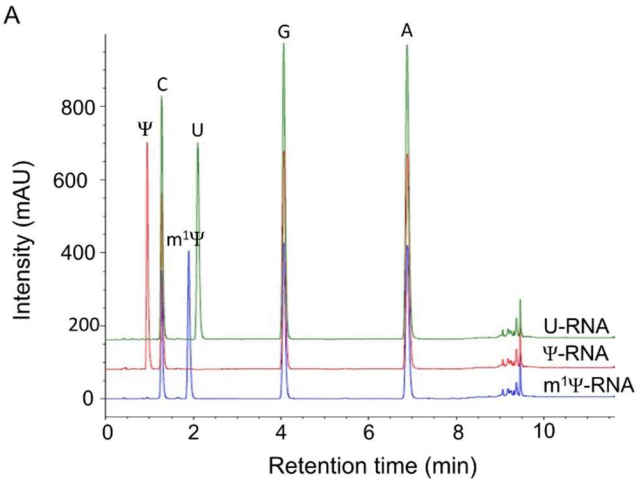

B

Nucleotide	U	Ψ	$m^1Ψ$
rA	0.92	0.91	0.93
rC	0.83	0.85	0.83
rG	1	1	1
rU/Ψ/$m^1Ψ$	0.71	0.73	0.72

Figure 22 *(**A**) Base composition of each RNA base detected by LC-MS, relative to guanosine. (**B**) Incorporation efficiency of modified nucleotides was assessed by Liquid Chromatography-Mass Spectrometry (LC-MS).*

Expression of Unmodified and Modified Luciferase mRNA in HEK293 Cells

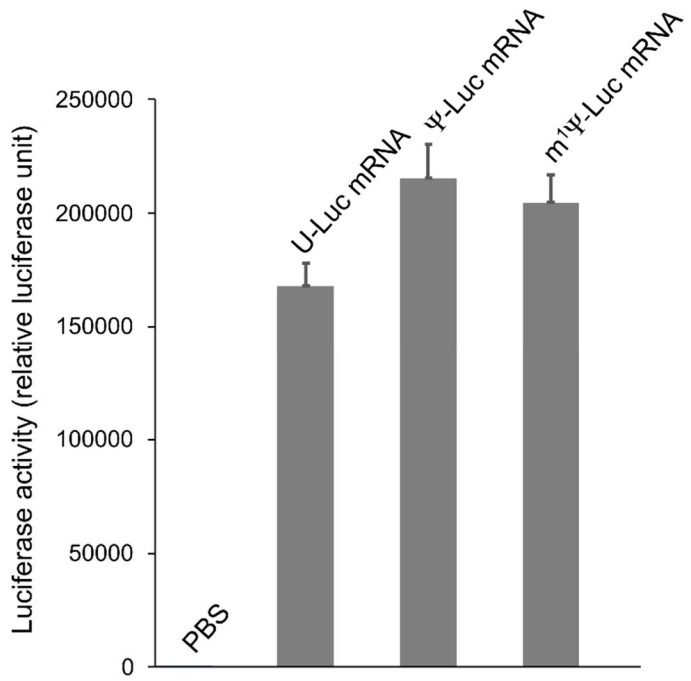

Figure 23 *Expression of m1Ψ modified luciferase mRNA in vivo. Luciferase activity assay demonstrating functionality of unmodified and modified luciferase mRNAs*

Protein Yields from Unmodified and Modified Luciferase mRNA in HEK293 Cells

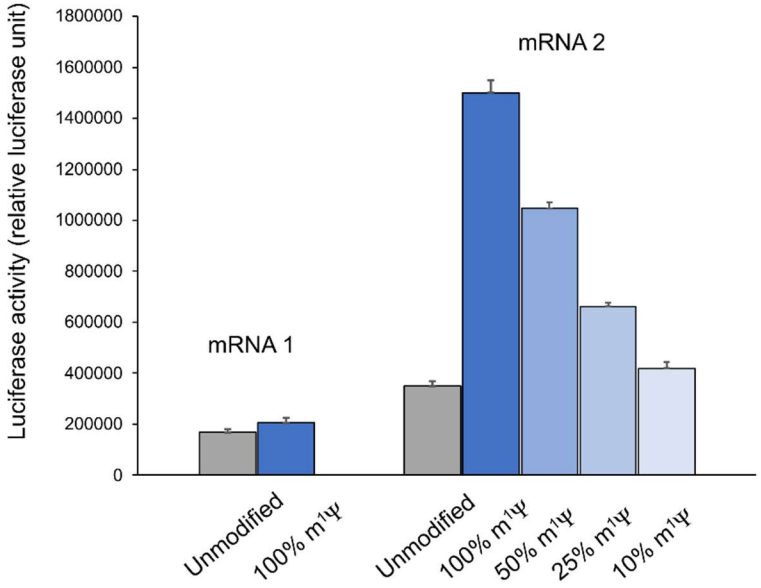

Figure 24 *The yield of active protein from m1Ψ modified mRNAs depends on the level of modification and sequence context. Two mRNAs coding for luciferase but with silent coding region changes were in vitro transcribed in the presence of varying ratios of uridine and m*^{1}*Ψtriphosphate. Purified mRNAs were transfected into cultured mammalian cells and luciferase activity was assayed at a single time point.*

Change in Energy based on Molecular Modeling of Cognate Decoding by Non-Hypermodified tRNA of Modified mRNA

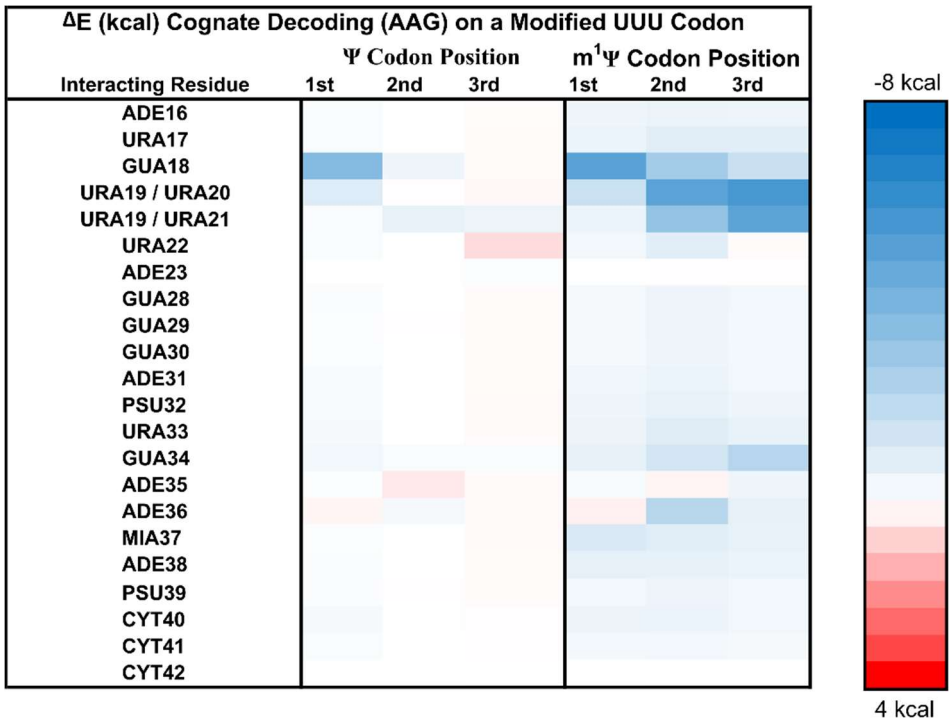

Figure 25 *The change in energy (ΔE kcal) for a Phe (AAG) decoding on a modified UUU codon. This interaction is modeling a decoding interaction in which the hypermodification immediately adjacent to first position in the anticodon (position 37) is absent. This modeling data supports our experimental data those chemical modifications to mRNA change the molecular interactions during translation. It indicates that different modifications alter decoding interactions in different ways. Generally, with the exception of 3MP, the strongest interactions occurred between the mRNA codon residues as intramolecular interactions. The $m^1\Psi$ and m^5U modifications produced the largest favorable changes in intramolecular interactions with ~ -7 kcal and ~ -4 kcal, respectively. Both Ψ and $m^3\Psi$ displayed unfavorable intramolecular interactions at the third position of about 2 kcal. The intermolecular interactions had overall had smaller magnitudes except for 3MP. The large unfavorable energy observed for 3MP is most likely the result of the replacement of the hydrogen bond donor with a methyl group.*

Change in Energy from Non-Hypermodified Cognate Decoding to Decoding by Hypermodified tRNA of Modified mRNA

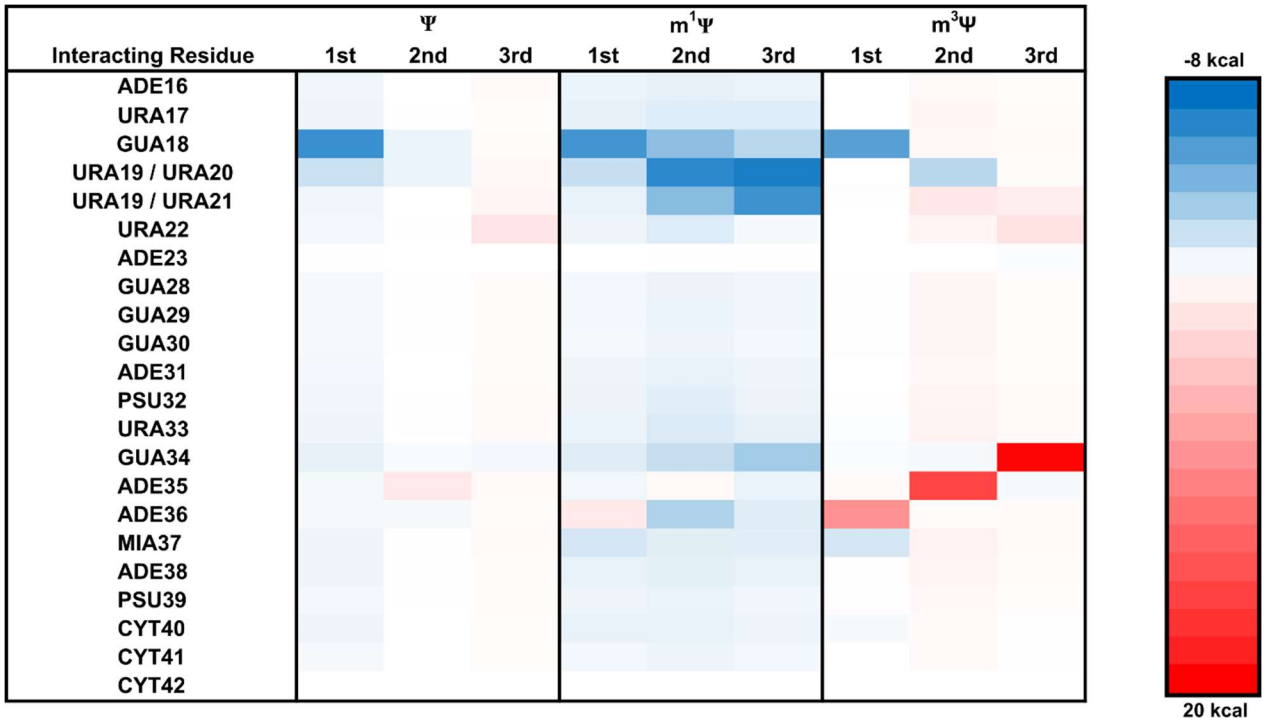

Figure 26 *The change in energy (ΔΔE kcal) for a Phe (AAG) decoding on a modified UUU codon when the MIA modification is present at position 37, compared to an unmodified position adenosine at position 37. When MIA is present it significantly alters how energetics of modifications interact both intramolecularly and intermolecularly, particularly with the first position of the codon which makes sense given its proximately to it. However, the alterations are not uniform at the first position with 5MU and 1MP both displaying unfavorable interaction while PSU has an increase in favorable interactions. The change in energy (ΔΔE kcal) for a Phe (AAG) decoding on a modified UUU codon when the MIA modification is present at position 37, compared to an unmodified position adenosine at position 37*

Change in Energy for Non-Cognate Decoding by a Hypermodified Ile tRNA on a Modified mRNA Codon

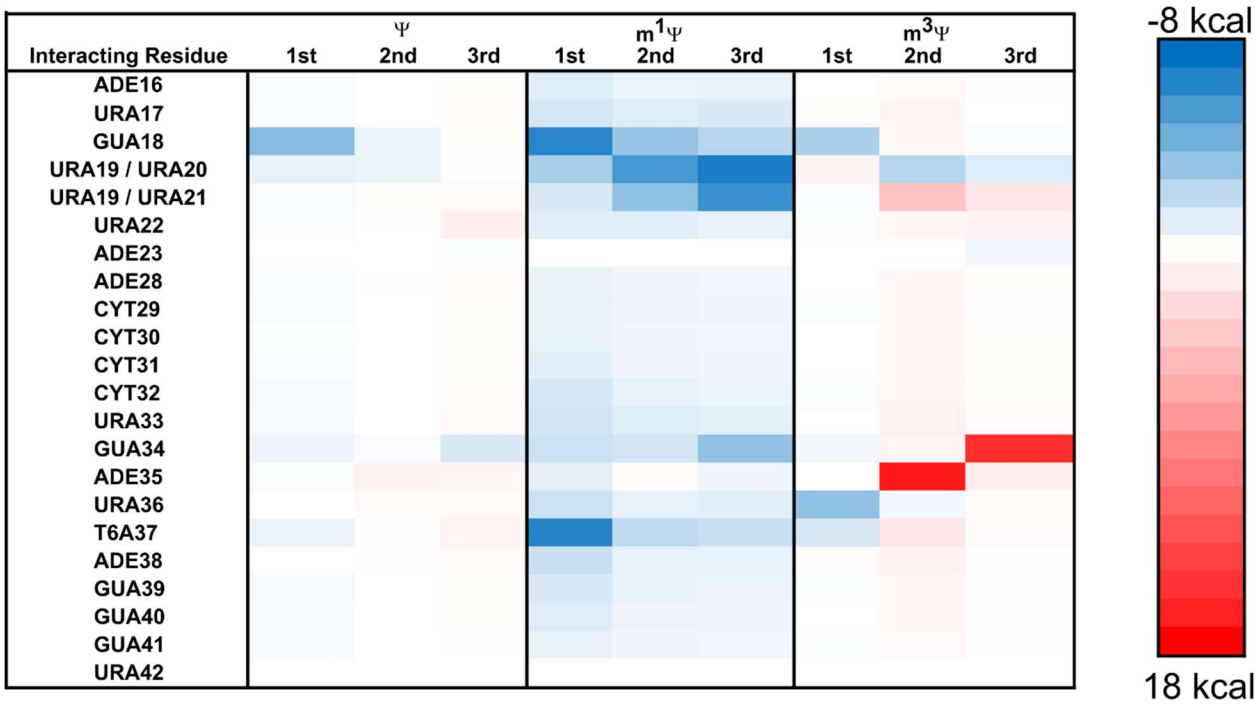

Figure 27 *The change in energy (ΔE kcal) for an Ile tRNA (AUG anticodon) decoding on a Ψ or $m^1Ψ$ modified UUU codon when the t^6A modification is present at position 37. There are significant favorable intramolecular interactions for both Ψ and $m^1Ψ$, apart from the Ψ modified wobble position. There are favorable codon anticodon interactions when the first position of the codon is modified.*

Detection of a P-Site Surveillance Mechanical on a m$^1\Psi$ Modified Codon

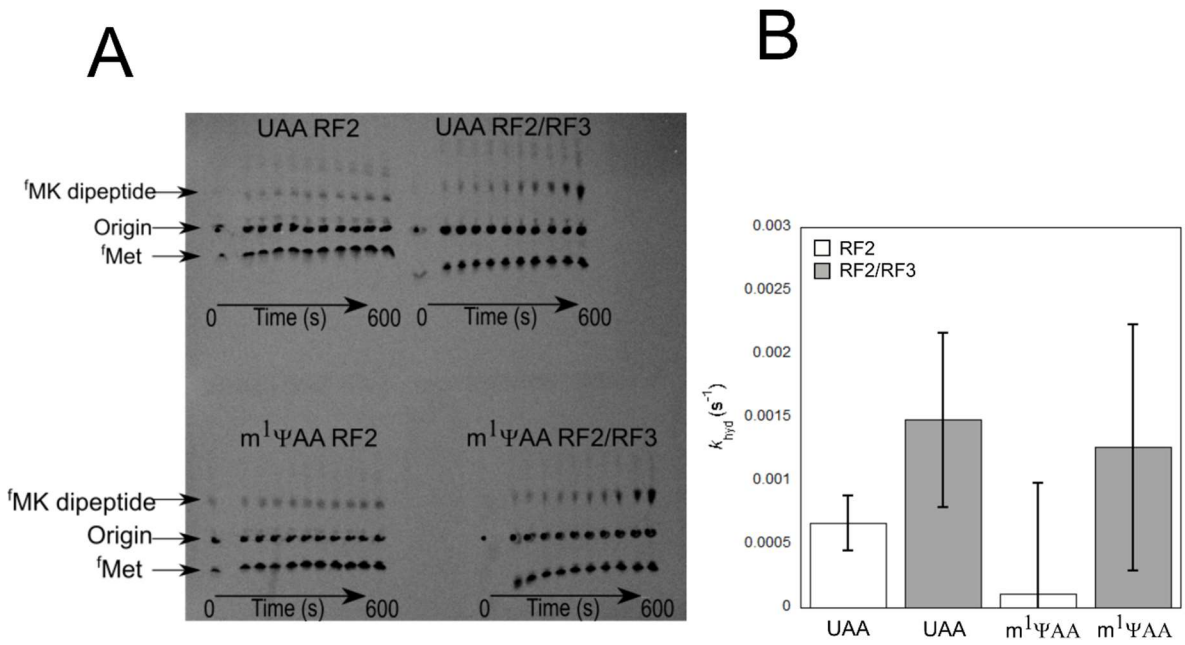

Figure 28 *P site mismatch surveillance is triggered by both modified and unmodified mRNA:tRNA interactions.* ***(A)*** *There is a mismatch between the tRNA anticodon and mRNA codon in the P site, MK dipeptides are released in an RF2-RF3 dependent manner from the ribosome. In both cases (**B**), the rate constant for peptide release is enhanced by at least 10-fold when RF3 is present.*

4.6 Supplemental Tables

Amino Acid Addition on an unmodified and m$^1\Psi$ modified Phenylalanine Codon

Rates of dipeptide formation		
Codon	**Rate (s^{-1})**	**Error**
UUU	1.7	0.1
m$^1\Psi$UU	1.5	0.1
Um$^1\Psi$U	1.6	0.2
UUm$^1\Psi$	3.4	0.5

Table 9 *This table reflects the values plotted in Figure 1A for the ribosome catalyzing the addition of a single phenylalanine on unmodified and modified codons, The reported k_{obs} and standard error values are from the fit of a single curve to all replicate time courses.*

Titration of Release Factor 1 on an unmodified and $m^1\Psi$ modified Stop Codon

Release Factor 1 Assays (k_{hyd} s^{-1})				
Concentration (μM)	**UAA**	**Error**	**$m^1\Psi$AA**	**Error**
0.1	**0.06**	**0.022**	**0.01**	**0.002**
0.5	**0.04**	**0.009**	**0.02**	**0.003**
1.0	**0.10**	**0.011**	**0.05**	**0.008**
2.0	**0.15**	**0.024**	**0.08**	**0.013**
4.0	**0.08**	**0.009**	**0.06**	**0.008**
10.0	**0.11**	**0.012**	**0.12**	**0.001**

Table 10 *Pre-termination complexes were prepared on mRNAs containing the coding sequence AUG-UAA-GUU and AUG- $m^1\Psi$AA-GUU. Peptide release assays were performed in 1X219-Tris buffer at room temperature (70 nM pre-TCs, RF1 ranging from 100 nM to 10 μM final concentration). Reaction aliquots were quenched with 5% formic acid (final) at varying time points. Free f-[^{35}S]-Met was separated from f-[35S]-Met-tRNAfMet by electrophoretic TLC and quantified by phosphorimaging.*

Titration of Release Factor 2 on an unmodified and $m^1\Psi$ modified Stop Codon

Release Factor 2 Assays (k_{hyd} s^{-1})				
Concentration (μM)	**UAA**	**Error**	**$m^1\Psi$AA**	**Error**
0.1	**0.01**	**0.003**	**0.003**	**0.005**
0.5	**0.02**	**0.004**	**0.02**	**0.005**
1.0	**0.05**	**0.009**	**0.03**	**0.005**
3.0	**0.05**	**0.005**	**0.04**	**0.004**
10.0	**0.06**	**0.006**	**0.05**	**0.006**

Table 11 *Pre-termination complexes were prepared on mRNAs containing the coding sequence AUG-UAA-GUU and AUG- $m^1\Psi$AA-GUU. Peptide release assays were performed in 1X219-Tris buffer at room temperature (70 nM pre-TCs, RF2 ranging from 100 nM to 10 μM final concentration). Reaction aliquots were quenched with 5% formic acid (final) at varying time points. Free f-[^{35}S]-Met was separated from f-[35S]-Met-tRNAfMet by electrophoretic TLC and quantified by phosphorimaging.*

Rates of Misincorporation on an unmodified and m^{1}Ψ modified Phenylalanine Codon

	Amino Acid substitution k_{obs} (s^{-1})					
	Ile	**Error**	**Leu**	**Error**	**Ser**	**Error**
UUU	0.013	0.0009	0.04	0.008	0.002	0.0005
m^{1}ΨUU	0.04	0.003	0.03	0.003	0.002	0.0005
Um^{1}ΨU	0.002	0.0003	0.01	0.0015	0.012	0.0015
UUm^{1}Ψ	0.019	0.003	0.019	0.003	0.004	0.0004

Table 12 *The k_{obs} of dipeptide formation for an unmodified and m^{1}Ψ positionally modified UUU codon. The reported kobs and standard error values are from the fit of a single curve to 3 replicate time courses*

Rates of Misincorporation on an unmodified and Ψ modified Phenylalanine Codon

	Amino Acid substitution k_{obs} (s^{-1})					
	Ile	**Error**	**Leu**	**Error**	**Ser**	**Error**
UUU	0.0190	0.0030	0.0360	0.0078	0.007	0.0004
ΨUU	0.0074	0.0030	0.0180	0.0033	0.018	0.0020
UΨU	0.0018	0.0007	0.0135	0.0005	0.016	0.0021
UUΨ	0.0180	0.0030	0.0230	0.0020	0.004	0.0002

Table 13 *The k_{obs} of dipeptide formation for an unmodified and Ψ positionally modified UUU codon. The reported kobs and standard error values are from the fit of a single curve to 3 replicate time courses.*

Observed Amino acid substitution on some $m^1\Psi$ containing codons observed in 293HEK cells

	Substitutions observed	Frequency of substitution (%)
Phe	Ser, Ile	0.31
Tyr	Cys, His	0.13
Leu	Pro, Ser	0.22
Ile	Thr, Trp, Val	0.11
Val	Glu, Ala	0.14
Trp	None observed	0

Table 14 *This table summarizes the amino acid substitutions detected in the U-containing codons in the entire luciferase dataset for multiple peptides when mRNAs were synthesized with Ψ. For calculating the frequencies, an extracted ion chromatogram was generated at <5ppm for each of the peptides of interest from the total ion current, and the area under the curve for each EIC was calculated. This was then used to calculate the percentage of substitution (area under the curve for peptides with a specific substitution/[area under the curve for all wild-type peptides with no substitution + area under the curve for all peptides with substitutions]).*

$m^1\Psi$ containing codons in luciferase mRNA

Amino acids evaluated for miscoding in 293H cells	Codons evaluated for miscoding in 293H cells
Phe	**UUU, UUC**
Leu	**UUA, UUG, CUU, CUC, CUA, CUG**
Ile	**AUU, AUC, AUA**
Val	**GUU, GUC, GUA, GUG**
Trp	**UGG**
Tyr	**UAU, UAC**

Table 15 *Uridine-containing codons analyzed for elongation miscoding.*

$m^1\Psi$ Substituted Codons and their Corresponding Miscoding Events

Codon	Substitutions observed	Frequency of substitution (%)
Phe	Ser, Ile/Leu	0.31%
Tyr	Cys, His	0.14%
Leu	Pro, Ser	0.36%

Table 16 *This table summarizes the amino acid substitutions detected from U-containing Phe, Tyr, Leu codons in the KGPAPFYPLEDGTAGEQLHK peptide when mRNAs were synthesized with $m^1\Psi$. The frequencies of the substitutions are also denoted. For calculating the frequencies, an extracted ion chromatogram was generated at <5ppm for each of the peptides of interest from the total ion current, and the area under the curve for each EIC was calculated. This was then used to calculate the percentage of substitution (area under the curve for peptides with a specific substitution/[area under the curve for all wild-type peptides with no substitution + area under the curve for all peptides with substitutions]).*

4.7 References

[1] Frye M, Jaffrey SR, Pan T, Rechavi G, Suzuki T. RNA modifications: what have we learned and where are we headed? Nat Rev Genet 2016;17:365–72. https://doi.org/10.1038/nrg.2016.47.

[2] Nachtergaele S, He C. The emerging biology of RNA post-transcriptional modifications. RNA Biol 2016;14:156–63. https://doi.org/10.1080/15476286.2016.1267096.

[3] Roundtree IA, Evans ME, Pan T, He C. Dynamic RNA modifications in gene expression regulation. Cell 2017;169:1187–200. https://doi.org/10.1016/j.cell.2017.05.045.

[4] Zhao X, Yang Y, Sun B-F, Shi Y, Yang X, Xiao W, et al. FTO-dependent demethylation of N6-methyladenosine regulates mRNA splicing and is required for adipogenesis. Cell Res 2014;24:1403–19. https://doi.org/10.1038/cr.2014.151.

[5] Ke S, Pandya-Jones A, Saito Y, Fak JJ, Vågbø CB, Geula S, et al. m6A mRNA modifications are deposited in nascent pre-mRNA and are not required for splicing but do specify cytoplasmic turnover. Genes Dev 2017;31:990–1006. https://doi.org/10.1101/gad.301036.117.

[6] Martinez NM, Su A, Burns MC, Nussbacher JK, Schaening C, Sathe S, et al. Pseudouridine synthases modify human pre-mRNA co-transcriptionally and affect pre-mRNA processing. Molecular Cell 2022;82:645-659.e9. https://doi.org/10.1016/j.molcel.2021.12.023.

[7] Jonkhout N, Tran J, Smith MA, Schonrock N, Mattick JS, Novoa EM. The RNA modification landscape in human disease. RNA 2017;23:1754–69. https://doi.org/10.1261/rna.063503.117.

[8] Sloan KE, Warda AS, Sharma S, Entian K-D, Lafontaine DLJ, Bohnsack MT. Tuning the ribosome: The influence of rRNA modification on eukaryotic ribosome biogenesis and function. RNA Biology 2017;14:1138–52. https://doi.org/10.1080/15476286.2016.1259781.

[9] Pan T. Modifications and functional genomics of human transfer RNA. Cell Res 2018;28:395–404. https://doi.org/10.1038/s41422-018-0013-y.

[10] RNA modifications and cancer n.d. https://www.ncbi.nlm.nih.gov/pmc/articles/PMC7567502/ (accessed December 15, 2021).

[11] Jackman JE, Alfonzo JD. Transfer RNA modifications: nature's combinatorial chemistry playground. WIREs RNA 2013;4:35–48. https://doi.org/10.1002/wrna.1144.

[12] Jones JD, Monroe J, Koutmou KS. A molecular-level perspective on the frequency, distribution, and consequences of messenger RNA modifications. Wiley Interdiscip Rev RNA 2020;11:e1586. https://doi.org/10.1002/wrna.1586.

[13] Gilbert WV, Bell TA, Schaening C. Messenger RNA modifications: Form, distribution, and function. Science 2016;352:1408–12. https://doi.org/10.1126/science.aad8711.

[14] Hoernes TP, Hüttenhofer A, Erlacher MD. mRNA modifications: Dynamic regulators of gene expression? RNA Biol 2016;13:760–5. https://doi.org/10.1080/15476286.2016.1203504.

[15] Zhao BS, Roundtree IA, He C. Post-transcriptional gene regulation by mRNA modifications. Nat Rev Mol Cell Biol 2017;18:31–42. https://doi.org/10.1038/nrm.2016.132.

[16] Motorin Y, Helm M. Methods for RNA Modification Mapping Using Deep Sequencing: Established and New Emerging Technologies. Genes 2019;10:35. https://doi.org/10.3390/genes10010035.

[17] Limbach PA, Paulines MJ. Going global: the new era of mapping modifications in RNA. WIREs RNA 2017;8:e1367. https://doi.org/10.1002/wrna.1367.

[18] Li X, Xiong X, Yi C. Epitranscriptome sequencing technologies: decoding RNA modifications. Nat Methods 2017;14:23–31. https://doi.org/10.1038/nmeth.4110.

[19] Helm M, Motorin Y. Detecting RNA modifications in the epitranscriptome: predict and validate. Nat Rev Genet 2017;18:275–91. https://doi.org/10.1038/nrg.2016.169.

[20] Grozhik AV, Jaffrey SR. Distinguishing RNA modifications from noise in epitranscriptome maps. Nat Chem Biol 2018;14:215–25. https://doi.org/10.1038/nchembio.2546.

[21] Finet O, Yague-Sanz C, Kruger LK, Migeot V, Ernst FGM, Lafontaine DLJ, et al. Transcription-Wide Mapping of Dihydrouridine (D) Reveals that mRNA Dihydrouridylation is Essential for Meiotic Chromosome Segregation. Rochester, NY: Social Science Research Network; 2020. https://doi.org/10.2139/ssrn.3569550.

[22] Schwartz S. Cracking the epitranscriptome. RNA 2016;22:169–74. https://doi.org/10.1261/rna.054502.115.

[23] Monroe JG, Smith TJ, Koutmou KS. Investigating the consequences of mRNA modifications on protein synthesis using in vitro translation assays. Methods in Enzymology, Academic Press; 2021. https://doi.org/10.1016/bs.mie.2021.06.011.

[24] Arango D, Sturgill D, Alhusaini N, Dillman AA, Sweet TJ, Hanson G, et al. Acetylation of Cytidine in mRNA Promotes Translation Efficiency. Cell 2018;175:1872-1886.e24. https://doi.org/10.1016/j.cell.2018.10.030.

[25] Schwartz S, Bernstein DA, Mumbach MR, Jovanovic M, Herbst RH, León-Ricardo BX, et al. Transcriptome-wide Mapping Reveals Widespread Dynamic-Regulated Pseudouridylation of ncRNA and mRNA. Cell 2014;159:148–62. https://doi.org/10.1016/j.cell.2014.08.028.

[26] Tardu M, Jones JD, Kennedy RT, Lin Q, Koutmou KS. Identification and Quantification of Modified Nucleosides in Saccharomyces cerevisiae mRNAs. ACS Chem Biol 2019;14:1403–9. https://doi.org/10.1021/acschembio.9b00369.

[27] Xu L, Liu X, Sheng N, Oo KS, Liang J, Chionh YH, et al. Three distinct 3-methylcytidine (m3C) methyltransferases modify tRNA and mRNA in mice and humans. Journal of Biological Chemistry 2017;292:14695–703. https://doi.org/10.1074/jbc.M117.798298.

[28] Franco MK, Koutmou KS. Chemical modifications to mRNA nucleobases impact translation elongation and termination. Biophysical Chemistry 2022;285:106780. https://doi.org/10.1016/j.bpc.2022.106780.

[29] Eyler DE, Franco MK, Batool Z, Wu MZ, Dubuke ML, Dobosz-Bartoszek M, et al. Pseudouridinylation of mRNA coding sequences alters translation. PNAS 2019;116:23068–74. https://doi.org/10.1073/pnas.1821754116.

[30] Licht K, Hartl M, Amman F, Anrather D, Janisiw MP, Jantsch MF. Inosine induces context-dependent recoding and translational stalling. Nucleic Acids Res 2019;47:3–14. https://doi.org/10.1093/nar/gky1163.

[31] You C, Dai X, Wang Y. Position-dependent effects of regioisomeric methylated adenine and guanine ribonucleosides on translation. Nucleic Acids Res 2017;45:9059–67. https://doi.org/10.1093/nar/gkx515.

[32] Meyer KD, Jaffrey SR. The dynamic epitranscriptome: N6-methyladenosine and gene expression control. Nat Rev Mol Cell Biol 2014;15:313–26. https://doi.org/10.1038/nrm3785.

[33] Agrawal S. RNA Therapeutics Are Stepping Out of the Maze. Trends Mol Med 2020;26:1061–4. https://doi.org/10.1016/j.molmed.2020.08.007.

[34] Zhou L-Y, Qin Z, Zhu Y-H, He Z-Y, Xu T. Current RNA-based Therapeutics in Clinical Trials. Curr Gene Ther 2019;19:172–96. https://doi.org/10.2174/1566523219666190719100526.

[35] Sergeeva OV, Koteliansky VE, Zatsepin TS. mRNA-based therapeutics–Advances and perspectives. Biochemistry Moscow 2016;81:709–22. https://doi.org/10.1134/S0006297916070075.

[36] Gao M, Zhang Q, Feng X-H, Liu J. Synthetic modified messenger RNA for therapeutic applications. Acta Biomater 2021;131:1–15. https://doi.org/10.1016/j.actbio.2021.06.020.

[37] Nance KD, Meier JL. Modifications in an Emergency: The Role of N1-Methylpseudouridine in COVID-19 Vaccines. ACS Cent Sci 2021. https://doi.org/10.1021/acscentsci.1c00197.

[38] Parr CJC, Wada S, Kotake K, Kameda S, Matsuura S, Sakashita S, et al. N 1-Methylpseudouridine substitution enhances the performance of synthetic mRNA switches in cells. Nucleic Acids Research 2020;48:e35–e35. https://doi.org/10.1093/nar/gkaa070.

[39] Svitkin YV, Cheng YM, Chakraborty T, Presnyak V, John M, Sonenberg N. N1-methyl-pseudouridine in mRNA enhances translation through eIF2α-dependent and independent mechanisms by increasing ribosome density. Nucleic Acids Res 2017;45:6023–36. https://doi.org/10.1093/nar/gkx135.

[40] Karikó K, Muramatsu H, Welsh FA, Ludwig J, Kato H, Akira S, et al. Incorporation of Pseudouridine Into mRNA Yields Superior Nonimmunogenic Vector With Increased Translational Capacity and Biological Stability. Mol Ther 2008;16:1833–40. https://doi.org/10.1038/mt.2008.200.

[41] Karikó K, Buckstein M, Ni H, Weissman D. Suppression of RNA Recognition by Toll-like Receptors: The Impact of Nucleoside Modification and the Evolutionary Origin of RNA. Immunity 2005;23:165–75. https://doi.org/10.1016/j.immuni.2005.06.008.

[42] Svitkin YV, Gingras A-C, Sonenberg N. Membrane-dependent relief of translation elongation arrest on pseudouridine- and N1-methyl-pseudouridine-modified mRNAs. Nucleic Acids Res 2021:gkab1241. https://doi.org/10.1093/nar/gkab1241.

[43] Hoernes TP, Clementi N, Faserl K, Glasner H, Breuker K, Lindner H, et al. Nucleotide modifications within bacterial messenger RNAs regulate their translation and are able to rewire the genetic code. Nucleic Acids Res 2016;44:852–62. https://doi.org/10.1093/nar/gkv1182.

[44] Levi O, Arava YS. Pseudouridine-mediated translation control of mRNA by methionine aminoacyl tRNA synthetase. Nucleic Acids Research 2020. https://doi.org/10.1093/nar/gkaa1178.

[45] Kurland CG. Translational accuracy and the fitness of bacteria. Annu Rev Genet 1992;26:29–50. https://doi.org/10.1146/annurev.ge.26.120192.000333.

[46] Wohlgemuth I, Pohl C, Rodnina MV. Optimization of speed and accuracy of decoding in translation. EMBO J 2010;29:3701–9. https://doi.org/10.1038/emboj.2010.229.

[47] Sitron CS, Brandman O. Detection and Degradation of Stalled Nascent Chains via Ribosome-Associated Quality Control. Annu Rev Biochem 2020;89:417–42. https://doi.org/10.1146/annurev-biochem-013118-110729.

[48] Ramakrishnan V. Ribosome Structure and the Mechanism of Translation. Cell 2002;108:557–72. https://doi.org/10.1016/S0092-8674(02)00619-0.

[49] Jobe A, Liu Z, Gutierrez-Vargas C, Frank J. New Insights into Ribosome Structure and Function. Cold Spring Harb Perspect Biol 2019;11:a032615. https://doi.org/10.1101/cshperspect.a032615.

[50] Zaher HS, Green R. Quality control by the ribosome following peptide bond formation. Nature 2009;457:161–6. https://doi.org/10.1038/nature07582.

[51] Hetrick B, Lee K, Joseph S. Kinetics of Stop Codon Recognition by Release Factor 1. Biochemistry 2009;48:11178–84. https://doi.org/10.1021/bi901577d.

[52] Svidritskiy E, Madireddy R, Korostelev AA. Structural Basis for Translation Termination on a Pseudouridylated Stop Codon. Journal of Molecular Biology 2016;428:2228–36. https://doi.org/10.1016/j.jmb.2016.04.018.

[53] Pardi N, Tuyishime S, Muramatsu H, Kariko K, Mui BL, Tam YK, et al. Expression kinetics of nucleoside-modified mRNA delivered in lipid nanoparticles to mice by various routes. J Control Release 2015;217:345–51. https://doi.org/10.1016/j.jconrel.2015.08.007.

[54] Karijolich J, Yu Y-T. Converting nonsense codons into sense codons by targeted pseudouridylation. Nature 2011;474:395–8. https://doi.org/10.1038/nature10165.

[55] Weixlbaumer A, Murphy FV, Dziergowska A, Malkiewicz A, Vendeix FAP, Agris PF, et al. Mechanism of expanding the decoding capacity of tRNAs by modification of uridines. Nat Struct Mol Biol 2007;14:498–502. https://doi.org/10.1038/nsmb1242.

[56] Murphy FV, Ramakrishnan V, Malkiewicz A, Agris PF. The role of modifications in codon discrimination by tRNA(Lys)UUU. Nat Struct Mol Biol 2004;11:1186–91. https://doi.org/10.1038/nsmb861.

[57] Rodnina MV, Wintermeyer W. Fidelity of Aminoacyl-tRNA Selection on the Ribosome: Kinetic and Structural Mechanisms. Annual Review of Biochemistry 2001;70:415–35. https://doi.org/10.1146/annurev.biochem.70.1.415.

[58] Eyler DE, Franco MK, Batool Z, Wu MZ, Dubuke ML, Dobosz-Bartoszek M, et al. Pseudouridinylation of mRNA coding sequences alters translation. Proc Natl Acad Sci U S A 2019;116:23068–74. https://doi.org/10.1073/pnas.1821754116.

[59] Andries O, Mc Cafferty S, De Smedt SC, Weiss R, Sanders NN, Kitada T. N1-methylpseudouridine-incorporated mRNA outperforms pseudouridine-incorporated mRNA by providing enhanced protein expression and reduced immunogenicity in mammalian cell lines and mice. Journal of Controlled Release 2015;217:337–44. https://doi.org/10.1016/j.jconrel.2015.08.051.

[60] Choi J, Ieong K-W, Demirci H, Chen J, Petrov A, Prabhakar A, et al. N6-methyladenosine in mRNA disrupts tRNA selection and translation elongation dynamics. Nat Struct Mol Biol 2016;23:110–5. https://doi.org/10.1038/nsmb.3148.

[61] Gromadski KB, Rodnina MV. Kinetic Determinants of High-Fidelity tRNA Discrimination on the Ribosome. Molecular Cell 2004;13:191–200. https://doi.org/10.1016/S1097-2765(04)00005-X.

[62] Pape T. Induced fit in initial selection and proofreading of aminoacyl-tRNA on the ribosome. The EMBO Journal 1999;18:3800–7. https://doi.org/10.1093/emboj/18.13.3800.

[63] Charette M, Gray MW. Pseudouridine in RNA: What, Where, How, and Why. IUBMB Life 2000;49:341–51. https://doi.org/10.1080/152165400410182.

[64] Kierzek E, Malgowska M, Lisowiec J, Turner DH, Gdaniec Z, Kierzek R. The contribution of pseudouridine to stabilities and structure of RNAs. Nucleic Acids Res 2014;42:3492–501. https://doi.org/10.1093/nar/gkt1330.

[65] Davis DR, Veltri CA, Nielsen L. An RNA Model System for Investigation of Pseudouridine Stabilization of the Codon-Anticodon Interaction in tRNALys, tRNAHis and tRNATyr. Journal of Biomolecular Structure and Dynamics 1998;15:1121–32. https://doi.org/10.1080/07391102.1998.10509006.

[66] Davis DR. Stabilization of RNA stacking by pseudouridine. Nucleic Acids Res 1995;23:5020–6. https://doi.org/10.1093/nar/23.24.5020.

[67] Lucas X, Bauzá A, Frontera A, Quiñonero D. A thorough anion–π interaction study in biomolecules: on the importance of cooperativity effects. Chemical Science 2016;7:1038–50. https://doi.org/10.1039/C5SC01386K.

[68] Westhof E. Pseudouridines or how to draw on weak energy differences. Biochemical and Biophysical Research Communications 2019;520:702–4. https://doi.org/10.1016/j.bbrc.2019.10.009.

[69] Li S, Mason CE. The Pivotal Regulatory Landscape of RNA Modifications. Annu Rev Genom Hum Genet 2014;15:127–50. https://doi.org/10.1146/annurev-genom-090413-025405.

[70] Muramatsu T, Nishikawa K, Nemoto F, Kuchino Y, Nishimura S, Miyazawa T, et al. Codon and amino-acid specificities of a transfer RNA are both converted by a single post-transcriptional modification. Nature 1988;336:179–81. https://doi.org/10.1038/336179a0.

[71] Satpati P, Bauer P, Åqvist J. Energetic Tuning by tRNA Modifications Ensures Correct Decoding of Isoleucine and Methionine on the Ribosome. Chemistry – A European Journal 2014;20:10271–5. https://doi.org/10.1002/chem.201404016.

[72] Durant PC, Bajji AC, Sundaram M, Kumar RK, Davis DR. Structural effects of hypermodified nucleosides in the Escherichia coli and human tRNALys anticodon loop: the effect of nucleosides s2U, mcm5U, mcm5s2U, mnm5s2U, t6A, and ms2t6A. Biochemistry 2005;44:8078–89. https://doi.org/10.1021/bi050343f.

[73] Shi H, Chai P, Jia R, Fan X. Novel insight into the regulatory roles of diverse RNA modifications: Re-defining the bridge between transcription and translation. Mol Cancer 2020;19:78. https://doi.org/10.1186/s12943-020-01194-6.

[74] Boccaletto P, Machnicka MA, Purta E, Piątkowski P, Bagiński B, Wirecki TK, et al. MODOMICS: a database of RNA modification pathways. 2017 update. Nucleic Acids Research 2018;46:D303–7. https://doi.org/10.1093/nar/gkx1030.

[75] Garcia DM, Campbell EA, Jakobson CM, Tsuchiya M, Shaw EA, DiNardo AL, et al. A prion accelerates proliferation at the expense of lifespan. Elife 2021;10:e60917. https://doi.org/10.7554/eLife.60917.

[76] Monroe JG, Smith TJ, Koutmou KS. Investigating the consequences of mRNA modifications on protein synthesis using in vitro translation assays. Methods in Enzymology, Academic Press; 2021. https://doi.org/10.1016/bs.mie.2021.06.011.

[77] Roy B, Leszyk JD, Mangus DA, Jacobson A. Nonsense suppression by near-cognate tRNAs employs alternative base pairing at codon positions 1 and 3. Proc Natl Acad Sci U S A 2015;112:3038–43. https://doi.org/10.1073/pnas.1424127112.

[78] Roy B, Friesen WJ, Tomizawa Y, Leszyk JD, Zhuo J, Johnson B, et al. Ataluren stimulates ribosomal selection of near-cognate tRNAs to promote nonsense suppression. Proc Natl Acad Sci U S A 2016;113:12508–13. https://doi.org/10.1073/pnas.1605336113.

[79] Kitaura K, Ikeo E, Asada T, Nakano T, Uebayasi M. Fragment molecular orbital method: an approximate computational method for large molecules. Chemical Physics Letters 1999;313:701–6. https://doi.org/10.1016/S0009-2614(99)00874-X.

[80] Nakano T, Kaminuma T, Sato T, Akiyama Y, Uebayasi M, Kitaura K. Fragment molecular orbital method: application to polypeptides. Chemical Physics Letters 2000;318:614–8. https://doi.org/10.1016/S0009-2614(00)00070-1.

[81] Nakano T, Kaminuma T, Sato T, Fukuzawa K, Akiyama Y, Uebayasi M, et al. Fragment molecular orbital method: use of approximate electrostatic potential. Chemical Physics Letters 2002;351:475–80. https://doi.org/10.1016/S0009-2614(01)01416-6.

[82] Jo S, Kim T, Iyer VG, Im W. CHARMM-GUI: a web-based graphical user interface for CHARMM. J Comput Chem 2008;29:1859–65. https://doi.org/10.1002/jcc.20945.

[83] Lee J, Cheng X, Swails JM, Yeom MS, Eastman PK, Lemkul JA, et al. CHARMM-GUI Input Generator for NAMD, GROMACS, AMBER, OpenMM, and CHARMM/OpenMM Simulations Using the CHARMM36 Additive Force Field. J Chem Theory Comput 2016;12:405–13. https://doi.org/10.1021/acs.jctc.5b00935.

[84] Foloppe N, MacKerell AD Jr. All-atom empirical force field for nucleic acids: I. Parameter optimization based on small molecule and condensed phase macromolecular target data. Journal of Computational Chemistry 2000;21:86–104. https://doi.org/10.1002/(SICI)1096-987X(20000130)21:2<86::AID-JCC2>3.0.CO;2-G.

[85] Denning EJ, Priyakumar UD, Nilsson L, MacKerell AD. Impact of 2′-hydroxyl sampling on the conformational properties of RNA: Update of the CHARMM all-atom additive force field for RNA. J Comput Chem 2011;32:1929–43. https://doi.org/10.1002/jcc.21777.

[86] Lee MS, Feig M, Salsbury FR, Brooks CL. New analytic approximation to the standard molecular volume definition and its application to generalized Born calculations. J Comput Chem 2003;24:1348–56. https://doi.org/10.1002/jcc.10272.

[87] Takematsu K, Fukuzawa K, Omagari K, Nakajima S, Nakajima K, Mochizuki Y, et al. Possibility of Mutation Prediction of Influenza Hemagglutinin by Combination of Hemadsorption Experiment and Quantum Chemical Calculation for Antibody Binding. J Phys Chem B 2009;113:4991–4. https://doi.org/10.1021/jp810997c.

[88] Kurisaki I, Fukuzawa K, Nakano T, Mochizuki Y, Watanabe H, Tanaka S. Fragment molecular orbital (FMO) study on stabilization mechanism of neuro-oncological ventral antigen (NOVA)–RNA complex system. Journal of Molecular Structure: THEOCHEM 2010;962:45–55. https://doi.org/10.1016/j.theochem.2010.09.013.

[89] Mazanetz MP, Ichihara O, Law RJ, Whittaker M. Prediction of cyclin-dependent kinase 2 inhibitor potency using the fragment molecular orbital method. J Cheminform 2011;3:2. https://doi.org/10.1186/1758-2946-3-2.

[90] Okimoto N, Otsuka T, Hirano Y, Taiji M. Use of the Multilayer Fragment Molecular Orbital Method to Predict the Rank Order of Protein–Ligand Binding Affinities: A Case Study Using Tankyrase 2 Inhibitors. ACS Omega 2018;3:4475–85. https://doi.org/10.1021/acsomega.8b00175.

[91] Fedorov DG, Kitaura K, Li H, Jensen JH, Gordon MS. The polarizable continuum model (PCM) interfaced with the fragment molecular orbital method (FMO). Journal of Computational Chemistry 2006;27:976–85. https://doi.org/10.1002/jcc.20406.

[92] Suenaga M. Facio: New Computational Chemistry Environment for PC GAMESS. Journal of Computer Chemistry, Japan 2005;4:25–32. https://doi.org/10.2477/jccj.4.25.

[93] Suenaga M. Development of GUI for GAMESS / FMO Calculation. Journal of Computer Chemistry, Japan 2008;7:33–54. https://doi.org/10.2477/jccj.H1920.

[94] Barca GMJ, Bertoni C, Carrington L, Datta D, De Silva N, Deustua JE, et al. Recent developments in the general atomic and molecular electronic structure system. J Chem Phys 2020;152:154102. https://doi.org/10.1063/5.0005188.

[95] Fedorov DG, Kitaura K. Pair interaction energy decomposition analysis. J Comput Chem 2007;28:222–37. https://doi.org/10.1002/jcc.20496.

Chapter 5 Conclusions and Future Directions

5.1 Overview

The goal of the work presented here was to advance our understanding of how mRNA modifications impact translation and protein production. My findings highlight the importance of modifications within the coding region of mRNA transcripts to the rate and accuracy of amino acid selection, ribosome fidelity, and termination of translation. This work demonstrates that mRNA modification's role in the epitranscriptome and thus the Central Dogma of Biology is just beginning to be understood.

5.2 A Molecular Level Perspective on the frequency, distribution, and Consequences of mRNA Modifications Conclusions

Chemical modification of mRNA transcripts present the opportunity for the discovery of new regulators of mRNA function, stability and lifecycle, in addition to having been linked to human disease[1,2]. Key to the discoveries of mRNA modifications is the development of next generation sequencing technologies[3–5]. Sequencing has been crucial in identifying the location of modification(s) within mRNA messages. Discovery techniques such as LC/MS have also played an important role in the discovery of new mRNA modifications but provide no data as to site-specific location of a modification within a transcript. Locating the actual site of modification is important when making claims about the potential effects modifications can have upon translation because if the modification is located in the 5' or 3' untranslated regions (UTRs) their

impacts upon translation are unlikely to be as meaningful to the subsequent protein product as coding region modifications[5–8]. In addition to continuing advancements in sequencing and analytical techniques (LC/MS) future directions for improvements include better mRNA isolation/enrichment techniques and better spatial location of modification installation.

Both sequencing and LC/MS approaches suffer from prejudiced isolation techniques, namely poly(A) pull downs. Poly(A) pulldowns utilize the fact that most mature mRNA possess a poly(A) tail and can be isolated by annealing the poly(A) tail to the oligo(dT) beads. While this technique can be successfully used to enrich samples for mature mRNA it selects only for mRNA with long poly(A) tails while omitting the sub-populations of mRNA that have no poly(A) tails (poly(A)-), short poly(A) tails, or are bimorphic transcripts[9,10]. The neglection these mRNA subpopulations presents a knowledge gap regarding the modification state of mRNA transcripts responsible for the synthesis of vital proteins such as histones and a disproportionate amount of zinc finger proteins (ZNFs)[9]. While the current method of discovering modifications in mRNA using poly(A) enrichment is successful it leaves behind an unequal distribution of knowledge regarding mRNA transcript modification. Are these poly(A)- and bimorphic transcripts also modified and if so, are they modified to the same extent as mRNA transcripts with full length poly(A) tails? Given the lack of poly(A) tails it would be reasonable to assume that chemical modifications to these transcripts could replace, at least partially, the functionality of the poly(A) tail.

While progress has been made in discovering mRNA modifications further investigations into the cellular location of modification installation and/removal are needed. Answering these question demands the stringent purification of cellular components to establish the status of cellular spatial modification [2]. An example of a future study is whether the m^7G modification is

installed within the coding region of mRNA in the nucleus or the cytoplasm of a cell. This investigation would require the purification of mRNA from the cell's nucleus and cytoplasm. This study should be accompanied by multiple analysis methods (sequencing) to ensure the purity of the mRNA and that contamination from different cellular locations is kept to a minimum. These investigations would help to establish when (spatially) in the lifecycle a mRNA transcript is modified by writers and if those modification are later removed by erasers. Once a location(s) of modification installation and removal have been developed, insights into why cells install modifications can be gained. Transcript level information concerning modification occupancy and location depends on the continued development of analytical techniques such as LC/MS and sequencing, with nanopore sequencing holding great promise[11–13]. Understanding how mRNA modifications are impacting fundamental biological processes is vital to understanding their role in the epigenetic landscape and the Central Dogma of Biology.

5.3 Assessing the consequences of mRNA modifications on protein synthesis using in vitro translation assays Conclusions

Chemical modifications to mRNA residues have the potential to influence the rate and fidelity of protein synthesis. Given the complexity of translation it is hard to identify exactly where and how the rate and accuracy of translation can be influenced. The *in vitro* translation system derived from *E. coli* utilizes highly purified components which allows the direct molecular level investigation into the impacts of mRNA modifications on translation. Advantages of *in vitro* studies are that they can directly and discretely study single variable changes within an experiment. The downside to *in vitro* systems is the extensive material and time commitment required in order to utilize them. The *in vitro* system can be used to gain insights into how individual chemical modifications influence translation on the molecular level. Future directions for this system should

include detailed kinetic studies of the selection and accuracy of amino acid addition. Currently the effects of modifications on translation accuracy have only been observed on the k_{obs} level. In order to understand how mRNA modifications alter translation accuracy further investigations should utilize Equation 10 [14].

$$Accuracy\ (A) = (s) \times (p) \tag{10}$$

Where *s* is the tRNA selectivity during amino acid addition and *p* is the proofreading ability of the ribosome during amino acid addition. By comparing the ratio between cognate (c) and noncognate (nc) accuracy the kinetic efficiency of peptide bond formation can be established for each species of tRNA, as seen in equation 11.

$$A = \frac{(k_{obs}/K_{1/2})^{c}_{dipeptide}}{(k_{obs}/K_{1/2})^{nc}_{dipeptide}} \tag{11}$$

The ratio between the k_{obs} *and* $K_{1/2}$ for the cognate can provide an experimental double check on the values obtained from *in vitro* experiments since the ratio should be close to 1 in order to allow rapid and accurate addition of the correct amino acid, while non-cognate decoding ratio should have a relatively small number, which should give a high level of accuracy for the ribosome. These type of measurements by themselves will help to provide insight into relative decoding accuracies of the degenerate tRNA anticodons.

The selection and proofreading steps are separated by the GTPase activation and hydrolysis steps (**Figure 2**, steps 3,4) with selection taking place prior to GTPase activation and hydrolysis and proofreading occurring after. This means that selectivity can be defined as Equation 12.

$$s = \frac{(k_{obs}/K_{1/2})^{c}_{GTP}}{(k_{obs}/K_{1/2})^{nc}_{GTP}} \tag{12}$$

The proof-reading ability of the amino acid selection can then be derived by rearranging Equation 10 and substituting in the selectivity equation (Equation 12) to arrive at Equation 13[14,15].

$$p = \frac{A}{s} = \frac{\left(k_{obs}/K_{1/2}\right)^{nc}_{GTP}}{\left(k_{obs}/K_{1/2}\right)^{nc}_{dipeptide}} \Big/ \frac{\left(k_{obs}/K_{1/2}\right)^{c}_{GTP}}{\left(k_{obs}/K_{1/2}\right)^{c}_{dipeptide}} \quad (13)$$

These variables for these equations can all be measured using pre-existing techniques and in fact the rates for cognate addition have already been established for several species of tRNA [15]. Using the *in vitro* system to pick apart the kinetics of chemically modified mRNA will allow elucidation into just how exactly modification alter accuracy at the A-site of the ribosome. Additionally, it will help to establish the significant factors in codon:anticodon interactions (hydrogen bonding, geometry, base stacking, steric interactions, etc.) during translation[14,16,17].

5.4 N1-Methylpseudouridine and pseudouridine modifications impact amino acid misincorporation during translation

My studies with the $m^1\Psi$ and Ψ modifications show that they influence the ribosome's ability to discriminate between cognate and noncognate tRNA. This effect is most clearly seen in the fidelity of the ribosome since $m^1\Psi$ had little to no effect on the rate of amino acid addition or termination of translation. Insertion of $m^1\Psi$ alters the selection of near-cognate tRNAs both *in vitro* and HEK293 cells. My observations reveal that $m^1\Psi$ and Ψ modifications, can both increase and decrease the fidelity of the ribosome in a positional and tRNA dependent manner. Interestingly, this increase in fidelity is not observed during *in cellular* experiments where luciferase mRNA transcripts have every uridine replaced with Ψ or $m^1\Psi$, instead only an increase in amino acid misincorporation was observed in the resultant protein. This cancelation of increased ribosome fidelity when the entire codon is modified with $m^1\Psi$ or Ψ demonstrates that modification fidelity impacts are sensitive to their surrounding chemical environment. Further investigation into how different neighboring nucleotides alter the effects of modifications is needed since molecular level studies have focused on the homogeneous Phe (UUU) codon. The nearest neighbor theory

states that neighboring residues can change a nucleotide's interactions so it would follow that the impact of chemical modifications would also be changed by neighboring residues. Our work has shown that different codon sequences when modified will produce different level of protein production (SI Figure 4.4.9 and 4.4.10) . The question is not only how modification effects are influenced by surrounding residues but how they interact when their neighboring residues are also modified. So far, this question has not been investigated at the molecular level. This has implications for the design of mRNA therapeutics that plan to incorporate different nucleotide modifications within the same transcript such as the studies involving the incorporation of either Ψ or $m^1Ψ$ with m^5C [18]. In addition understanding how neighboring residues interact with modified residues could allow for codon accuracy optimization of mRNA transcripts. Codon optimization of transcripts for maximal protein production is already a common procedure with specific codons and codon combinations modulating translational speed, but these optimizations do not take modifications into account. Modifications could turn a rapidly translating codon into a suboptimal codon/codon pair. One way to test this hypothesis would be to use a combination of *in vitro* and data from *in cellular* experiments. *In vitro* experiments should resemble those described in Chapters 2 and 3. Initial studies should look at how preceding and proceeding codons impact a fully modified (with either Ψ or $m^1Ψ$) Phe UUU codon (Table 9).

Neighboring Codon Sequence Design		
Proceeding	**Preceding**	**Bounded**
AUG-GGG-ΨΨΨ-UAA	AUG-ΨΨΨ-GGG-UAA	AUG-GGG-ΨΨΨ-GGG-UAA
AUG-AAA-ΨΨΨ-UAA	AUG-ΨΨΨ-AAA-UAA	AUG-AAA-ΨΨΨ-AAA-UAA
AUG-CCC-ΨΨΨ-UAA	AUG-ΨΨΨ-CCC-UAA	AUG-CCC-ΨΨΨ-CCC-UAA
AUG-UUU-ΨΨΨ-UAA	AUG-ΨΨΨ-UUU-UAA	AUG-UUU-ΨΨΨ-UUU-UAA

Table 17 *Sequence design to examine the impact of different neighboring codons on the impact of fully modified Phe codons. These sequence present only the investigations needed to examine this effect.*

Starting from the premise of understanding these interactions on a chemical level homogenous codon will establish how a single nucleotide species will affect the modified codon. Once the homogenous codon impacts are understood then the proceed/preceeding/bounded codons can be altered and examined. When designing the follow on experiments investigators should examine miscoding events that occurred in fully modified transcripts such as the luciferase transcripts utilized in the *in cellular* experiments in chapter 4. Since the mass analysis of these miscoding events used mass spectrometry peptide fragment sequences were obtained. The longer of these fragments should be used to map and identify the coding region where the miscoding event occurred. Then using the *in vitro* system the proceeding and preceding codons can be altered without changing the resulting protein using synonymous codons, for example if the proceeding codon is an alanine GCC codon create an mRNA transcript that utilizes a GCU codon instead. This codon substitute even keeps the tRNA species the same (GGC) so that tRNA species population and tRNA modification status does not need to be taken into account and the only variable changed is the presence of uridine instead of a cytosine at the third position of the proceeding codon. Given that every amino acid (except methionine) has multiple codons which code for it investigations of this type will answer the question: do the Ψ or $m^1\Psi$ modifications interact different with different nucleotide neighbors? One downside to this type of investigation is that some amino acids only have two coding codons (i.e. phenylalanine UUU and UUC) which limits a full scale investigation of neighboring residues. This is only a slight downside however because all codon combinations will have biological relevance since they are all naturally occurring. These studies will require the analysis of dipeptide and tripeptide amino acid addition however these analysis are well

established and can be performed using kinetic simulation software [19]. These investigations will only continue as the altered nucleic acid chemistry of modifications in mRNA is uncovered.

Further work on the structural implications of modifications also remains. Molecular modeling suggests that electronically driven changes in mRNA:tRNA interactions largely account for the context specificity of the Ile-miscoding events we observe when Ψ and $m^1\Psi$ modifications are present at the second position of Phe codons. Our studies also reveal the impact that tRNA hypermodification play both in cognate and noncognate decoding by modified mRNA codons. The presence of hypermodifications ms^2i^6A and t^6A in cognate Phe tRNA or noncognate Ile tRNA, respectively, either enhanced or abated the modified mRNA interactions with the tRNA anticodon. Modified codon interactions with hypermodification have implications for mRNA vaccine design as well since not all tRNA have hypermodification present. These altered interactions drive the point home that RNA modifications can alter the chemistry of translation both individually and by acting in concert. Future work will have to elucidate how modification individually and in combination alter fundamental biological processes. This can be accomplished by more complete crystallography and NMR studies which should at a bare minimum include native, and thus fully modified, tRNA, and codons modified at each location (1^{st}, 2^{nd}, 3^{rd}) as well as completely modified codons when possible, such as the Phe (UUU) codon. These studies will be able to elucidate just how mRNA modifications alter not only the codon:anticodon interactions but the changed the structures of the tRNA-mRNA complex. Indeed, one structure has already shown that a ΨUU modified codon alters the CAA end of a Phe tRNA [20]. I would expect that a codon modified at the second position will display similar if not greater structural alterations.

Additionally I would call for the investigation into how modifications alter the thermal stability of the codon anticodon complex. Work has already been done by the Kierzek lab in Poland

which showed that the thermodynamic stability of RNA complexes was altered by the presence of hypermodifications (i^6A and ms^2i^6A) [21,22]. These experiments would consist of reacting fully modified tRNA with unmodified/selectively/fully modified mRNA duplexes and melting the complexes in an isothermal calorimeter to obtain melting curves. These curves can inform on differences in entropy, enthalpy, and melting temperature (T_M) allowing for the calculation of Gibbs free energy. This investigation will allow validation/insight into the molecular modeling performed in Chapter 4 with Ψ and $m^1Ψ$. It should be noted that this experiment will only examine the codon anticodon complex and further studies into the role the ribosome plays in tRNA mRNA complex stability should not be forgotten. These investigations will direct the study of how mRNA modifications alter translational complexes and structures.

5.5 Chapter 5 References

[1] Franco MK, Koutmou KS. Chemical modifications to mRNA nucleobases impact translation elongation and termination. Biophysical Chemistry 2022;285:106780. https://doi.org/10.1016/j.bpc.2022.106780.

[2] Gilbert WV, Bell TA, Schaening C. Messenger RNA modifications – Form, distribution, and function. Science 2016;352:1408–12. https://doi.org/10.1126/science.aad8711.

[3] Amort T, Rieder D, Wille A, Khokhlova-Cubberley D, Riml C, Trixl L, et al. Distinct 5-methylcytosine profiles in poly(A) RNA from mouse embryonic stem cells and brain. Genome Biol 2017;18:1. https://doi.org/10.1186/s13059-016-1139-1.

[4] Delatte B, Wang F, Ngoc LV, Collignon E, Bonvin E, Deplus R, et al. Transcriptome-wide distribution, and function of RNA hydroxymethylcytosine. Science 2016;351:282–5. https://doi.org/10.1126/science.aac5253.

[5] Helm M, Motorin Y. Detecting RNA modifications in the epitranscriptome: predict and validate. Nat Rev Genet 2017;18:275–91. https://doi.org/10.1038/nrg.2016.169.

[6] Chan CTY, Dyavaiah M, DeMott MS, Taghizadeh K, Dedon PC, Begley TJ. A Quantitative Systems Approach Reveals Dynamic Control of tRNA Modifications during Cellular Stress. PLoS Genet 2010;6:e1001247. https://doi.org/10.1371/journal.pgen.1001247.

[7] Tardu M, Jones JD, Kennedy RT, Lin Q, Koutmou KS. Identification and Quantification of Modified Nucleosides in Saccharomyces cerevisiae mRNAs. ACS Chem Biol 2019;14:1403–9. https://doi.org/10.1021/acschembio.9b00369.

[8] Xu L, Liu X, Sheng N, Oo KS, Liang J, Chionh YH, et al. Three distinct 3-methylcytidine (m3C) methyltransferases modify tRNA and mRNA in mice and humans. Journal of Biological Chemistry 2017;292:14695–703. https://doi.org/10.1074/jbc.M117.798298.

[9] Yang L, Duff MO, Graveley BR, Carmichael GG, Chen L-L. Genomewide characterization of non-polyadenylated RNAs. Genome Biology 2011;12:R16. https://doi.org/10.1186/gb-2011-12-2-r16.

[10] Tudek A, Lloret-Llinares M, Jensen TH. The multitasking polyA tail: nuclear RNA maturation, degradation and export. Philos Trans R Soc Lond B Biol Sci 2018;373. https://doi.org/10.1098/rstb.2018.0169.

[11] Lin B, Hui J, Mao H. Nanopore Technology and Its Applications in Gene Sequencing. Biosensors (Basel) 2021;11:214. https://doi.org/10.3390/bios11070214.

[12] Wang Z, Gerstein M, Snyder M. RNA-Seq: a revolutionary tool for transcriptomics. Nat Rev Genet 2009;10:57–63. https://doi.org/10.1038/nrg2484.

[13] Wang Y, Zhao Y, Bollas A, Wang Y, Au KF. Nanopore sequencing technology, bioinformatics and applications. Nat Biotechnol 2021;39:1348–65. https://doi.org/10.1038/s41587-021-01108-x.

[14] Indrisiunaite G. Accuracy of protein synthesis and its tuning by mRNA modifications n.d.:46.

[15] Indrisiunaite G, Pavlov MY, Heurgué-Hamard V, Ehrenberg M. On the pH Dependence of Class-1 RF-Dependent Termination of mRNA Translation. Journal of Molecular Biology 2015;427:1848–60. https://doi.org/10.1016/j.jmb.2015.01.007.

[16] Gromadski KB, Rodnina MV. Kinetic Determinants of High-Fidelity tRNA Discrimination on the Ribosome. Molecular Cell 2004;13:191–200. https://doi.org/10.1016/S1097-2765(04)00005-X.

[17] Pape T, Wintermeyer W, Rodnina MV. Complete kinetic mechanism of elongation factor Tu-dependent binding of aminoacyl-tRNA to the A site of the E. coli ribosome. EMBO J 1998;17:7490–7. https://doi.org/10.1093/emboj/17.24.7490.

[18] Andries O, Mc Cafferty S, De Smedt SC, Weiss R, Sanders NN, Kitada T. N1-methylpseudouridine-incorporated mRNA outperforms pseudouridine-incorporated mRNA by providing enhanced protein expression and reduced immunogenicity in mammalian cell lines and mice. Journal of Controlled Release 2015;217:337–44. https://doi.org/10.1016/j.jconrel.2015.08.0510

[19] Smith TJ, Tardu M, Khatri HR, Koutmou K. mRNA and tRNA modification states influence ribosome speed and frame maintenance during poly(lysine) peptide synthesis. J Biol Chem. 2022 May 17:102039.

[20] Eyler DE, Franco MK, Batool Z, Wu MZ, Dubuke ML, Dobosz-Bartoszek M, et al. Pseudouridinylation of mRNA coding sequences alters translation. Proc Natl Acad Sci U S A 2019;116:23068–74. https://doi.org/10.1073/pnas.1821754116.

[21] Kierzek E, Kierzek R. Influence of N6-isopentenyladenosine (i(6)A) on thermal stability of RNA duplexes. Biophys Chem. 2001 Jul 2;91(2):135-40.

[22] Kierzek E, Kierzek R. The thermodynamic stability of RNA duplexes and hairpins containing N6-alkyladenosines and 2-methylthio-N6-alkyladenosines. Nucleic Acids Res. 2003 Aug 1;31(15):4472-80.

Appendix A The cAMP Signaling Pathway Regulates Epe1 Protein Levels and Heterochromatin Assembly

The cell's ability to maintain homeostasis requires variable expression of the genome but without the alteration of the genome's DNA sequence. Non-sequence altering methods of variable gene expression can include modifications (DNA methylations, histone modification), repressor proteins, and repressive structures. One of these repressive structures is heterochromatin, which consists of condensed DNA[1,2]. This condensed DNA is less accessible to transcription factors and can repress the expression of genes. In yeast the formation of heterochromatin is partially regulated by the protein Epe1. In turn the protein levels of Epe1 were regulated by the cAMP signaling pathway as seen by interruptions in the cAMP pathway affecting Epe1 and heterochromatin landscapes[3]. However, the exact mechanism of how cAMP controls Epe1 is unknown. One possible mechanism of control is

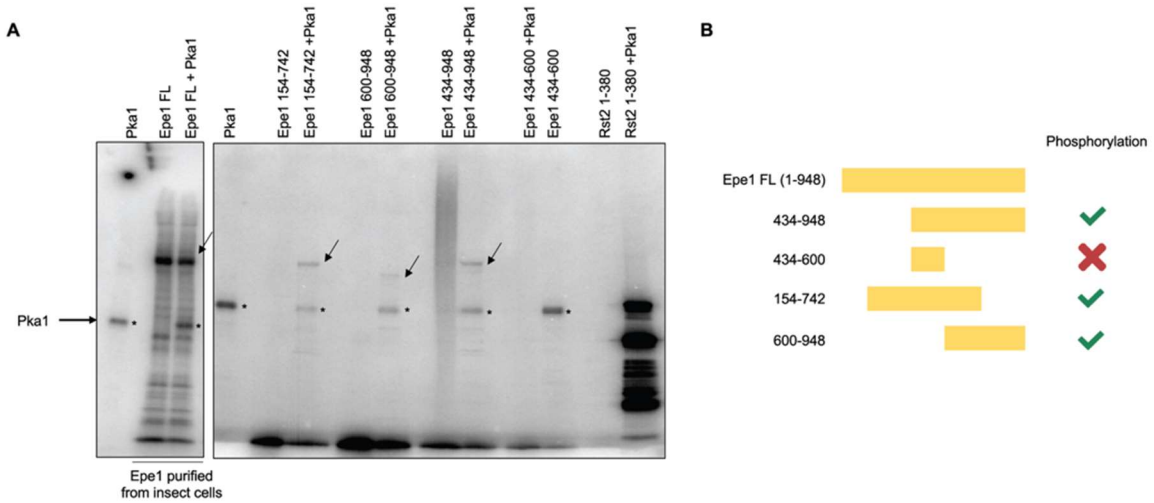

Figure 29 *In vitro phosphorylation assay*

through the phosphorylation of Epe1 by kinase Pka1. Indeed, the result of an *in vitro* assays (Figure 15) show that Epe1 is able to be phosphorylated by Epe1. This result was confirmed by mass-spec analysis showed that the S717 residue is phosphorylated. However, when the S717 residue was mutated to S717D the Epe1 level were still responsive to alterations in the cAMP signaling pathway. This indicates that the Epe1 is not regulated through cAMP signaling pathway-controlled by phosphorylation.

Appendix B Thermal Stability of Pus 7

Cells can alter the structure and stability of their RNAs by incorporating chemical modifications to nucleotides within RNA species. These modifications are installed by "writer" proteins. One of the most abundant RNA modifications, pseudouridine, is installed by pseudouridine synthetase enzymes (Pus) with pseudouridine synthase 7 being the prominent modifier of mRNA. Pus7 preferentially binds to the consensus sequence UGUAR (R representing any purine), of multiple RNA species and transcripts regardless of structural motifs[4]. Despite its indiscriminate binding pseudouridine modification levels do not match UGUAR site levels present in mRNA transcripts thus indicating that other factors play a role in Pus7 substrate selection. Given the fact pseudouridinalyation level have been observed to increase in cells under heat stress, one of these factors could be melting of RNA secondary structure and the dissociation of other RNA binding proteins that obstructed Pus7 from binding to the UGUAR consensus sequence[5]. I modeled the thermal stability of Pus7 in order to determine if it would even be stable at elevated temperatures. This model used the relationship between solvent accessible surface area and thermal dynamic parameters to model stability, seen in Equation 14 [6].

$$\Delta G(N,T) = \Delta H_R + \Delta C_p(T - T_R) - T\Delta S_R - T\Delta C_p \ln\left(\frac{T}{T_R}\right) \tag{14}$$

Where m_h and b_h are the slope and intercept of ΔH_R , m_s and b_s are the slope and intercept of ΔS_R and m_c and b_c are the slope and intercept of ΔC_p when these parameters are plotted as a function

of N. Where ΔH_R and ΔS_R are the enthalpy and entropy at reference temperature, T_R is the reference temperature and T is the temperature [6].

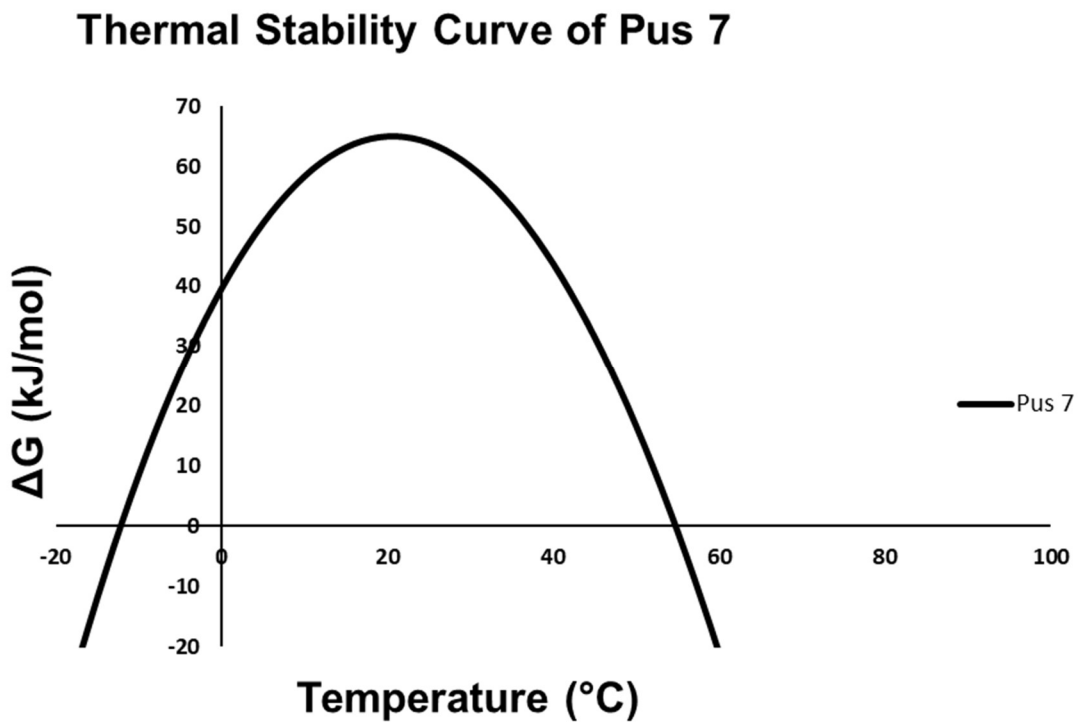

Figure 30 *Thermal Stability of Pus7*

Pus7 is stable at elevated temperatures with a max stability of approximately 22 °C. This stability could allow Pus7 to modify RNA consensus sequences that becomes unmasked during times of thermal stress.

Appendix C CGG Repeats Trigger Translational Frameshifting

Translational frameshifting occurring when the ribosome is shifted by one or two nucleotides during the translation of an mRNA transcript. This shifting of a single or double nucleotides creates an entirely new mRNA message and corresponding protein output. Frameshifting events can be triggered by structure or mRNA sequence. Frame shift triggering sequences are typically composed of repeated nucleotide triplets such as those found in repeat associated non-ATG (RAN) translation sites [7]. The FMRP translational regulator 1 (FMR1) human gene is essential for cognitive and reproductive development contains the repeated CGG trinucleotide which can induce RAN translation. Frameshifts by the ribosome within this RAN translation region can result in increased protein product toxicity. In order to elucidate whether CGG frameshift was the result of sequence or structure *in vitro* translation experiments were conducted. Using the prokaryotic *in vitro* translation system described in Chapter 3. The mRNA sequences tested consisted of an AUG start codon followed by either an arginine CGG repeat, an

arginine repeat AGG/AGA with structure, an arginine AGG/AGA repeat without structure, a glycine GGC repeat, or an alanine GCG repeat. The results can be seen in

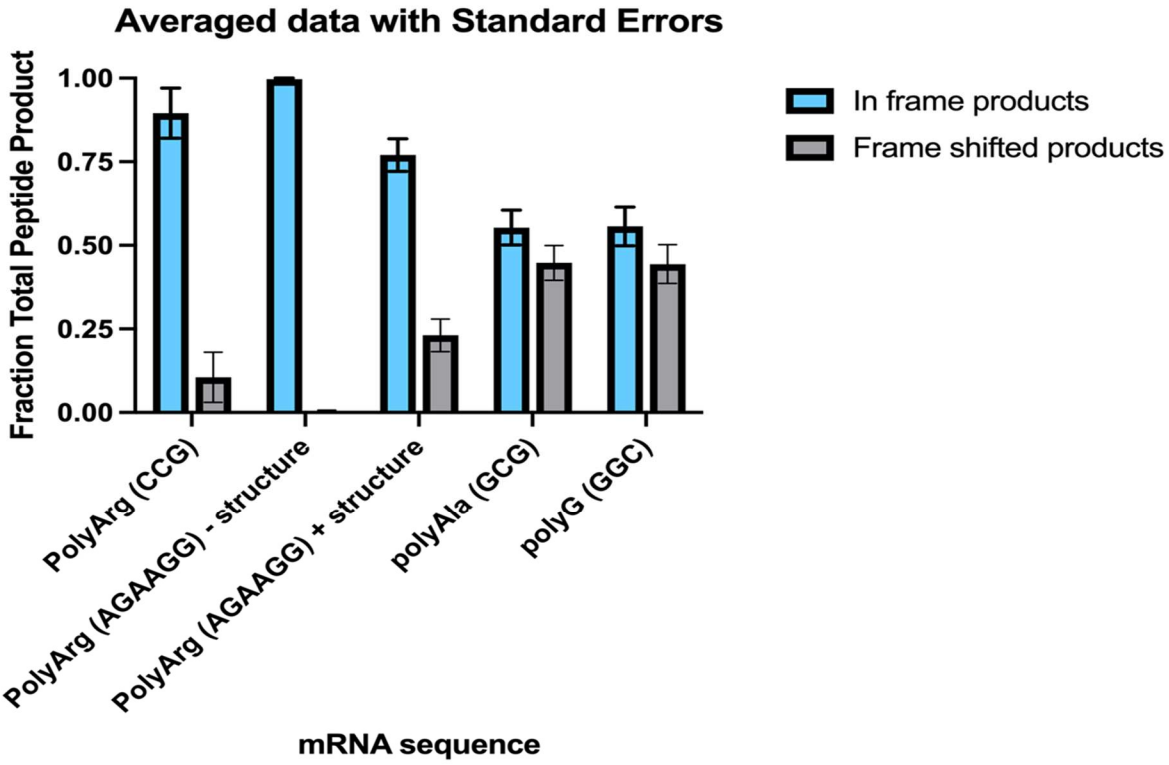

Figure 31 *Ribosome frameshifting*

The experiment indicates that both structure and sequence play a role in frame shifting. Most likely these frameshifting events are initiated by the repeated sequences and then enhanced by mRNA secondary structure.

5.6 References

[1] Allshire RC, Madhani HD. Ten principles of heterochromatin formation and function. Nat Rev Mol Cell Biol 2018;19:229–44. https://doi.org/10.1038/nrm.2017.119.

[2] Grewal SIS, Jia S. Heterochromatin revisited. Nat Rev Genet 2007;8:35–46. https://doi.org/10.1038/nrg2008.

[3] Bao K, Shan C-M, Chen X, Raiymbek G, Monroe JG, Fang Y, et al. The cAMP signaling pathway regulates Epe1 protein levels and heterochromatin assembly. PLoS Genet 2022;18:e1010049. https://doi.org/10.1371/journal.pgen.1010049.

[4] Gilbert WV, Bell TA, Schaening C. Messenger RNA modifications – Form, distribution, and function. Science 2016;352:1408–12. https://doi.org/10.1126/science.aad8711.

[5] Purchal MK, Eyler DE, Tardu M, Franco MK, Korn MM, Khan T, et al. Pseudouridine synthase 7 is an opportunistic enzyme that binds and modifies substrates with diverse sequences and structures. Proceedings of the National Academy of Sciences 2022;119:e2109708119. https://doi.org/10.1073/pnas.2109708119.

[6] Watson MD, Monroe J, Raleigh DP. Size-Dependent Relationships between Protein Stability and Thermal Unfolding Temperature Have Important Implications for Analysis of Protein Energetics and High-Throughput Assays of Protein-Ligand Interactions. J Phys Chem B 2018;122:5278–85. https://doi.org/10.1021/acs.jpcb.7b05684.

[7] Malik I, Kelley CP, Wang ET, Todd PK. Molecular mechanisms underlying nucleotide repeat expansion disorders. Nat Rev Mol Cell Biol 2021;22:589–607. https://doi.org/10.1038/s41580-021-00382-6.